UCRL-11861

University of California

Ernest O. Lawrence Radiation Laboratory

STRUCTURES AND STRENGTH OF AUSFORMED STEELS

TWO-WEEK LOAN COPY

This is a Library Circulating Copy which may be borrowed for two weeks. For a personal retention copy, call Tech. Info. Division, Ext. 5545

Berkeley, California

DISCLAIMER

This document was prepared as an account of work sponsored by the United States Government. While this document is believed to contain correct information, neither the United States Government nor any agency thereof, nor the Regents of the University of California, nor any of their employees, makes any warranty, express or implied, or assumes any legal responsibility for the accuracy, completeness, or usefulness of any information, apparatus, product, or process disclosed, or represents that its use would not infringe privately owned rights. Reference herein to any specific commercial product, process, or service by its trade name, trademark, manufacturer, or otherwise, does not necessarily constitute or imply its endorsement, recommendation, or favoring by the United States Government or any agency thereof, or the Regents of the University of California. The views and opinions of authors expressed herein do not necessarily state or reflect those of the United States Government or any agency thereof or the Regents of the University of California.

UCRL-11861

UNIVERSITY OF CALIFORNIA

Lawrence Radiation Laboratory
Berkeley, California

AEC Contract W-7405-eng-48

STRUCTURES AND STRENGTH OF AUSFORMED STEELS

Om Johari

Ph.D. Thesis

January 1965

CONTENTS

Abstract..... v

I. Introduction..... 1

II. Experimental..... 6

III. Results..... 8

A. Structure of Austenite..... 8

1. 0 and 8% Deformation..... 8

2. 30% Deformation..... 8

3. Twinned Austenites..... 14

B. Structure of Martensites..... 15

1. 0 and 8% Ausformed Steels..... 15

2. 30% Ausformed Steels..... 18

C. Summary of Observations on Austenites..... 21

D. Summary of Observations on Martensites..... 22

IV. Discussion..... 24

A. Precipitation in Austenite..... 24

B. Retained Austenite and Effect of Deformation on Martensites..... 26

C. Twinning..... 27

D. Strength of Ausformed Steels..... 31

1. Martensite Grain Size..... 31

2. Twinning..... 31

3. Carbon Content..... 31

4. Precipitation..... 32

5. Dislocation Density..... 33

E. Parameters of Ausforming 35

F. Control of Properties 37

V. Conclusions 40

Acknowledgments 42

Appendix I 43

Appendix II 44

References 50

Figure Captions 52

STRUCTURES AND STRENGTH OF AUSFORMED STEELS

Om Johari

Inorganic Materials Research Division, Lawrence Radiation Laboratory,
Department of Mineral Technology, College of Engineering,
University of California, Berkeley, California

January 1965

ABSTRACT

Substructures of conventional and ausformed steels were examined using transmission electron microscopy to determine the causes of strengthening of these steels and to better understand the role of the parameters of ausforming. Steels based on Fe-25% Ni-0.3%C, with carbide forming alloying elements (Cr, V and Mo) were examined in both austenitic and martensitic conditions. Undeformed steels were studied and compared with steels ausformed 8 and 30% at 100°C and 500°C. Dark field analyses were done in most cases to study substructural features such as precipitates and twinning.

Precipitates and a high density of dislocations were observed in austenites and martensites of all 30% ausformed steels. A critical amount of ausforming was necessary to nucleate the precipitates and this amount was between 8 and 30% in all the steels examined. The precipitates are identified as Fe_3C, VC, MoC and probably $Cr_{23}C_6$. For the steels containing carbide formers, neither the precipitates could be grown nor the dislocation density reduced by low temperature tempering in the microscope. Similar treatments produced extensive growth of cementite in Fe-Ni-C steel and this accounts for their

the two temperatures of deformation and different compositions of the steels showed little substructural differences.

The higher strength resulting from ausforming is primarily due to the increased dislocation density. The precipitates play an important role by providing sites for dislocation multiplication and pinning. The role of carbon in strengthening was mainly through providing precipitates. No systematic variation of martensite plate sizes with ausforming parameters could be detected.

The extent of twinning in martensites decreased with increasing amount of ausforming. This suggested that the occurrence of transformation twinning was favored by a low Ms temperature. Twinning in some austenites was observed. This may be due to the effects of solutes in lowering the stacking fault energy. The absence of twinning and the high density of dislocations probably accounts for the better ductility of ausformed steels.

It is proposed that explosive deformation of ausformed steels, alloying and ausforming to give deformable precipitates, and explosive deformation of dispersion hardened materials containing suitable precipitates be investigated further to obtain materials with higher strength and better ductility.

I. INTRODUCTION

Cold working has always been used as a way of strengthening materials, though usually at the expense of ductility. However, with the increasing demand for stronger and tougher materials, new ways of strengthening have been developed. Thermal-mechanical treatments, consisting of introducing mechanical strain at some point of a heat treatment cycle, have been developed to obtain further improvement in strength and toughness. Ausforming is one such thermal mechanical treatment in which metastable austenite is deformed without recrystallization before transformation to martensite.[1] In this process the steel selected has to be such that a suitable metastable austenite region (the so-called bay region) is produced in which austenite can be worked, and the hardenability of the steel is so adjusted that it does not transform to non-martensitic products anywhere during the deformation. By this process the tensile strength is raised as much as 30 - 50%,[2] with usually an enhancement of ductility and toughness. The increased strength of ausformed steels is directly proportional to the amount of deformation.[3]

This ausforming process has been the subject of numerous investigations which have been recently reviewed by Phillips and Duckworth,[4] and Marshall.[5] The main metallurgical interest has centered around optimizing the process parameters so that the best combination of strength and ductility is obtained. These parameters (viz., temperature of deformation, amount of deformation, carbon content, alloy content, tempering time and temperature, and austenitizing conditions) are,

however, intimately related and it is difficult to make generalizations about the process (see e.g. Phillips and Duckworth[4]).

For ausforming to be beneficial, it is essential that the steel contain some carbon (>0.1%). The results of Floreen et al.[6] on stainless steels clearly prove that in steels where carbon is absent, cold working gives higher strength than ausforming. However, the exact role played by carbon has been rather unclear, although a number of suggestions have been recently put forward, e.g. precipitation hardening from alloy carbides,[7-11] although no direct evidence for precipitation has been found until this research was done. Solid solution strengthening by carbon is known to be an important factor in martensite strength (e.g. Cohen[12]), and it should be a contributing factor in ausformed steels also. However, the carbon content has to be kept low to obtain better ductility[13] and to avoid large amounts of retained austenites.

Apart from the three factors mentioned so far, viz. work hardening due to mechanical working of austenite, precipitation hardening due to possible carbide precipitation during or after deformation and solid solution hardening due to carbon, two other effects have been considered for strengthening in martensitic steels. They are twinning[14] due to the transformation strain and refinement of martensite plates due to worked austenite.[11,15] Speich and Swann[16] have shown in the case of Fe-Ni martensites that internal twins are not an important strengthening mechanism, because no sharp increase in strength was observed when internally twinned martensite plates appeared. The work on explosively deformed nickel[17] also showed that twinning does not appreciably increase

the strength. These results indicate that twinning is not an important mode of strengthening. Although refinement of martensite plates was previously thought to be an important factor in strengthening,[15] there are observations which would suggest that this may not be so.[7]

With deformation of austenite there is an increase in dislocation density. If these dislocations are to be effective in strengthening, it is essential that they survive the transformation austenite to martensite. The dislocations could aid in inducing precipitation by increasing directly or indirectly the diffusivity of alloying elements. Before precipitation occurs, it is likely that carbon forms atmospheres about dislocations. Depending on the temperature and amount of deformation, the nucleation of carbides may be very high, but the growth rate would be limited. From thermodynamical considerations, alloy carbides rather than cementite are likely to precipitate under usual conditions. The alloy carbides formed would therefore be very fine and difficult to detect. Previous thin foil, and extraction replica work have not been successful in determining the existence of such carbides.[7-9] Thus, so far, there has been no direct evidence of carbide precipitates. This briefly summarizes the current thinking about strengthening of ausformed steels.

From the review so far, it is apparent that most of the work done on ausformed steels has been either on mechanical properties or on explaining these on the basis of some metallographic and extraction replica work, but no attempt has been made to study the substructure in detail. The present work is an attempt in this direction. Steels were

designed with a view to provide a range of temperatures for deformation to enable examination of both metastable deformed austenite at room temperature, and of martensite obtained by quenching these austenites in liquid nitrogen. A base composition of Fe-25 Ni-0.3C was utilized. With a constant carbon content of 0.3%, the alloying elements and nickel content were adjusted to provide a favorable Ms. Three different alloying elements, V, Cr and Mo, were investigated to find which of the three was most beneficial. Three important parameters were chosen for this work, viz. degree of deformation (undeformed, 8% and 30%), temperature of deformation (100° and 500°C), and composition. The steel compositions and their Ms temperatures are listed in the table below. The steels will be referred to by their heat numbers.

TABLE I

Heat No.	%C	%Ni	%Alloying Element	Austenitizing Temperature	Ms
1410	0.3	27.94	---	1200°C	- 8°C
1398	0.28	24.92	4.50 Mo	1200°C	Below-77°C
1541	0.32	16.40	4.72 Cr	1200°C	-16°C
1402	0.29	24.73	1.85 V	1290°C	- 3°C

This work was jointly undertaken with the research laboratories of the Ford Motor Company at Dearborn, Michigan and Newport Beach, California, who prepared the steels and carried out the mechanical testing. The electron metallography and correlation to mechanical properties was the objective of this thesis. Preliminary results of the investigation were

reported at the Berkeley Conference in June, 1964.[18] Reference to the mechanical property data therein reported will be made where necessary.

II. EXPERIMENTAL

The composition of the steels investigated is given in Table I. The steels were given thermal mechanical treatments at the Ford Laboratory (described in Appendix I). For the electron microscopy, 10 samples were taken from each steel as described below: two from steels with no deformation - one austenitic, and one transformed to martensite; four from steels deformed at 100°C -two 8% and two 30% deformed, one each for each deformation in untransformed and transformed conditions; and similarly four from steels deformed at 500°C.

As was found later, the Ms of steel 1398 was too low and hence very little martensite was detected in the microscope. The Ms for steel 1402 was higher, and almost all steels showed the presence of martensite, more so in case of deformed steels because Ms is raised by deformation.

Specimens 0.005 ins. thick, obtained by chemical polishing in 30% H_2O_2 - phosphoric acid solution after thermal mechanical treatment, were supplied by the Ford Laboratory. These were then electropolished using the window technique in chromic acid-acetic acid (270 cc glacial acetic acid, 14 cc distilled water and 60 gm chromic acid) solution. Thin foils were cut from the polished sheets, mounted in single or double tilt stages, and examined in a Siemens Elmiscope Ib microscope, operated at 100 KV. In order to preserve as clean a surface as possible the specimens were examined immediately after preparation, but traces of films (probably oxide) were observed in some cases.

The dark field technique was mostly used to study the precipitates,

twins, or other fine structures. It will become clear during the discussion of results that dark field work is an absolute necessity in this type of electron microscopic investigation. The dark field images can be obtained either by gun tilt or without gun tilt. Although it is quicker to obtain dark field images without tilting the gun, maximum resolution is obtained only when the electron gun is tilted so that the diffracted rays pass down the optical axis of the electron microscope.

Emphasis is placed on a detailed metallographic analysis of the various substructural features in austenite and martensite. These include dislocation arrangements, precipitation, and microtwinning, and involved examination of many electron micrographs and diffraction patterns.

III. RESULTS

The steels will be referred to by their heat numbers (Table I). When "alloy steels" are referred to, this means steels containing carbide forming alloying elements in addition to nickel and carbon (e.g. steels 1398, 1402 and 1541).

A. Structure of Austenite

1. 0 and 8% Deformation

Figure 1 shows the structure of austenite for steel 1410 in the undeformed state. The structure shows that in many areas very few dislocations are present (e.g. 1(a)), but some areas show a relatively high density (e.g. Figs. 1(b), 2). This indicates that the austenitizing treatment does not anneal out all of the dislocations, which is not surprising because of the relatively low temperature (Table I). The dislocations in Fig. 2(a) all lie along the traces of {111} slip planes, (lying at 60° to each other, the foil orientation being [111]). This was also true of steels deformed 8% (e.g. Fig. 3). In all these cases no evidence for any precipitation was observed. These structures are similar to dislocation substructures observed in other plastically deformed metals and indicate that the deformation normally takes place by slip and not twinning. The density of dislocations observed depends on the orientation of the area being examined and its relation to the deformation process, i.e. the amount of resolved shear strain.

2. 30% Deformation

In contrast to the structure of 0 and 8% deformed steels, the

structure after 30% deformation was different. Structures such as shown in Fig. 4(for steel 1398), consisting mainly of dislocation tangles were now observed. The cell walls do not lie parallel to slip planes, indicating considerable cross slip has occurred. Dislocations lie along the slip planes for metals with low stacking fault energy and the observation of tangles would suggest a rise in stacking fault energy which favors cross slip. This is taking place by the removal of alloying elements by precipitation, although this micrograph and likewise many other plates were taken which showed no visible evidence of precipitation in bright field. However, when dark field work was done, it became clear that small precipitates were present in the steels. Figure 5 shows a bright and dark field pair from steel 1398, 30% deformed at 500°C. The diffraction pattern in (c) is $[01\bar{1}]$, with the dark field micrograph taken on spot A, which as shown in the following, includes a precipitate reflection as well as the (111) matrix reflection. Reversal of contrast indicates the presence of precipitates.

Some of the austenitic steels were also examined using the XRD-5 diffractometer. This gave a lattice parameter of about 3.60Å for austenite and showed no evidence for the presence of carbides. The electron diffraction pattern (Fig. 5(c)) shows streaks near the 200 and 220 type spots, which are seen more clearly in Fig. 6(c), along with faint continuous rings. From the measurements of the distances of these streaks, the 'd' values corresponding to these can be approximately obtained from the camera constant equation. The two average 'd' values so calculated for streaks near 200 and 220 spots for the electron

diffraction patterns in Figs. 5, 6 and 7, and others (not submitted here), correspond to nearly 2.10Å and 1.45Å, respectively.

For austenites, d_{111} = 2.08Å, so that one of the carbide diffraction spots (with d ≈ 2.10Å) will coincide with the matrix spot, and the precipitates will change contrast when the dark field micrograph is taken at a (111) spot (e.g. Fig. 5(b)), as well as at the streaks. Normally, however, the streak or ring is too faint to be seen on the microscope screen (Fig. 6(c)), and the dark field micrographs are taken with the objective aperture placed over a 200 matrix spot. The corresponding streak is also included in the aperture so that contrast reversal for carbides is also obtained (Fig. 6(b)). Some times this can give rise to striking contrast reversal (Fig. 7(b)). The presence of precipitates in this steel is thus confirmed. Precipitates are not producing strain contrast because their dark field image is of uniform intensity (Figs. 5, 6 and 7 for steel 1398), i.e. not black-white "lobed" images expected from coherent precipitates such as G.P. zones.[19] It is concluded, therefore, that they are incoherent, i.e. discreet dispersoids rather than clusters or zones.

Similar observations regarding the presence of precipitates were made on the other steels. Figure 8 shows the substructure containing a high density of dislocations and precipitates in chromium and vanadium* steels, (steels 1541 and 1402, respectively). It was observed from the diffraction patterns in all cases that the streaks or faint rings (as in Figs. 5, 6 and 7) due to precipitates appeared again

*In the case of deformed vanadium steel, as mentioned earlier, it always contained some martensite. The area shown is therefore retained austenite.

near the 200 and 220 spots. This may suggest the possibility of some orientation relationship between the precipitate and the matrix; however, this cannot be derived because of insufficient reflections. The observations of these streaks does not necessarily imply an orientation relationship because the intensity of precipitate reflection may be enhanced due to some overlap with the intensity of the matrix reflection (e.g. in Fig. 6, the intensity of the faint continuous ring is higher near the matrix spot than elsewhere).

Sometimes thin edges of the foil polygonized and in these regions the precipitates were observed to be larger than elsewhere. This is probably associated with the ease with which the dislocations anneal from very thin edges as a result of heating of the sample in the microscope because of the electron beam. One such case is shown in Fig. 9 for steel 1398. The measurements from the ring pattern and the results therefrom are recorded in Table II. The dark field image from a point on the first ring shows the contrast reversal for precipitates. The carbide rings also include the same d-spacings as were obtained from the spot patterns (Figs. 5, 6 and 7). Although the 'd' values of carbides obtained are not very accurate, it is possible to identify the carbides for steel 1398. In the literature,[20] there are two carbides reported for molybdenum, MoC and Mo_2C, both of which are hexagonal. Within the accuracy of results in Table II, both carbides show lines at 'd' values of 1.46Å and lower. However Mo_2C shows no line with 'd' value in the neighborhood of 2.1Å. The existence of a 'd' value of ≈ 2.1Å proves that the precipitates are MoC and not Mo_2C.

TABLE II

Measurements from Fig. 9, for steel 1398 (Mo steel)

Ring No.	Observed Diameter of Rings in Cm	Austenitic Rings Ratios	Austenitic Rings hkℓ for Matrix	Probable Carbide 'd' values*
1	4	1	111	2.08Å
2	4.6	1.15	200	
3	5.6			1.46Å
4	6.55	1.63	220	
5	7.0			1.18Å
6	7.65	1.91	311	
7	8.0	2.00	222	
8	8.1			0.99Å
9	8.6			0.94Å
10	9.10	2.28	400	
11	10.0	2.50	331	
12	10.3	2.58	420	

*These values are calculated from the camera constant equation.

Similar observations in the polygonized part of the foil were made on Cr steels (Fig. 10). Calculations of 'd' values from the ring pattern and its comparison with the 'd' values obtainable from the ASTM card file[20] presented similar difficulties as in the case of steel 1398 where the rings for lower 'd' values could not be used to identify the carbides definitely due to the limited accuracy of the calculated results. The line in the neighborhood of 2.1Å is present in all the three Cr-carbides reported (e.g. at 2.05Å for $Cr_{23}C_6$, 2.12 and 2.04Å for Cr_7C_3 and 2.12 and 2.10Å for Cr_3C_2). In this case, therefore, from these observations positive identification of carbides cannot be made. These results are, however, not in disagreement with extraction replica work[18] in which the precipitates were found to be $Cr_{23}C_6$. Similar diffraction experiments enabled the precipitates in vanadium steel (1402), to be identified as VC and in steel 1410 as cementite. These identifications are based on the best fit obtained from the comparison of the electron diffraction data of the present work with the previous published x-ray results.[20] However, since only a few lines could be observed for each carbide the results of identification may not be conclusive.

In Fig. 10 two dark field micrographs are shown (b and c), one of which (c) is taken with the aperture inside the first ring. Most carbides have 'd' spacings which are higher than the minimum 'd' spacings for the matrix (2.1Å for (111) in the case of fcc austenite and 2.08Å for (110) in the case of martensites), e.g. there are six more lines with 'd' spacings higher than 2.05Å for $Cr_{23}C_6$. If enough carbides are

present, these will give rise to some faint spots (which may not be easily visible) inside the first ring. A dark field micrograph inside the first ring may, therefore, under appropriate conditions, show contrast reversal for some precipitates. This is seen in Fig. 10(c). It is obvious, however, that for such effects to show up, many precipitates of different orientations should be present. This is unlikely to be the case when precipitates are small and possibly not random.

Observations were made on steels deformed at 100°C also, and they showed similar evidence of precipitation. Due to the complexities of the structure observed, it is not possible to meaningfully measure and compare the sizes of the precipitates or dislocation densities obtained at 100°C and 500°C. From the observations there is very little difference in the structures observed after the 100°C and the 500°C ausforming.

3. Twinned Austenites

In a few areas of 30% deformed austenite of Mo stel (steel 1398) some evidence of mechanical twinning was observed, both for 500°C and 100°C deformation. An example is shown in Fig. 11. The diffraction pattern is [110] and the twins lie on either (111) or $(11\bar{1})$ planes, so that the twin spots coincide with some of the matrix spots.[21] The analysis of this pattern (see Appendix II) and the dark field work show that the structure is twinned. The dark field at spot A shows no reversal of contrast for twins, but it does change contrast for the precipitates and some of the dislocations in the matrix, showing that it is not a twin spot. At spot B, contrast reversal for twins takes place, as would be expected, because this $\bar{2}20$ spot remains the same after twinning

on either of the {111} planes mentioned above.

Although very few twinned areas were found in Mo steel, no evidence for twinning was found in austenites of the other steels. This is the first time that mechanical twinning has been observed in austenitic steels that can undergo the martensitic transformation.

B. Structures of Martensites

1. 0 and 8% Ausformed Steels

During the transformation austenite to martensite the lattice invariant shear occurs by slip or twinning.[22] Previous work has shown that twinned substructures are preferred when the solute content is high, i.e. when the Ms temperature is low. The occurrence of twinning may also be related to stacking fault energy although no direct evidence for this has yet been reported. Thus, Kelly and Nutting[14] found a few internally twinned martensite plates in plain carbon steels containing as low as 0.14%C. The relative number of these plates increased with carbon content. Swann and Speich[16] found twinning in Fe-Ni alloys above 25% Ni. There is not a sharp transition from dislocations to twinning and both are usually observed even in concentrated solid solutions. The densest twinned area seem to coincide with the so called mid-rib near the centers of martensite plates.

The martensites of unausformed steels showed both twinned and untwinned structures. This is to be expected because the steel composition is based on 25% Ni and 0.3%C. Figure 12 shows two of the mid-rib twinned structures from an unausformed specimen. The high density of twinning at the mid-rib decreases outwards to the edge of the plate.

These twins are not always continuous. A high dislocation density can also be seen in the micrograph of Fig. 12(b).

The twins lie along the traces of $(112)_M$ planes and the analysis of their diffraction pattern is greatly simplified by a technique described by Johari and Thomas.[21] The stereographic projection is an aid in solving these patterns, and some of the stereograms are submitted in Appendix II.

Similar transformation twinning was also observed in alloy steels and an example is shown in Fig. 13 for steel 1398. Figure 13(a) shows the structure as observed in bright field, while the dark field image of the reflection A showed some evidence of twinning (Fig. 13(b)), the contrast of which could be considerably improved by proper tilting (Fig. 13(c)). The twins, as seen in Fig. 13(c), do not seem to be continuous, but are broken along the line, which in this case is the trace of the $(01\bar{1})$ plane, the slip plane in bcc structures. Observations of such discontinuous twins have been made before on steels[23,24,25], as well as explosively deformed Cu-Al alloys.[26] As the martensitic reaction takes place over a range of temperature, the region to transform could first be transformed by slip or twinning shears. If it transformed first by a twinning shear, twinning will take place and the deformation produced as a result of later transformation may cause the twins to slip. If the first shear is slip, many dislocations will be introduced in the matrix, and if the twinning shear occurs afterwards, in these areas, the twins would not be continuous but broken because of their interaction with dislocations already present. More experiments are

required before the phenomenon of discontinuous twinning can be fully understood.

The structures of 8% ausformed steels were similar to those of unausformed steels, except that the relative amount of twinning was much less than in unausformed steels. Figure 14 shows two micrographs from 8% ausformed steel 1410. In both cases the twins lie along the traces of $\{112\}_M$ planes. In Fig. 14(a), a dark field micrograph is submitted showing that some of the features of the twinned structure are better resolved in dark field than in bright field.

Both martensite and retained austenite were observed after 0 and 8% ausforming. Figure 15 shows two such structures for unausformed and Fig. 16 for 8% ausformed 1410 steel. Structures similar to Fig. 15(a) have been previously observed by Kelly and Nutting.[27] From observations of these steels it was not possible to suggest any change in size of martensite plates as a result of prior austenite deformation, e.g. a comparison of the four micrographs in Figs. 15 and 16 as well as others not included here show clearly that the change in martensite plate size, if any, is not uniform.

Specimens ausformed 8% at either 100°C or 500°C showed no evidence for precipitation either before or after transformation to martensite. It was possible to induce precipitation, in a few cases in steel 1410, by slight beam heating (i.e. tempering in the microscope), an example of which is shown in Fig. 17. There are no extra spots but streaks along directions perpendicular to the habit planes of the precipitates are seen in the diffraction patterns. It is not possible to identify

the precipitates in this case, although they must be a form of iron carbide. The plates seem to be lying on {112} planes and this suggests[25] that the precipitates are probably cementite. Tempering of bulk 1410 conventional martensite also produces Fe_3C as shown by carbon extraction replicas.[18]

2. 30% Ausformed Steels

The substructures observed in martensites formed after 30% ausforming in all the steels showed evidence for precipitation which is not surprising since the austenites after 30% deformation also showed precipitates (section III-A-2). Figure 18(a) shows a bright field image in which it is difficult to resolve precipitation. However, once the dark field micrograph (Fig. 18(b)) is taken, then, as in the case of austenites, precipitation is clearly evident. By similar dark field work, it was proved that precipitates were also present in the other steels. There appears to be no change in the number or distribution of carbides from the austenitic to the martensitic state.

Rings and streaks were not observed in the case of martensites obtained from deformed austenites, though as seen in some of the dark field micrographs, contrast reversal for precipitates was obtained (Fig. 18(b)). The reason for the non-observance of precipitate reflections is simply due to the fact that the d-spacings of precipitate and matrix are nearly the same; hence, both sets of reflections coincide (e.g. for the first two allowed reflections for martensites $d_{110} \sim 2.03$Å and $d_{200} \cong 1.47$Å and the observed d-spacings for carbides (Table II) are 2.08 and 1.46Å).

The structure of these steels was, in general, very complex due to the effects of working and precipitation and because retained austenite was always present. Figure 19 shows such a complex structure for steel 1402, from which it is seen that the dislocation density for retained austenite (γ) is very high. The martensitic areas also contain a high density of dislocations (Fig. 20). These may not be revealed in some areas (Fig. 21(a)), because of the orientation, but once the specimen is tilted, dislocations are clearly seen as shown in Fig. 21(b).

The diffraction patterns of these steels are very complex and show very many spots, e.g. due to the small size of martensite plates various orientations of the martensites and precipitates are illuminated. This was, at times, further complicated by diffraction from retained austenite. Figure 22 shows such a diffraction pattern and its analysis, while in Fig. 23 the corresponding image and dark field micrographs from three spots are shown.

The analysis of this diffraction pattern is facilitated by forming the dark field images of separate reflections arising from different parts of the area under investigation. As seen in Fig. 23(b) and (c), dark fields of spots A and C separate out two martensite plates which are in $[1\bar{1}1]$ and [001] orientation, respectively. The dark field micrograph at spot B, however, also includes part of the reflection from spot A (due to the limited aperture size). When these areas are separated, the austenite lying between the two martensite plates M_1 and M_2, is seen to reverse in contrast. Reflection B is from the austenite (γ) having orientation $[1\bar{1}0]$, and it is seen from the diffraction pattern

that the [110] axis for both M_1 and M_2 is parallel to the [111] axis of the austenite. This is one of the orientation relationships expected from a Bain transformation and has been reported in some of the Fe-Ni martensites.[22] Sometimes areas showing only one martensite and one austenite orientation could be observed (Fig. 24), which satisfied the relationship $[110]_M \parallel [111]_\gamma$ within 3°. From these observations, it is not possible to arrive at the general orientation relationships as have been reported in other examples of martensitic transformations.[22,28]

Unlike unausformed steels the structure of martensites after 30% ausforming showed very little twinning. In some cases no evidence for twinning was found, while in others, very few areas were twinned, i.e. Fig. 25 for steel 1398 (Mo). Twinning is also present in the austenite of this steel (after 30% deformation, Fig. 11). As steel 1398 had a very low Ms, most of the structure in this case was retained austenite containing a heavy density of dislocations and precipitates. The retained austenite also showed mechanical twins in a few areas of steel 1398 (Fig. 26). Figure 27 shows similar examples of twinned martensite in steels 1410 and 1541. In <u>all</u> cases the twin plane in martensite is one of the {112} variants and dislocations and precipitates are always present in the martensites.

The effect of slight beam heating during microscopy observation of martensite was also investigated. It was found that, in general, beam heating produced no visible effects on the size of the precipitates or distribution of dislocations in the three 30% ausformed alloy steels.

The behavior of 30% ausformed steel 1410 was different, and as

mentioned in describing martensites from 8% deformed austenites, precipitation of cementite was observed. Figure 28 shows the martensites with precipitates and dislocations after slight beam heating. On heating a little longer, the precipitates grow in size and give rise to a Widmanstätten structure, as observed in Fig. 29(b). The cementite precipitates lie on $(1\bar{1}2)$ and $(1\bar{2}1)$ planes, i.e. the twin planes, the foil being in approximately [115] orientation. Figure 30 shows bright and dark field images from steel 1410 deformed at 100°C, and the diffraction pattern with its analysis is given in Fig. 31. This pattern clearly verifies that the precipitates are cementite, as well as affording the following orientation relationships:

$$\begin{aligned} [211]_\alpha &\parallel [001]_{Fe_3C} \\ [0\bar{1}1]_\alpha &\parallel [100]_{Fe_3C} \\ [1\bar{1}\bar{1}]_\alpha &\parallel [010]_{Fe_3C} \end{aligned} \qquad (1)$$

Besides the above (1), there is another orientating relationship[29] reported for cementite which is as follows:

$$\begin{aligned} (013)_{Fe_3C} &\parallel (011)_\alpha \\ [010]_{Fe_3C} &\parallel [111]_\alpha \end{aligned} \qquad (2)$$

The present results clearly establish that the valid relationship is as given in relations (1) above.

C. Summary of Observations on Austenites

1. The dislocations lie along the traces of slip planes up to at least 8% deformation. This would probably continue to be so with further deformation unless precipitation takes place.

2. A critical amount of deformation is necessary to nucleate observable precipitates. The results suggest that in all the four steels examined this critical value lies between 8 and 30% deformation.

3. The deformation substructure consists of tangles of dislocations with precipitates after 30% deformation.

4. The precipitates are found to be Fe_3C (for steel 1410), VC (for steel 1402), and MoC (for steel 1398). The precipitates in the case of Cr steel (steel 1541) could not be uniquely identified but are probably $Cr_{23}C_6$.

5. In the case of alloy steels it was not possible to reduce the dislocation density or increase the size of precipitates by slight beam heating of thick areas, but thin areas near the edges polygonized.

6. In the case of Mo steel (1398), some mechanical twinning in austenite was observed after 30% deformation. This effect has not been reported previously.

7. The dark field technique has been shown to be of considerable significance in studying important substructures like precipitates, twinning, etc.

D. Summary of Observations on Martensites

1. As for the austenites, martensites from 0 and 8% deformed steels show no precipitation, while those of 30% deformed steels show precipitation.

2. The amount of transformation twinning decreases as the extent of deformation increases, until after 30% ausforming very little twinning is observed.

3. Retained austenite from 30% ausformed steels show precipitation and a very high density of dislocations.

4. Ausformed steel 1410 is found to be most susceptible to low temperature tempering in the microscope with rapid growth of Fe_3C precipitates. Ausformed alloy steels resist tempering, in that the precipitates do not grow appreciably and the dislocation density does not drop.

5. No generalizations can be made regarding the influence of temperature or change of size of the martensite plates, after various ausforming treatments.

IV. DISCUSSION

A. Precipitation in Austenite

The experimental observations have shown that precipitation of carbides in austenite takes place in ausformed steels after a certain deformation. Previous workers have shown [7,18] by thermodynamic arguments that the diffusivity for the various alloying elements involved is favorable for such a precipitation. In almost all investigations of precipitation on substructures in iron base alloys (reviewed by Keh et al.[30]), a high density of dislocation favors formation of fine precipitates, probably because dislocations provide a high density of nucleation sites, and/or that diffusion is increased as a result of the high concentration of vacancies which are generated during plastic deformation. The absence of precipitation in steels deformed 8% or less and the comparatively lower mechanical properties of such steels suggest that precipitation is favored by large deformations. The difficulty of precipitation is thus probably one of nucleation since when precipitation takes place on closely spaced nucleation sites, the volume of material in the matrix from which precipitating constituents can diffuse to a site is limited. Thus, nuclei, in order to grow, will have to redissolve and diffuse to other sites. This process is likely to occur only on tempering at high temperatures. In the absence of any tempering effect, the higher the amount of deformation, the greater are the number of nucleation sites possible, and this means that precipitates are finer and more

closely spaced. Both these favor high mechanical strength as has been observed.[3]

It is likely that some tempering takes place in the microscope during observation. It should be emphasized, however, that all the specimens in the electron microscopes are examined under identical conditions and, therefore, if precipitation occurred by beam heating alone, specimens deformed 0 and 8% would have also shown evidence for precipitation. Since this is not found, it is concluded that the precipitation observed is essentially deformation dependent. The size and separation of precipitates is therefore dependent on the temperature and degree of deformation and subsequent tempering. After precipitates have reached their maximum size, no further change can take place, unless the steel is subjected to a temperature high enough to redissolve some of the precipitates so that others can grow.

The observations also show that precipitates are retained by martensite during the phase transformation. The effect of tempering on growing precipitates should be more rapid in the case of martensite than in the case of austenite, because the solubility of carbon in martensite is lower. Precipitation is also observed in Ni-steel (steel 1410), but this steel does not have as high mechanical properties as the other ausformed steels. In this steel (1410), the precipitates produced by deformation are cementite. From the tempering behavior of conventional steels, containing noncarbide-forming elements, it is known that cementite particles grow easily and this is accompanied by a deterioration of tensile strength during the early stages of the

tempering process. It is also observed in the present case, that cementite precipitates grow easily (Figs. 17 and 29), and that purposely heating the foils in the microscope causes rapid growth into a Widmanstätten pattern. It is therefore suggested that the comparatively poor properties of steel 1410 are due to the ease with which precipitates can grow.

Similar experiments in the microscope on the other steels showed no evidence for growth of precipitates. This result is attributed to the fact that the temperature was not high enough to favor growth. Indeed, this is confirmed by the observed tempering behavior of ausformed steels where the mechanical properties are maintained to a temperature as high as 500°C.[13]

B. Retained Austenite and Effect of Deformation on Martensite

The retained austenite observed in ausformed martensites contains a high density of dislocations, which represents a contribution from the austenite to martensite transformation as well as the dislocations inherited from the deformed austenite. It was not possible to arrive at any quantitative calculations of dislocation density for deformed austenites or martensites because the density was very high. It is estimated that the latter is certainly about $10^{12}/cm^2$ or higher.

The amount of retained austenite observed in 30% deformed ausformed steels is larger compared to the retained austenite of undeformed steels. This is explained by Thomas et al.[18] on the basis that the propagation of martensite nuclei is hindered by the presence of high density of dislocations and carbide particles in the path of the growing nuclei.

The martensite plates, in general, had no uniform shape or size as can be seen by the various micrographs (Figs. 19, 21, 24). Some of the areas (e.g. Figs. 20, 23) showed martensite plates side by side, while others did not (Fig. 19). This is possibly dependent on the reasons given earlier and also the fact that the growth of martensite plates may be stopped at times by other martensite plates.

From the analysis of various diffraction patterns (as is obvious from the micrographs also), it was found that martensites of varying orientations were present, and that the relationship of austenite orientation to martensite orientation could not be generalized in the case of deformed specimens. It was always found, however, that one of the $[111]_A$ was nearly parallel to one of the $[110]_M$, even though the same region may contain martensites of two or more orientations (Figs. 22, 23, 24).

The substructure of ausformed martensites, i.e. the presence of high density of dislocations and absence of twinning is believed to be responsible for the higher ductility of ausformed steels compared to normally treated steels.[31] The high density of dislocations prevents the nucleation of cracks by slip. Twinning in body centered structures is known to be an important cause of fracture.[32] From its almost complete absence in ausformed steels examined in this investigation, it would seem that the decreased amount of twinning is of considerable importance for enhanced ductility of ausformed steels.

C. Twinning

In this section only the factors influencing the presence of

twinning in ausformed steels will be considered. The electron diffraction patterns from twinned regions and their crystallographic aspects are explained in Appendix II.

The experimental observations clearly show that the extent of transformation twinning in martensites decreases with increasing amount of deformation of the metastable austenite prior to transformation. It is very likely that twins may be entirely absent for greater deformations.

The factors known to affect transformation twinning in martensite are:

1. There is more twinning the higher the carbon[14] and/or nickel[16] contents. As both these elements lower the Ms temperature of steel, this means that a low Ms temperature favors twinning. This is to be expected since in most metals (Cu for example[33]), low temperature favors mechanical twinning. The important factor must be the temperature dependence of the critical resolved shear stress for slip or twinning.
2. All alloying elements in steels except Co are known to lower the Ms and thus should favor twinning.
3. Little is known about the effect of stacking fault energy on the transformation substructure, though Kelly and Nutting[27] postulated that twinning is favored by high stacking fault energy of the austenites. This agrees with the observation of twinning by Swann and Speich[16] in Fe-Ni steels, as Ni is known to raise the stacking fault energy of austenite. However, from work on face centered cubic metals[26,33], it is expected that the lower the stacking fault energy, the higher is the tendency to twin. This would suggest that with regard to trans-

formation twinning, the effect of solutes on Ms is more important than their effects on stacking fault energy.

The present results show clearly that increasing deformation of austenite opposes twinning. This can be due to the effect of deformation and the associated precipitation of carbides which dilute the solid solution; both these factors are known to raise Ms. All the solutes examined in the present case (e.g. V*, Cr, and Mo) are known to lower the stacking fault energy.[34,35,36] Their depletion by precipitation should, therefore, raise the stacking fault energy and favor twinning according to Kelly and Nutting.[27] Since this was not so, it further shows that Ms temperature rather than stacking fault energy of the austenites is the important factor in determining twinning.

It is also worth noting that transformation twinning occurs in body centered martensite and since the body centered structures in general have high stacking fault energy, the latter parameter cannot be very important in steels which undergo the martensitic transformation. No observation of faulted martensites have been made in steels whereas Cu-Al alloys of low stacking fault energy undergo the lattice invariant shear by propagation of faults.[37]

In the present work twinning was also observed in a few cases of mechanically deformed austenites and retained austenites (see Figs. 11 and 26). This effect can be explained on the basis of stacking fault energy alone. While there are no accurate measurements of the stacking fault energies of the alloys examined here, Mo is known to strongly lower the stacking fault energy of austenite.[35] As mentioned previously

*No data are available on effect of V on stacking fault energy of austenites, but observations on effect of other solutes suggest that V also lowers the stacking fault energy.

for fcc metals, therefore, this low stacking fault energy favors deformation by twinning. In the areas showing twinning, the stacking fault energy may be still lower because of local segregation.

Since the removal of alloying elements from solid solution by precipitation would raise the stacking fault energy and hence oppose twinning in austenite, it would indirectly seem (from the observation of precipitates within the twins in austenites, e.g. Figs. 11 and 26), that precipitation cannot take place concurrently with deformation of austenite, at least in the early stages. This is supported by the observations of serrated yielding of austenite during tensile tests.[18] Furthermore, no large precipitates were observed, even in steels deformed at 500°C. If the precipitation had taken place side by side or preceding the deformation, there would be at least some particles which would have been of comparatively large size or at least there would be a broad range or precipitate sizes observed. The observations (Figs. 5, 6, 18) seem to suggest that this is not so, and that it may be that the nucleation starts during the later stages of deformation, with slow growth occurring with the passage of time. This is similar to strain aging, with possibly the aging taking place in a short time. As the martensites observed in this work were not obtained by quenching immediately after deformation, but the quenching was done at a later time, aging could have taken place in the time before quenching. So far there is no experimental evidence to suggest this kind of aging phenomenon, but the observations of substructure and serrated yielding[18] would indicate such a possibility.

D. Strength of Ausformed Steels

In this section the observation of substructure will be related to strength. Neglecting the inherent lattice friction stress τ_o, and solid solution strengthening due to substitutional alloying elements, as they are comparatively small, there are five main factors which are important in strengthening. Substructural observations of the present work suggest the following about each of these five factors:

1. Martensitic Grain Size

Although optical metallographic examination of ausformed steels indicates a decrease in martensitic grain size with ausforming, when individual martensite plates are examined in the electron microscope, no such trend is apparent. In fact, martensite grain sizes (i.e. width of plates) were observed from as small as 300Å (some of the martensites in Fig. 28) to a few microns and greater (e.g. as in Fig. 25, which shows a single plate). This work would therefore clearly indicate that there is no systematic variation of martensite plate size with ausforming, so that it is difficult to correlate grain size with strengthening. In view of other overriding parameters to be discussed in the following, it is felt that this contribution is small.

2. Twinning

As already discussed in Section IV-C, the almost complete absence of twinning in 30% ausformed steels would eliminate twinning as a factor in strengthening of ausformed steels. However, the absence of twinning is favorable to ductility.

3. Carbon Content

Carbon is the most important factor in strengthening of conventional

martensites, the strength levels achieved vary from 80,000 psi for 0%C to 280,000 psi for 0.8%C.[12] In the present case, the base composition had a carbon content of 0.3%. However, since ausforming results in precipitation of alloy carbides, carbon is depleted from the solid solution. The amount of carbon remaining in solution would be dependent on the amount of carbide forming element present, and on the extent to which precipitation has progressed (i.e. depending on the amount of deformation and temperature). In steel 1398, for example, MoC precipitates prior to the transformation. A simple calculation shows that the ratio of atomic percentages of carbon to molybdenum is 1:2, and thus, the probability of carbon remaining in solution is small. Similarly, for steel 1402 in which VC precipitates the amount of vanadium is nearly 1.5 times that which would be required to use up all of the carbon as VC. These considerations would suggest that the effect of carbon in solution must be small. Furthermore, in practice, steels are subsequently tempered, so that almost all of the carbon would be removed from solid solution.

4. Precipitation

From the structural observations, dislocations and precipitates are the dominant features and thus presumably control the strength. Their contribution, however, is related in the sense that creation of dislocations and accompanying point defects aid in precipitation, while creation of precipitates aid in increasing the dislocation density by pinning the dislocations and by providing sites for dislocation multiplication. To be beneficial in strengthening, the precipitate

particles should be strong enough to resist shearing. Kelly and Nicholson[38] have shown that the critical size, r_c, of a particle which would resist shearing is given by $r_c = \frac{2G\ b^2}{\pi\gamma}$ where G is shear modulus, b the Burger's vector, γ is dependent on the values of shear modulus G' and Burger's vector b' for the particle. They derive a value of $r_c = 2b$ for $G' = 10G$ and $b' = b$ and $r_c = 20b$ for $G' = G$ and $b' = b$. As the particle size in the present case is higher than these values (though no data for G' of carbides are available, they are in the range of G – 5G) e.g., from Fig. 18(a) the carbide size of 50 - 150Å is obtained, it is unlikely that carbides will be sheared by dislocations. Since the values of G' and b' for carbides are not available, Thomas et al.[18] proposed that γ may be related to the bond energies of the carbides. Their calculations also show that carbides are unlikely to be sheared.

The strengthening due to carbides, if considered alone, will be essentially of an Orowan type. However, the material is already in a work hardened state due to the presence of a high density of dislocations. Thus, the engineering yield strength is really a flow stress measurement which will not depend on the particle-particle spacing, but rather on the total dislocation density. The contribution to strength of the particles must therefore be accounted for, not on the basis of Orowan yielding, but rather on their effect on the total dislocation density. This is considered in the next section.

5. Dislocation Density

The substructural observations of ausformed steels on both austenites and martensite clearly indicate an increase in dislocation density with

prior deformation of austenite. The total dislocation density is the sum of contributions from the effects of deformation, dislocation multiplication at the precipitates, and dislocations generated during the phase transformation. Although it is not possible to measure the dislocation density accurately from the observations of thin foils, the maximum value in a crystal cannot exceed 10^{16} lines/cm^2. The structure is essentially work hardened and using the usual relationship for flow stress τ,[39] and neglecting the friction stress, $\tau = \beta G b \sqrt{N}$, where β is a constant $\simeq 1/4$, G is the shear modulus, b $\simeq$ Burger's vector of the dislocation and N the dislocation density. In general, for plastically deformed metals, N has been observed to range from 10^{10} to 10^{12} lines/cm^2.[39] In dispersion strengthened materials, provided the second phase is not cut by dislocations, the dislocation multiplication rate is greater than in the absence of dispersoids because of dislocation-particle interactions. Previous work has estimated that the rate is increased by about a factor of five.[40-42] This would give a dislocation content of ausformed martensite of about 10^{13} lines/cm^2, which is consistent with estimates from the micrographs.

Putting this number into the flow stress equation, τ is of the order of G/50. For steels G = 12 x 10^6 psi so the strength is calculated to be about 240,000 psi. The maximum strength for the alloy steels is 210,000 psi. The agreement is close enough to state that the high strength of ausformed martensite is primarily due to the high dislocation density.

E. Parameters of Ausforming

From substructural observations alone, it was not possible to determine any influence of temperature of ausforming, as has also been reported.[8] The substructural differences between ausformed steels containing carbide forming alloying elements and steel 1410 were not found to be large. Precipitation of Fe_3C in ausformed 1410 increases the strength slightly over conventionally treated 1410. However, the tendency for growth of Fe_3C with tempering rapidly causes a deterioration in strength. The difference between carbide forming alloying elements on the dislocation density and size and distribution of precipitates could not be established by substructural investigation alone, though Thomas et al., using thermodynamical considerations have shown that Mo is most beneficial and Cr least, which is in agreement with the mechanical property measurements.[18] From the slight tempering work done in the microscope, it seems that the alloy steels are little affected, though systematic tempering experiments may be necessary to arrive at the full importance of this parameter.

In future studies it would be difficult from the observed substructural changes alone to correlate carbon content, total alloy composition or austenitizing temperature and their influence on dislocation density or size and distribution of precipitates. However, the presence or absence of twinning is easily recognized by electron microscopy.

The carbon content is of considerable practical importance. On the basis of the present work, one of the roles of deformation is established as causing precipitation. Theoretically therefore, for a given size and distribution of precipitation desired, one can calculate

the amount of carbon required, e.g. for MoC precipitation, say average precipitate particles of 50Å diameter, uniformly distributed at 100Å separation, would require theoretically 1.75% Mo and 0.22%C. It would thus seem that in an alloy of say 3% Mo, a carbon content of 0.3% would be enough for MoC precipitation. Whatever excess carbon is present in solid solution will be an added benefit in solid solution strengthening but its limitations should be pointed out, too. A higher percentage of carbon gives rise to poorer ductility and more retained austenite. Also, greater stresses will be required for the ausforming deformation.

A higher percentage of carbon would tend to give internally twinned martensite plates, and this should adversely effect the ductility. One can apply similar theoretical considerations in selection of substitutional alloying elements. The solid solution strengthening from these is probably small, unless the stacking fault energy is changed appreciably.[16] One function of solutes is to cause a favorable Ms and a bay region in the TTT diagram for the process to be carried out at appropriate temperatures and for sufficient times without transformation. Secondly, enough of the most beneficial carbide formers (those which will diffuse easily and whose precipitates will not be sheared under stress) should be present. Some of the alloying elements will have to be controlled on the basis of other specific properties of steels, e.g. weldability, corrosion resistance, etc., and they are not considered here.

Most alloying elements which could be beneficial in ausforming are also those which lower Ms and consequently favor transformation twinning

in martensite. In addition, as observed in the present case for steel 1398, a large addition of a particular alloying element may lower the stacking fault energy of austenite and favor mechanical twinning during deformation. A large addition of alloying elements may also lower the M_f temperature such that large amounts of retained austenite may be obtained.

F. Control of Properties

In this section, in the light of previous and present observations, possible ways of achieving the highest possible engineering strength (i.e., high U.T.S. and desirable ductility) will be discussed.

Obtaining higher strengths would require that as many barriers to dislocation motion be provided as possible, without introducing other substructures such as twinning which might impair the ductility. As shown in the present work, two effective barriers to dislocation motion are the high density of dislocations and precipitates.

As mentioned previously, the strengthening due to the dislocations is given by $\tau = \beta\ G\ b \sqrt{N}$ (page 34). The maximum value N can have is $\simeq 10^{16}$, in which case strengths of the order of G will be obtained. Since the theoretical strength limit is G/15, the maximum dislocation density will be $\simeq 10^{14}$. However, in these cases little or no plastic flow can be expected. Even so, there is a limit to the possible dislocation density obtainable by static deformation, though , conventional ausforming static deformation induces precipitation and so provides more sites for dislocation multiplication. It is believed that explosive deformation as a means for substantially increasing

dislocation densities needs to be explored more, especially in the case of ausformed steels.

It is known that the dislocation density can be considerably increased with explosive deformation, e.g. by explosively deforming nickel, cell sizes of half those obtained by static deformation are obtained.[17] This would roughly double the dislocation density. As multiplication at precipitates increases the dislocation density by about a factor of 5, dislocation densities as high as those allowed by theoretical strength may be attained. However, it is known,[17,26] that explosive deformation can induce twinning in FCC metals after a particular value of pressure (depending on the technique of shock loading) is attained. This value of pressure has been shown to depend on the stacking fault energy of the Cu-Al FCC alloys.[26] In iron[43] explosive deformation has been shown to induce allotropic transformations at high pressures (170 kbar and higher). Thus, if the composition and pressure can be properly controlled so that occurrence of twinning and other phase changes are avoided, it will be interesting to see how much rise in dislocation density and strength can be obtained by shock loading ausformed steels in austenitic and martensitic states. The role of the precipitates in dislocation multiplication in this case should be interesting also.

Precipitates in alloys can be either already present (e.g. in dispersion hardened alloys) or later induced by some heat treatment (as in age hardening). If the particles do not deform, they control the yield strength by the Orowan relationship, i.e., $\tau = \frac{2Gb}{\ell}$, ℓ

being the particle-particle separation in the slip plane. However, in the present case, precipitation was induced by deformation, i.e. there are large numbers of dislocations and precipitates simultaneously built into the structure. In this case the role of precipitates in strengthening is through increasing the dislocation density. The precipitates may be deformable or undeformable. As shown by Kelly and Nicholson,[38] whether a precipitate is deformable or not depends on γ, the surface energy of the precipitate. It can be shown that γ is directly dependent on the bond energy of the precipitating phase, and thus the higher the bond energy, the stronger the particle in resisting shearing. For higher strengths then, stronger particles of small sizes would be more beneficial (where the size and distribution is controlled through composition and degree of deformation), than particles which would deform easily. However, easily deformable particles may give greater ductility by their deformation at the levels of the critical stress to shear these particles. By proper selection of these particles, i.e. by a study of the dependence of γ on bond strength, it should be possible to obtain materials with desirable ductilities at higher strength levels. It may also be possible to introduce some such deformable particles beforehand and then introduce dislocations through explosive deformation. A combination of various of these parameters should enable stronger and tougher materials to be made.

V. CONCLUSIONS

1. Precipitation is observed in all of the 30% ausformed steels in both austenitic and martensitic conditions. Precipitation is not observed in undeformed or 8% ausformed steels. It is shown that a critical amount of deformation is necessary to nucleate the precipitates, and that their growth rate is very small, unless the temperature is high enough to redissolve the precipitates.

2. The benefit of precipitates to properties is by providing sites for dislocation multiplication and by pinning the dislocations.

3. Carbon in steels is essential if ausforming is to improve properties. Solid solution strengthening due to carbon is small because of its removal due to precipitation of carbides. A high carbon content in solution is harmful to ductility, it increases the amount of retained austenite, and probably changes the desired microstructure from dislocated to twinned martensite.

4. The high strength of ausformed steels is primarily due to the very high dislocation density ($\sim 10^{13}/cm^2$). The total dislocation density includes contributions from deformation of austenite, multiplication at the precipitates, and from the invariant shear strain during the phase transformation.

5. Precipitates are also observed in ausformed Fe-28Ni-0.3C, but due to the ease with which cementite can grow, as compared to in other steels, its strength is inferior.

6. In conventional steels, transformation twinning during the martensitic reactions is favored primarily by the effect of solutes on the

Ms temperature of the steel. The rise of Ms, due to deformation and depletion of solutes by precipitation, consideraby decreases the extent of twinning in ausformed steels.

7. The absence of twinning and presence of a very high density of dislocations are favorable to ductility of ausformed steels.

8. Mechanical twinning was observed in austenites of some steels and is thought to be due to the effect of solutes on the stacking fault energy of austenite.

9. The selection of suitable carbide forming alloying elements and their amounts should depend on their diffusivity, their effects on stacking fault energy and Ms and M_f temperatures, besides considerations specific for a particular application.

10. To achieve still higher strengths, explosive deformation of ausformed steels as a means of increasing dislocation density may be used. For better ductility, at high strengths, explosively deformed dispersion hardened materials containing deformable dispersoids or ausformed steels of proper composition so as to result in deformable precipitates may be beneficial.

ACKNOWLEDGMENTS

The author is deeply grateful to Prof. G. Thomas for his personal guidance, encouragement and support during this research. Helpful discussions with Dr. V. F. Zackay are also acknowledged. Special thanks are due to the Ford Research Laboratory, through Mr. D. Schmatz, for kindly supplying the material used in this investigation. I wish to thank Mrs. Joan Forney for her special efforts in typing this thesis.

This work was done under the auspices of the U. S. Atomic Energy Commission through the Inorganic Materials Research Division of the Lawrence Radiation Laboratory.

APPENDIX I

The following is quoted from a letter from the Ford Laboratory[44] regarding the thermal mechanical treatment of steels used in this work. "The steels used were vacuum melted and vacuum cast in 25 lb. ingots. They were hot worked to a rough blank size at 1200°C. Prior to ausforming the steels were machined to various sizes such that each deformation would produce a finished flat sample 0.125 in. thick, 1.5 in. wide and about 8 in. long. The samples were re-solutioned at 1200°C or 1290°C* for 1 hour, air cooled to 500°C or 100°C and deformed 8 and 30% reduction in thickness, and water quenched. The samples were thinned by chemically polishing to 0.005 in. thick."

---

*Alloy 1402 was resolution heat treated at 1290°C.

APPENDIX II

Standard Projections and Analysis of Electron Diffraction Patterns from Twinned Regions

A. Standard Projection

All through this work, standard projections of different orientations were often needed, and as they are not readily available, each time they had to be drawn for future use. Some of these are included here. All standard projections drawn have been obtained by use of two zone laws, viz., (1) poles of planes belonging to the same zone lie on the same great circle, and (2) if (h_1, k_1, ℓ_1), and (h_2, k_2, ℓ_2) are indices of two planes belonging to a zone [uvw], all (H, K, L) planes whose indices are $H = mh_1 \pm nh_2$, $K = mk_1 \pm nk_2$ and $L = m\ell_1 \pm n\ell_2$, m and n being any integers, belong to the same zone. For example if in Fig. 48 (115 standard projection), the location of pole $0\bar{1}3$ is desired, it is seen that this pole lies on the great circle joining $\bar{1}\bar{1}2$ and 101 [as $\bar{1}\bar{1}2 + 101 = 0\bar{1}3$], and the great circle joining $0\bar{1}1$ and 001 [as $2 \times 001 + 0\bar{1}1 = 0\bar{1}3$]. Hence, the intersection of these two great circles gives the required pole. This method is more accurage than drawing angles, in which the measurement is limited by graduations on the Wulff net (e.g. only 2° graduations on a 20 cm net). Any other standard projection can be drawn this way. The projections included here are 001, 011, 111, 012, 112, 122, 013, 113, 023, 123, 223, 331, 332, 014, 114, 015 and 115 [Figs. 32 to 48]. In each projection all 001, 011, 111 and 112 poles are shown.

B. Twinning

Analyses of some electron diffraction patterns from twinned regions submitted in this work is explained here. The tetragonality of Fe-Ni-C martensite is so small[45] that it is not detectable within the accuracy of this work and hence the martensite is treated as bcc.

The analyses of electron diffraction patterns require the aid of stereographic projections, use of dark field technique, and at times, calculations from the transformation matrix arrived at in previous publications.[21] From the application of the matrix it is seen that (1) in fcc structures where twinning planes are {111}, the first two allowed spots of an electron diffraction pattern 111 and 200 would be superposed on spots as listed in Table III, and similarly (2) in bcc structures, where the twinning planes are {112}, the first two allowed spots 110 and 200 become coincident with those listed in Table III. To avoid fractions, poles like 333, 600, 330 have been used in the Table because when a spot like 111 transforms to $\frac{5}{3}\,\frac{1}{3}\,\frac{1}{3}$ by twinning, it means that a 333 spot becomes coincident with 511, similarly in the case of bcc a 411 spot shall coincide with 330. When analyzing the diffraction patterns, the first step (especially in cases such as the ones under consideration), is to establish whether the structure is fcc or bcc. This is easily done by the use of distance ratio tables obtained from camera constant equations and angle tables. Once this is done, fcc spots like 511 are watched for, e.g. in Fig. 26 (for austenite) where the orientation is between [001] and [015], $1\bar{5}1$ spot is present. It is expected that after twinning a 333 spot may coincide with $1\bar{5}1$, and

TABLE III

New Indices PQR of the Pole pqr After Twinning* on hkℓ for bcc and fcc Using the Relations-

$$P = -p + \frac{2h\,(hp + kq + \ell r)}{h^2 + k^2 + \ell^2}$$

$$Q = -q + \frac{2k\,(hp + kq + \ell r)}{h^2 + k^2 + \ell^2}$$

$$R = -r + \frac{2\ell\,(hp + kq + \ell r)}{h^2 + k^2 + \ell^2}$$

hkℓ → / pqr ↓	111	hkℓ → / pqr ↓	112
333	$\bar{3}\bar{3}\bar{3}$	330	$\bar{1}\bar{1}4$
		303	033
$33\bar{3}$	$\bar{1}\bar{1}5$	033	303
		$\bar{3}30$	$3\bar{3}0$
$3\bar{3}3$	$\bar{1}5\bar{1}$	$30\bar{3}$	$4\bar{1}1$
		$03\bar{3}$	$\bar{1}\bar{4}1$
$\bar{3}33$	$5\bar{1}\bar{1}$	600	$\bar{4}24$
		060	$2\bar{4}4$
600	$\bar{2}44$	006	442
060	$4\bar{2}4$		
006	$44\bar{2}$		

*Since the twinning has been treated as reflection about the twinning plane in stereograms and rotation about the twin axis in the Table, the two are related such that indices obtained by one are negative of the other [21] because in crystallography a twofold axis and a mirror plane normal to the axis also means a center of symmetry.

since in fcc the presence of a 333 spot would require the presence of a 111 spot, a 111 spot is seen near 020. Indeed, dark field work at this faint spot A changes contrast for the twins (Figs. 26(b)). From the stereogram (Fig. 49) it is easily verified that the twinning plane is (111).

Similarly, in Fig. 25(b) (which is from bcc) where orientation is $[\bar{1}\bar{1}3]$, a $4\bar{1}1$ spot is present. By twinning it is likely to coincide with a 330 twin spot, the exact value of which depends on the particular plane on which the twins lie. The presence of a 330 spot implies the presence of the 110 spot, and it is seen that such a spot is present, (Figs. 25(b)). Since in this case the twinning plane is established as (121), being perpendicular to the foil surface, no stereogram is required because the twinning can be treated by rotation along the twin axis (e.g. a line through origin perpendicular to 121). The extra spot present is therefore $(1\bar{1}0)_T$.

However, this might not always turn out to be so easy. Considering, for example, Fig. 13(from martensite) it is first established that the foil orientation is between [122] and [133], and $\bar{4}11$ spot is present. This suggests the possibility that this spot may coincide with 330 after twinning, in which case a 110 spot at 1/3 the distance will also show up. In this case, however, the exact twinning plane is not established without the stereographic analysis. From the stereogram in Fig. 50, it is seen that the twins lie on the $(12\bar{1})$ plane, and the $\bar{3}03$ spot is actually superposed on the $\bar{4}11$ spot. From the same stereogram it is also seen that the twins are discontinuous along the

trace of $(01\bar{1})$, the slip plane in this case. The dark field micrograph at the $(\bar{1}10)_T$ spot in Fig. 51 verifies this analysis.

The method described so far has been found to be applicable in most of the cases found in this work. Another example for twins in Fig. 16(b) shall be given. Figure 52(b) gives the diffraction pattern and Fig. 52(a) gives the dark field micrograph at spot A. It is easily found that the matrix is bcc with [115] orientation. By stereographic analysis, Fig. 53, the twinning plane is found to be $(\bar{1}21)$ so that after twinning the $41\bar{1}$ spot coincides with $(330)_T$, and the dark field work at $(110)_T$ spot which now shows up, reverses the contrast for the twins. It is also seen that the twins are discontinuous along the slip plane $(1\bar{1}0)$.

The analysis of electron diffraction patterns in which all the twin reflections superimpose on some of the matrix reflections has been described elsewhere[21] and will not be discussed here. Figure 11(d) is an example of the diffraction pattern anticipated there. It is verified by the stereographic analysis in Fig. 54.

This treatment of electron diffraction patterns from twinned crystals is by no means complete as the specific cases may have to be separately treated. However, the present analysis is shown as part of the experience gained during this work and to establish some starting procedures for analyzing such patterns.

References

1. V. Zackay and W. Justusson, in "High Strength Steels", Iron and Steel Institute Special Report 76, p. 14 (1962).

2. J. Shyne, V. Zackay and D. Schmatz, Trans. ASM, 52, 346 (1960).

3. W. M. Justusson and D. Schmatz, Trans. ASM, 55, 640 (1962).

4. R. Phillips and W. E. Duckworth, Proceedings 2nd International Symposium on High Strength Materials, Berkeley, (1964). (To be published).

5. C. M. Marshall, DMIC Report 192, Oct. 11 (1963).

6. S. Floreen and G. Tuffnell, Trans. ASM, 57, 301 (1964).

7. A. McEvily, R. Bush, F. Schaller, and D. Schmatz, Trans. ASM, 56, 753 (1963).

8. W. Gerberich, C. F. Martin and L. Raymond, Trans. ASM, 57, 324 (1964).

9. F. Schaller and D. Schmatz, Acta Met., 11, 1193 (1963).

10. G. Ansell and A. Arrott, Trans. AIME, 227, 1080 (1963).

11. W. E. Duckworth, P. R. Taylor and D. A. Leak, Journal of Iron and Steel Institute, 202, 135 (1964).

12. M. Cohen, Trans. AIME, 224, 638 (1962).

13. D. Schmatz, F. Schaller and V. Zackay, in "The Relation Between the Structure and Mechanical Properties of Metals", NPL Symposium 15, Her Majesty's Stationary Office, London (1963), p. 613.

14. P. M. Kelly and J. Nutting, Proc. Roy. Soc. London, Series A, 259, 45 (1961).

15. R. A. Grange and J. B. Mitchell, Met. Eng. Quart. 1, 41 (1961).

16. G. R. Speich and P. R. Swann, to be published in Journal of Iron and Steel Institute.

17. R. L. Nolder and G. Thomas, Acta Met., 12, 227 (1964).

18. G. Thomas, D. Schmatz and W. Gerberich, Proceedings 2nd International Symposium on High Strength Materials, Berkeley (1964). (To be published).

19. M. F. Ashby and L. M. Brown, Phil. Mag., 8, 1083 (1963); Phil. Mag. 8, 1649 (1963).

20. X-Ray Powder Data File, ASTM Special Technical Publication 48-M2; American Society for Testing Materials, Philadelphia, Pennsylvania (1963).

21. O. Johari and G. Thomas, Trans. AIME, 230, 597 (1964).

22. B. A. Bilby and J. W. Christian, The Mechanism of Phase Transformations in Metals (The Institute of Metals, London) (1956), p. 121.

23. R. L. Patterson and C. M. Wayman, Acta Met., 12, 1306 (1964).

24. K. Schimizu, J. Phys. Soc., Japan, 17, 508 (1962).

25. M. H. G. Wells, Acta Met., 12, 389 (1964).

26. O. Johari and G. Thomas, Acta Met., 12, 1153 (1964).

27. P. M. Kelly and J. Nutting, Journal of Iron and Steel Institute, 197, 199 (1961).

28. A. H. Geisler, Acta Met., 1, 260 (1953).

29. I. V. Isaichev, Zhurnal Technicheskoi Fiziki, 17, 835 (1947).

30. A. S. Keh, W. C. Leslie and G. R.Speich, paper presented at a symposium on The Role of Substructure in the Mechanical Behavior of Metals, at Orlando Air Force Base, Orlando, Florida (Dec. 1962).

31. A. S. Tetelman, discussion to the paper by Thomas et al., Proceedings 2nd International Symposium on High Strength Materials,

Berkeley, (1964). (To be published).

32. R. W. Armstrong, in Deformation Twinning, ed. by R. E. Reed-Hill, Gordon and Breach Publishers, New York (1964).

33. J. A. Venables, in Deformation Twinning, ed. by R. E. Reed-Hill, Gordon and Breach Publishers, New York (1964).

34. D. L. Douglas, G. Thomas and W. R. Roser, Corrosion, 20, No. 1, 15t (1964).

35. S. Barnartt, R. Stickler and D. Van Rooyen, Corrosion Science, 3, 9 (1963).

36. A. J. Goldman and C. N. J. Wagner, Acta Met., 11, 405 (1963).

37. P. R. Swann and H. Warlimont, Acta Met., 11, 511 (1963).

38. A. Kelly and R. B. Nicholson, Prog. Mat. Sci., 10, 149 (1963).

39. J. Friedel, Dislocations, Pergamon Press, New York, 1964.

40. L. I. Van Torne and G. Thomas, Acta Met., 11, 881 (1963).

41. J. B. Mitchell, S. K. Mitra and J. E. Dorn, Trans. ASM, 56, 236 (1963).

42. M. von Heimendahl and G. Thomas, Trans. AIME, 230, 1520 (1964).

43. W. L. Leslie, D. W. Stevens, and M. Cohen, Proceedings 2nd International Symposium on High Strength Materials, Berkeley, (1964). (To be published).

44. D. Schmatz, private communication.

45. P. G. Winchell and M. Cohen, Trans. ASM, 55, 347 (1962).

FIGURE CAPTIONS

1. Dislocations in undeformed austenite steel 1410 showing that some dislocations remain after austenitizing. In some areas, e.g., (b) a relatively high residual dislocation density is observed.
2. Residual dislocations in steel 1398 after austenitizing at 1200°C. The foil orientation is [111] and the dislocations lie along the {111} planes.
3. Dislocation substructures in 8% deformed austenites.
   (a) Steel 1410, the foil orientation is [123] and the dislocations again lie along the traces of the {111} planes.
   (b) Steel 1402, the foil orientation is [111], and as in Fig. 2, the dislocations lie on {111} planes.
   (c) Steel 1541. Clusters of dislocations, most of which are parallel to (111) or $(11\bar{1})$ plane, the orientation of the foil being [110].
4. Dislocations in austenite of steel 1398 after 30% deformation at 500°C showing random cell structure.
5. (a) Bright field micrograph of austenite in steel 1398, 30% deformed at 500°C. The substructure shows dislocation tangles and precipitates which are clearly seen in the dark field micrograph, (b) taken of the 111 spot A in the diffraction pattern, (c) notice the streaks near the 200 and $0\bar{2}\bar{2}$ spots in (c). The diffraction pattern is in $[01\bar{1}]$ orientation.

6. Steel 1398 as Fig. 5, showing dislocation substructures and precipitation in (a) bright field, and (b) dark field taken of spot A of diffraction pattern in (c). Notice the faint rings from carbides and increased intensity of these rings near matrix shots, e.g. near $\bar{2}00$, $\bar{2}20$, etc., the diffraction pattern being [001].
7. Austenite in steel 1398, 30% ausformed at 500°C, showing a bend contour in (a) bright field and (b) dark field. Since the dark field micrograph taken at spot A (in diffraction pattern (c)) also includes the streak near the spot 200, contrast reversal for precipitates is also obtained.
8. Dislocation cell substructures in austenites of 30% deformed (a) Cr steel (1541) and (b) V steel (1402). The dark field micrographs of these, as in Figs. 5 to 7 show similar contrast reversal for precipitates.
9. A very thin edge of 30% deformed 1398 steel after polygonization in the electron microscope due to slight beam heating. Precipitates are seen to reverse contrast when the dark field micrograph (b) is taken of A. The ring diffraction pattern in (c) proves that austenite is polygonized and the carbides are of random orientations. Notice that the precipitates here are larger compared to previous examples (Figs. 5 to 7). The precipitates are identified as MoC, (see Table II and text).
10. Polygonized area in a very thin foil of 30% deformed Cr-steel 1541. The dark field (b) is taken on a point A at the first ring of the diffraction pattern (d), while the dark field (c) is taken from inside this ring.

11. Mechanical twinning in austenite of steel 1398, deformed 30% at 100°C.

12. Mid-rib twinned structures in martensite of undeformed transformed steel 1410. The density of twins decreases outwards from the mid-rib.

13. Twinning in undeformed transformed steel 1398. Though the twinning is not apparent in (a), dark field at spot A shows presence of twinning in (b), which can be brought to better contrast by tilting as in (c) (bright field). The diffraction pattern in this case is between [122] and [133]. The twins lie on $(12\bar{1})$, while they are discontinuous along the $(01\bar{1})$ plane. See Appendix II for details of diffraction pattern analysis. The orientation after twinning becomes [001].

14. Two twinned structures in martensites of 8% ausformed 1410 steel. In Fig. (a), a dark field micrograph very clearly shows the discontinuity of the twins along a sharp direction which corresponds to the trace of the slip plane. The twin density is seen to decrease away from mid-rib. In (b) extensive twinning is shown in another region of the same steel. In both cases the twinning plane is $(112)_M$.

15. Martensitic structures in undeformed steel 1410. The size of the martensite plates in (a) are much smaller compared to that for 8% ausformed steel 1410 in Fig. 14(a), in which the mid-rib twinned structure actually continues for about four times the length shown here. Notice also the dislocation substructure of untwinned martensite in (b).

16. (a) Martensite of various plate sizes in 8% ausformed steel 1410, the plates are of varying sizes, though nearly regular in shape.

    (b) Twinned martensites and retained austenite in same steel, the twins lie along the $(\bar{1}21)_M$ plane in a matrix of [115] orientation and are again discontinuous along the slip plane $(\bar{1}10)$. Notice the smaller martensite plates (some of them only in weak contrast) at the left of the photographs.

17. (a) Cementite precipitation in 8% ausformed steel 1410 induced by tempering in the microscope. The cementite gives streaks in the diffraction pattern (b), which lie normal to their habit plane.

18. Precipitation in martensite of 30% ausformed steel 1402. The precipitates are not visible in bright field, but are clearly seen in the dark field micrograph (b). The precipitates are from 50 - 150Å in size, and about 150 - 250Å apart.

19. Retained austenite (γ) and martensite (M) in 30% ausformed steel 1402 showing precipitation and heavy dislocation density in both. Notice the nonuniform shape of martensite plates in dark field micrograph in (b).

20. Retained austenite and martensite in 30% ausformed steel 1541 showing a very high density of dislocation.

21. Martensite in 30% ausformed steel 1402. (a) some plates (e.g. M), show no dislocations in one orientation, but tilting, as in (b) reveals the dislocation substructure.

22. (a) Diffraction pattern from a martensitic-austenitic area in Fig. 23.

    (b) The analysis of Fig. 22(a).

23. 30% ausformed steel 1402, the circled area in (a), shows where the diffraction pattern in Fig. 22 was taken. (b), (c) and (d) are the dark field micrographs taken at spots A, C and B, respectively. Martensite plate M_1 changes contrast in (b) and M_2 in (c), while M_2 and (γ) are seen to change contrast in (d).

24. (a) Martensite and retained austenite in 30% ausformed steel 1541.

    (b) The diffraction pattern from the area circled in (a).

25. Twinning in martensite of a 30% ausformed steel 1398. The diffraction pattern in (b) is in $[\bar{1}\bar{1}3]$ orientation and the twins lie on a (121) plane, normal to the foil surface.

26. Twinning in retained austenite of 30% ausformed transformed steel 1398. The twins are seen clearly in dark field micrograph (b), taken of the $1\bar{1}1$ twin spot A. The diffraction pattern is between [001] and [015] orientations. Notice the streak near the 200 spot as observed in austenite (e.g. Figs. 5 to 7).

27. Transformation twinning in martensites of 30% ausformed steels (a) 1410 and (b) 1541. The twinning plane in both structures of $(112)_M$.

28. (a) Martensite after slight tempering in steel 1410 30% ausformed at 500°C.

    (b) In another area of the same foil, the precipitates at some places (e.g. A) have grown.

29. 30% ausformed and transformed steel 1410, after more tempering in

the microscope. The precipitates have grown considerably on preferential planes, (b) the continuation of the area in the left of micrograph in (a) area A being the same in both micrographs. The orientation of the micrograph in (b) in between [001] and [115] and the precipitates lie on traces on $(1\bar{1}2)$ and $(1\bar{2}1)$ planes.

30. Cementite precipitation by slight tempering in the microscope in steel 1410, ausformed 30% at 100°C.

31. Diffraction pattern from the circled area in Fig. 30. The orientation is $[211]_\alpha$ and [001] Fe_3C.

32. Standard 001 projection for cubic crystals.

33. Standard 011 projection for cubic crystals.

34. Standard 111 projection for cubic crystals.

35. Standard 012 projection for cubic crystals.

36. Standard 112 projection for cubic crystals.

37. Standard 122 projection for cubic crystals.

38. Standard 013 projection for cubic crystals.

39. Standard 113 projection for cubic crystals.

40. Standard 023 projection for cubic crystals.

41. Standard 123 projection for cubic crystals.

42. Standard 223 projection for cubic crystals.

43. Standard 331 projection for cubic crystals.

44. Standard 332 projection for cubic crystals.

45. Standard 014 projection for cubic crystals.

46. Standard 114 projection for cubic crystals.

47. Standard 015 projection for cubic crystals.

48. Standard 115 projection for cubic crystals.

49. Stereogram showing the analysis of diffraction pattern in Fig. 26.

50. Stereographic analysis of diffraction pattern in Fig. 13, showing the trace of twin plane and the trace of the plane along which twins are discontinuous.

51. Dark field micrograph of $(\bar{1}10)_T$ spot in Fig. 13(d) verifying the analysis described in text and Fig. 50.

52. (a) Dark field micrograph at spot A.

    (b) Selected area diffraction pattern for twinned area in Fig. 16(b).

53. 115 stereogram illustrating the analysis of diffraction pattern in Fig. 52(b). The twin plane and the trace of the plane of discontinuity of twins is also shown.

54. Stereographic analysis of the diffraction pattern in Fig. 11(d).

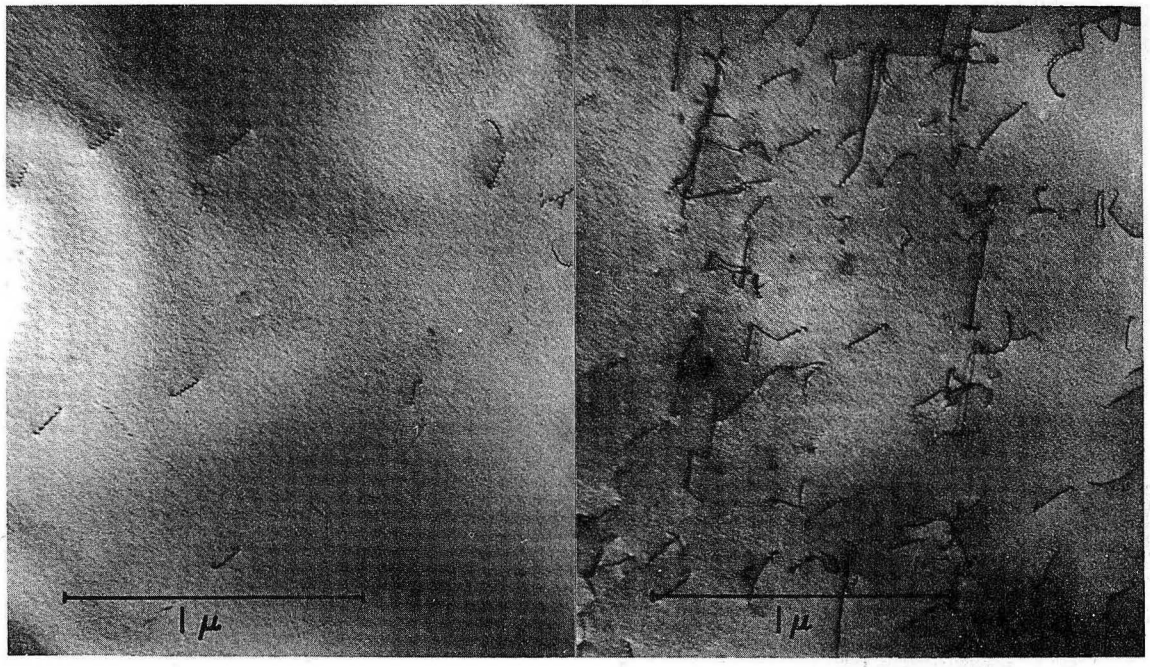

(a) (b)

ZN-4611

Fig. 1

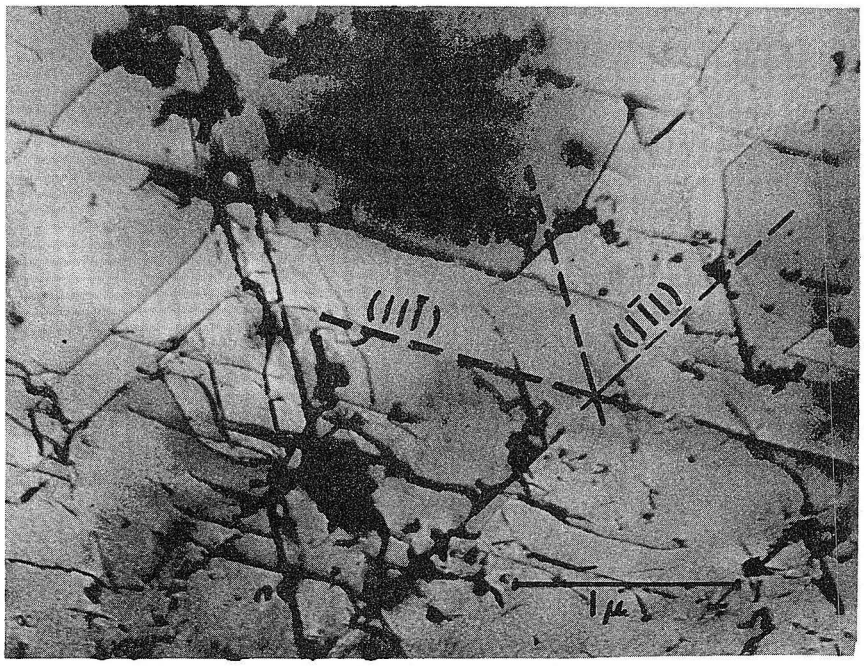

ZN-4612

Fig. 2

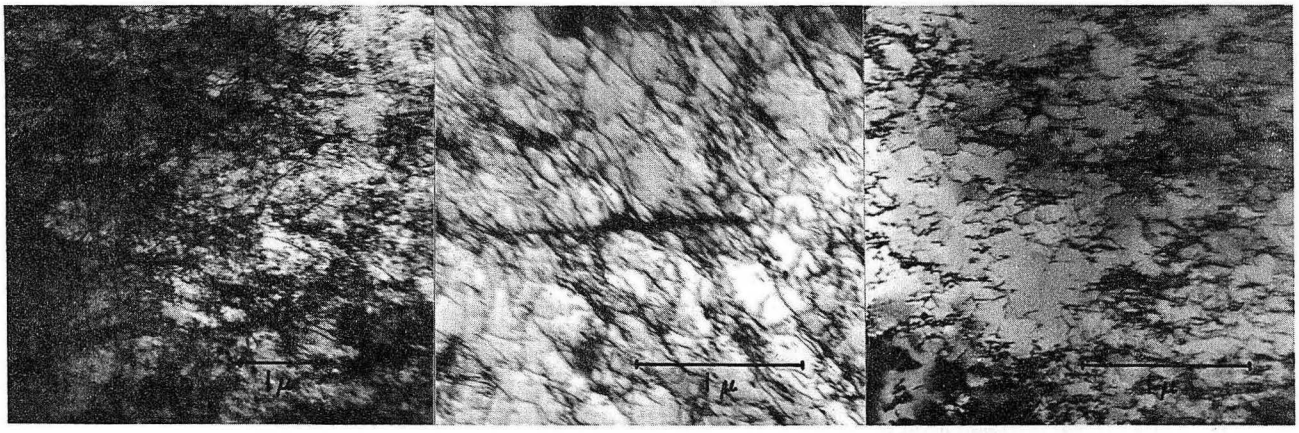

(a) (b) (c)

ZN-4613

Fig. 3

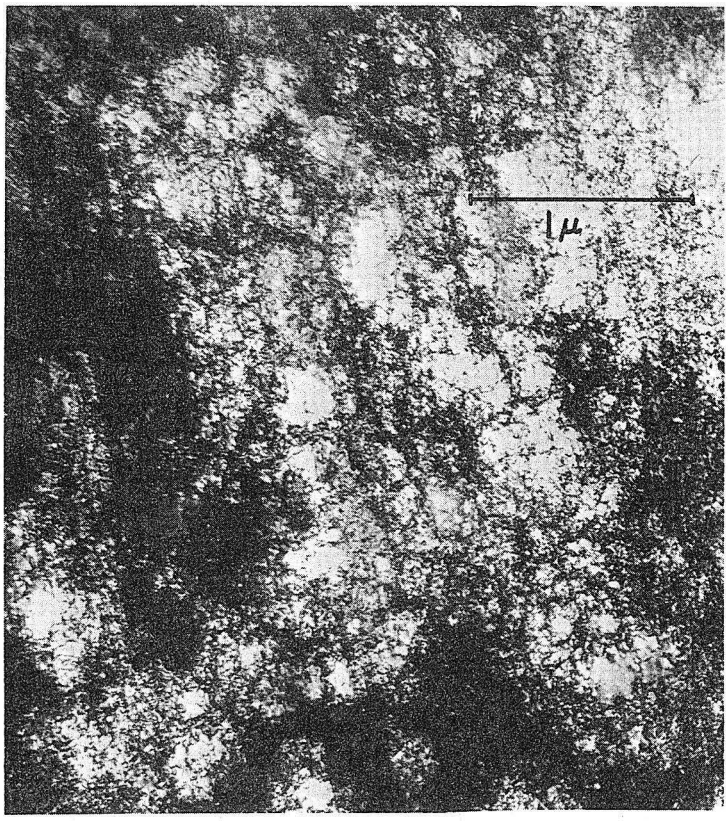

ZN-4614

Fig. 4

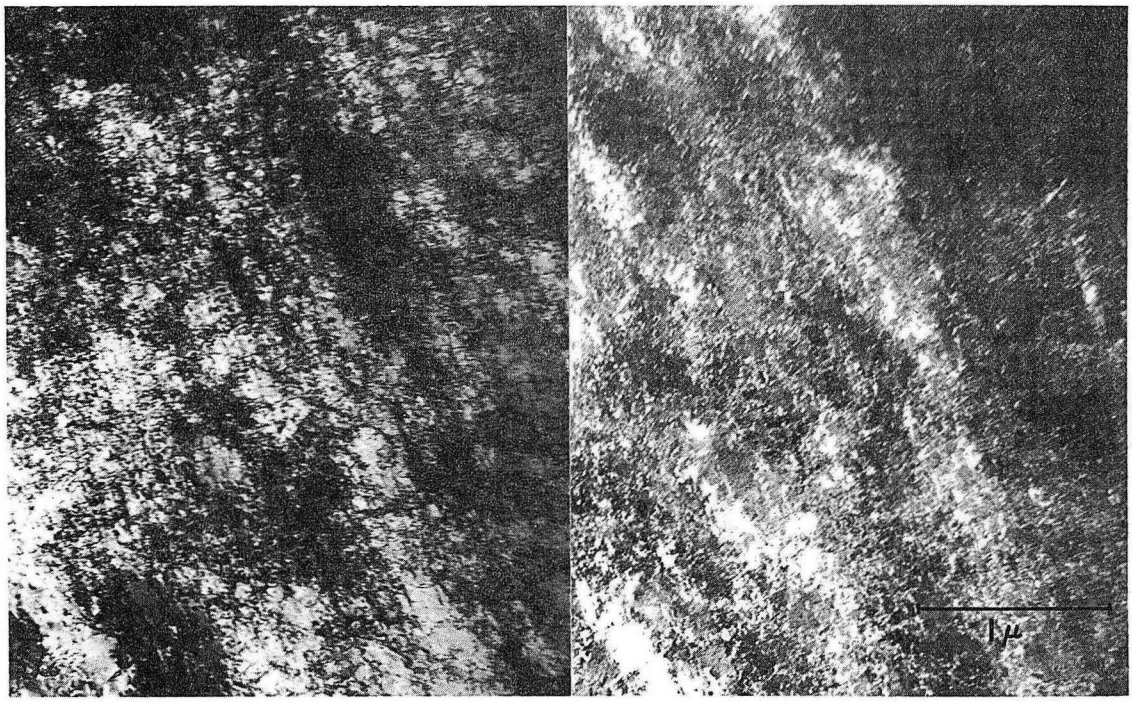

(a) (b)

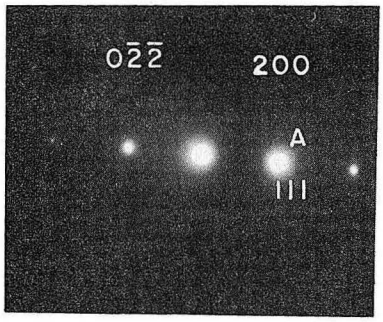

(c)

ZN-4615

Fig. 5

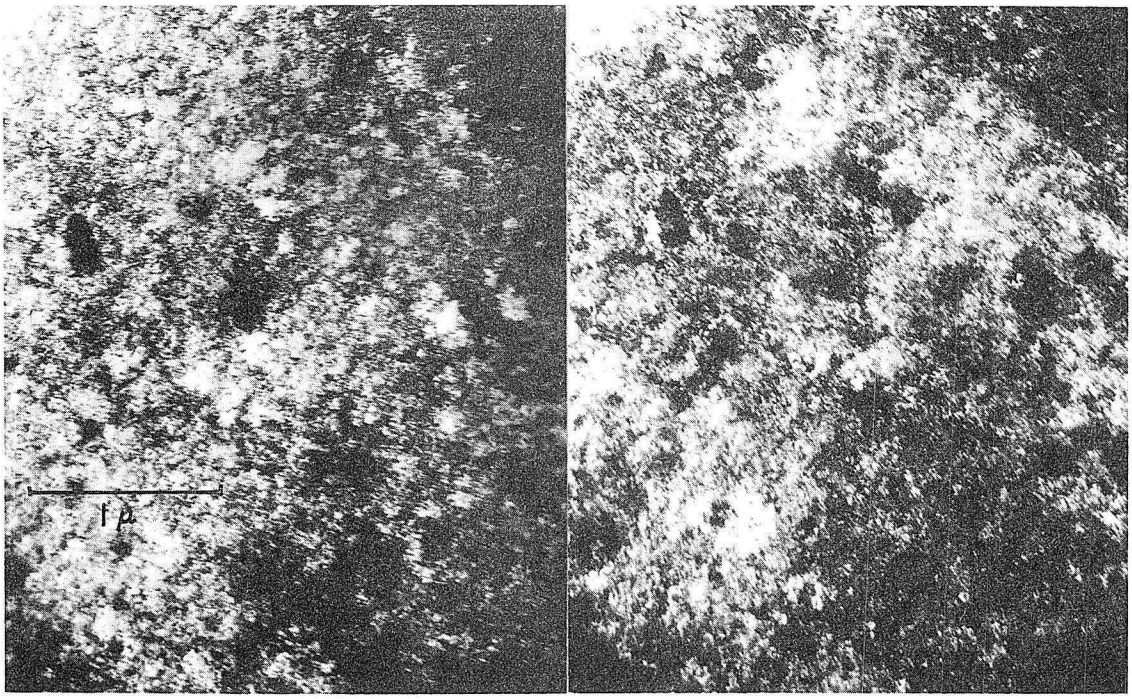

(a) (b)

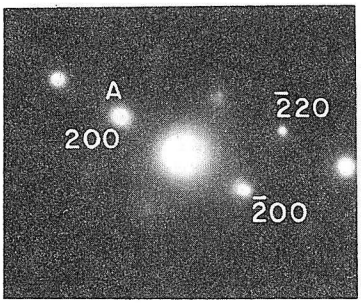

(c)

ZN-4616

Fig. 6

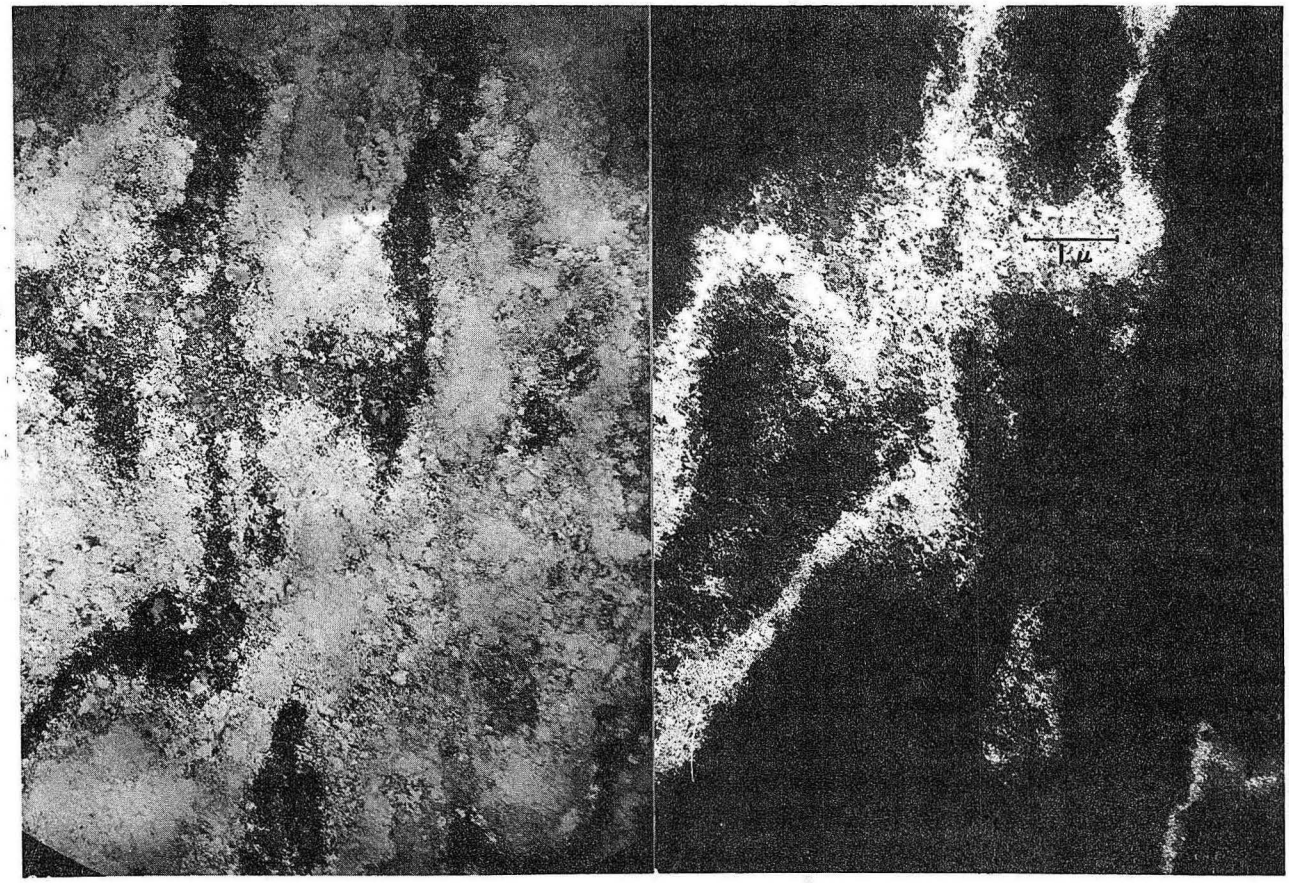

(a) (b)

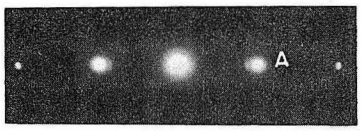

(c)

ZN-4617

Fig. 7

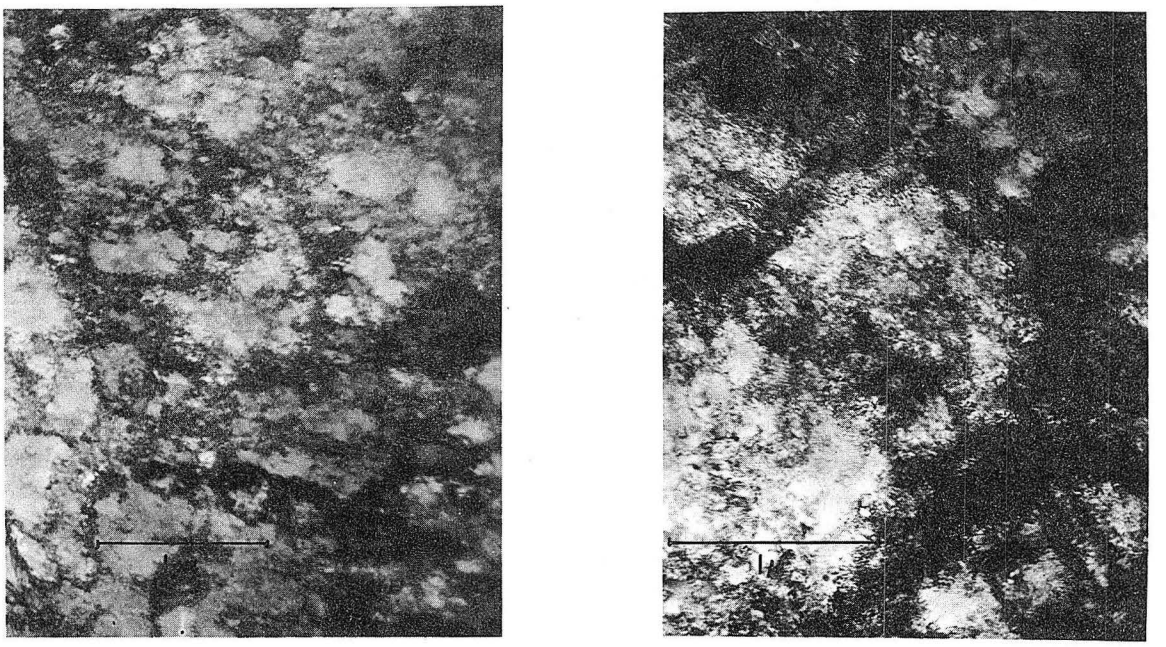

(a) (b)

ZN-4618

Fig. 8

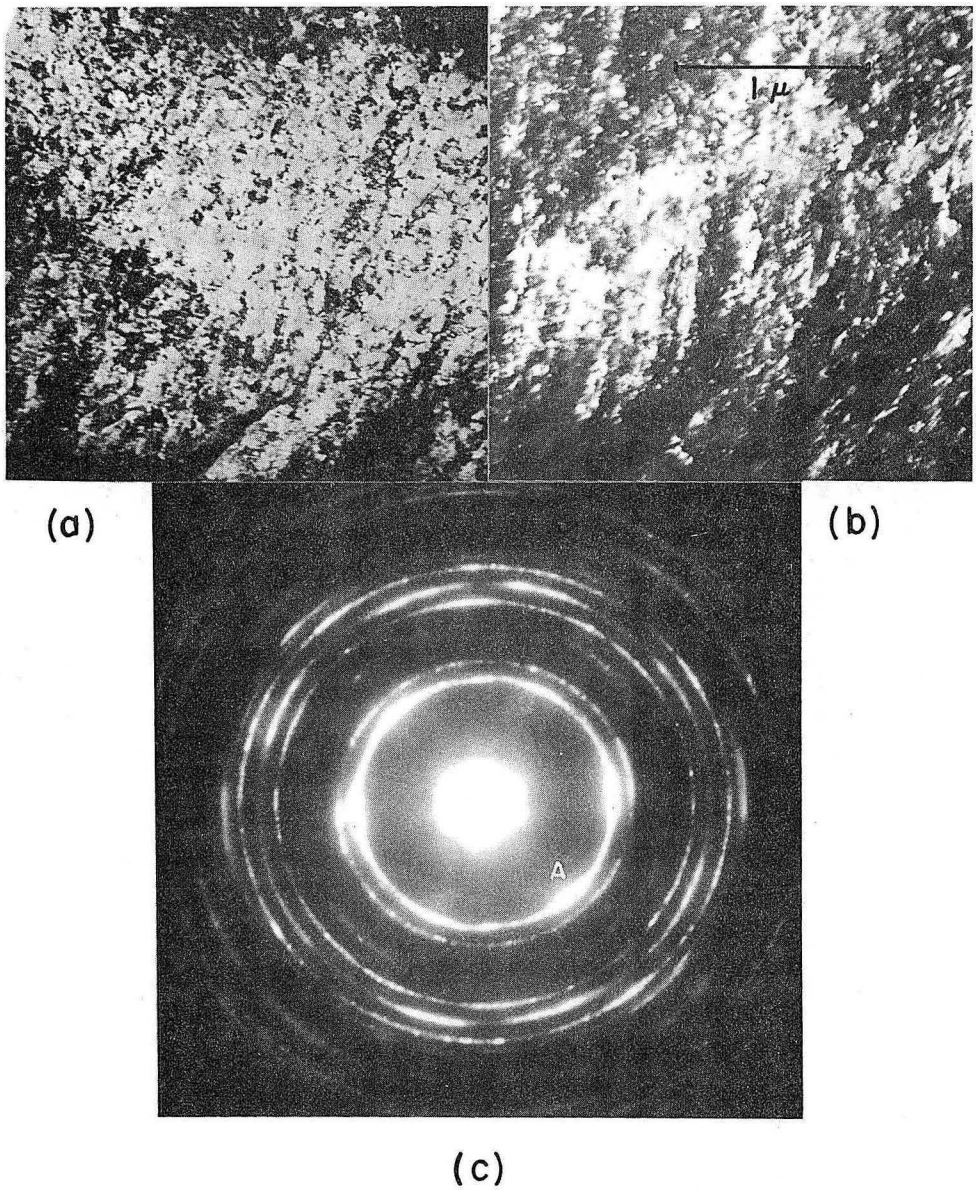

ZN-4619

Fig. 9

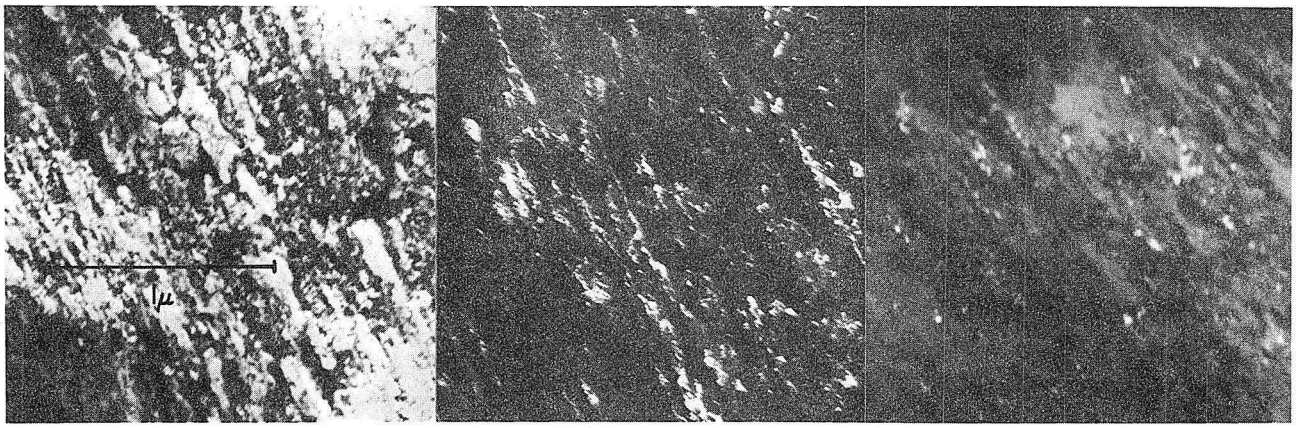

(a) (b) (c)

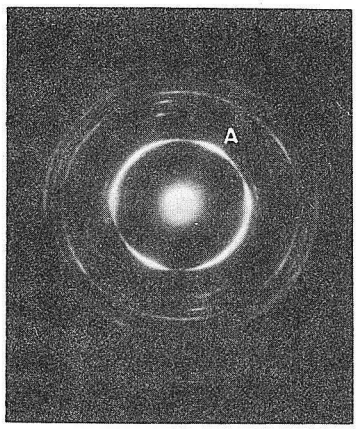

(d)

ZN-4620

Fig. 10

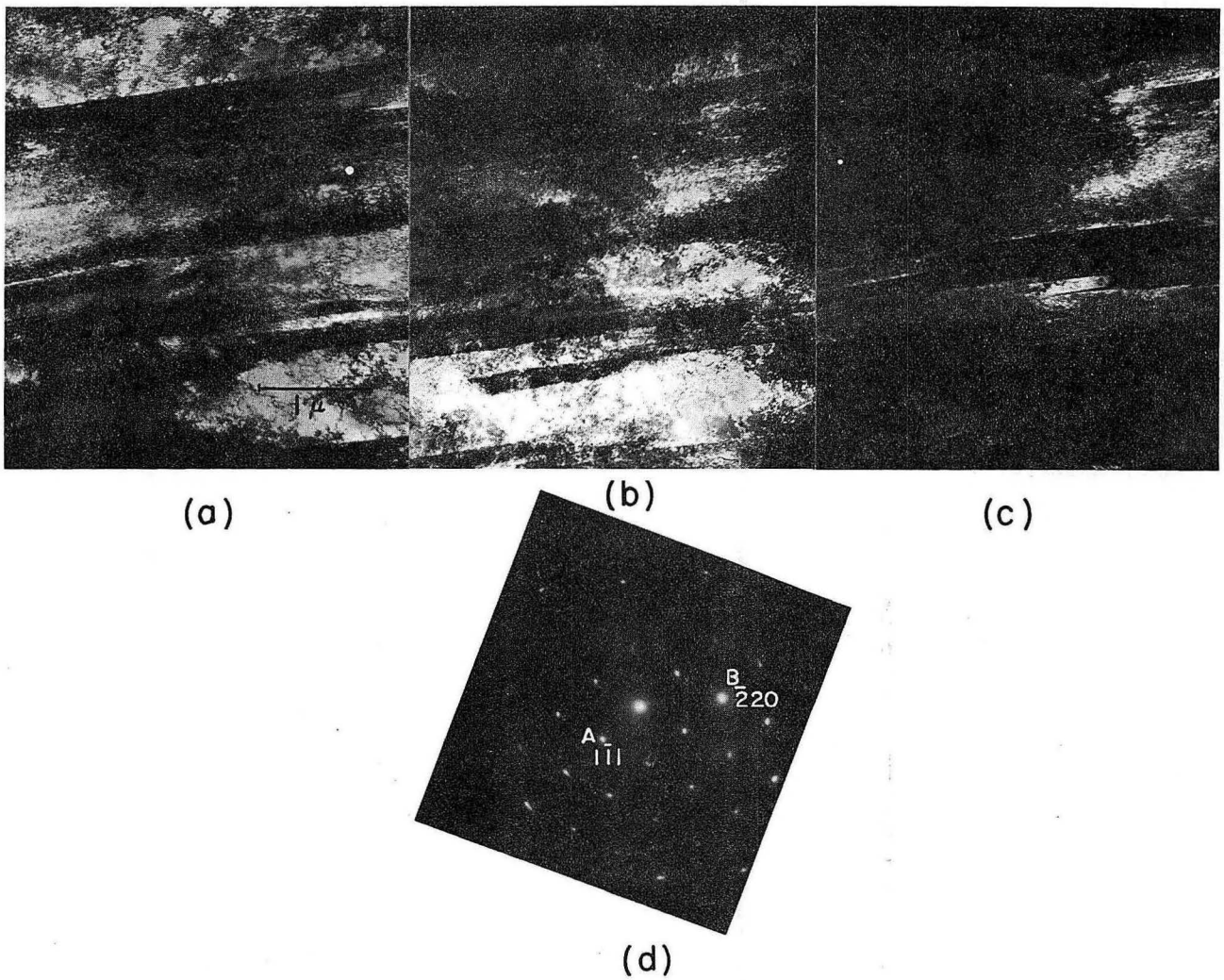

ZN-4621

Fig. 11

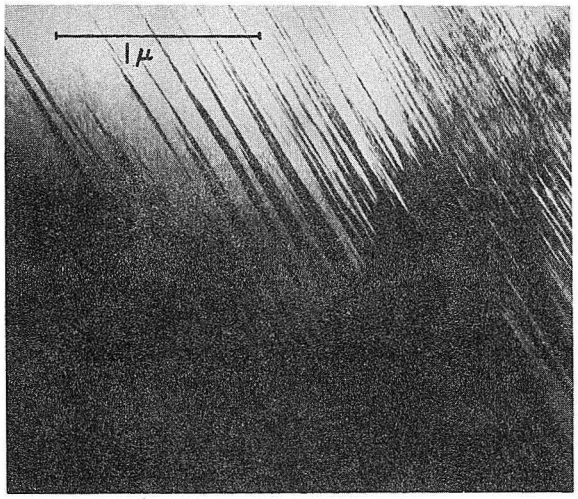

(a)

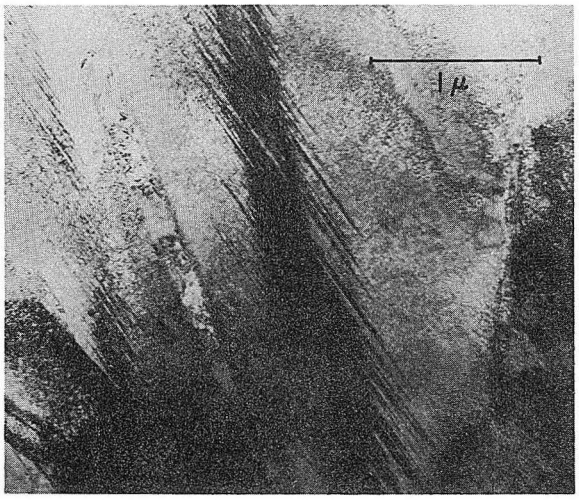

(b)

ZN-4622

Fig. 12

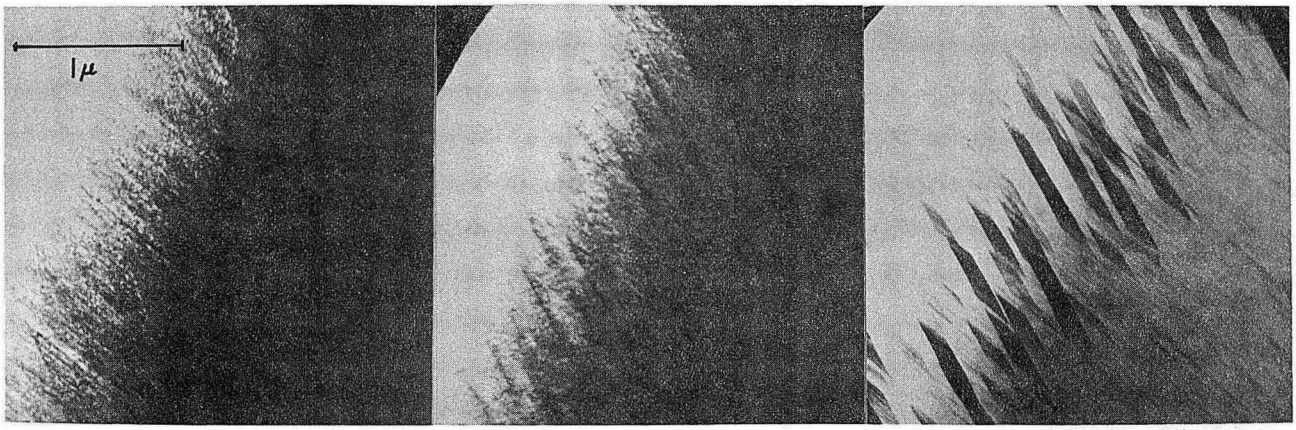

(a) (b) (c)

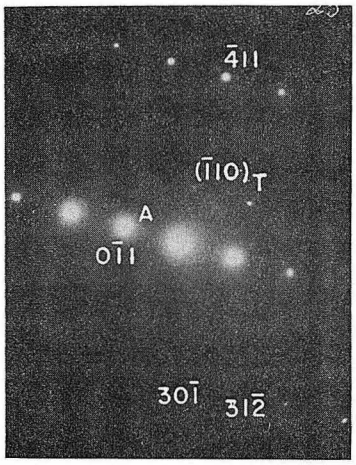

(d)

ZN-4623

Fig. 13

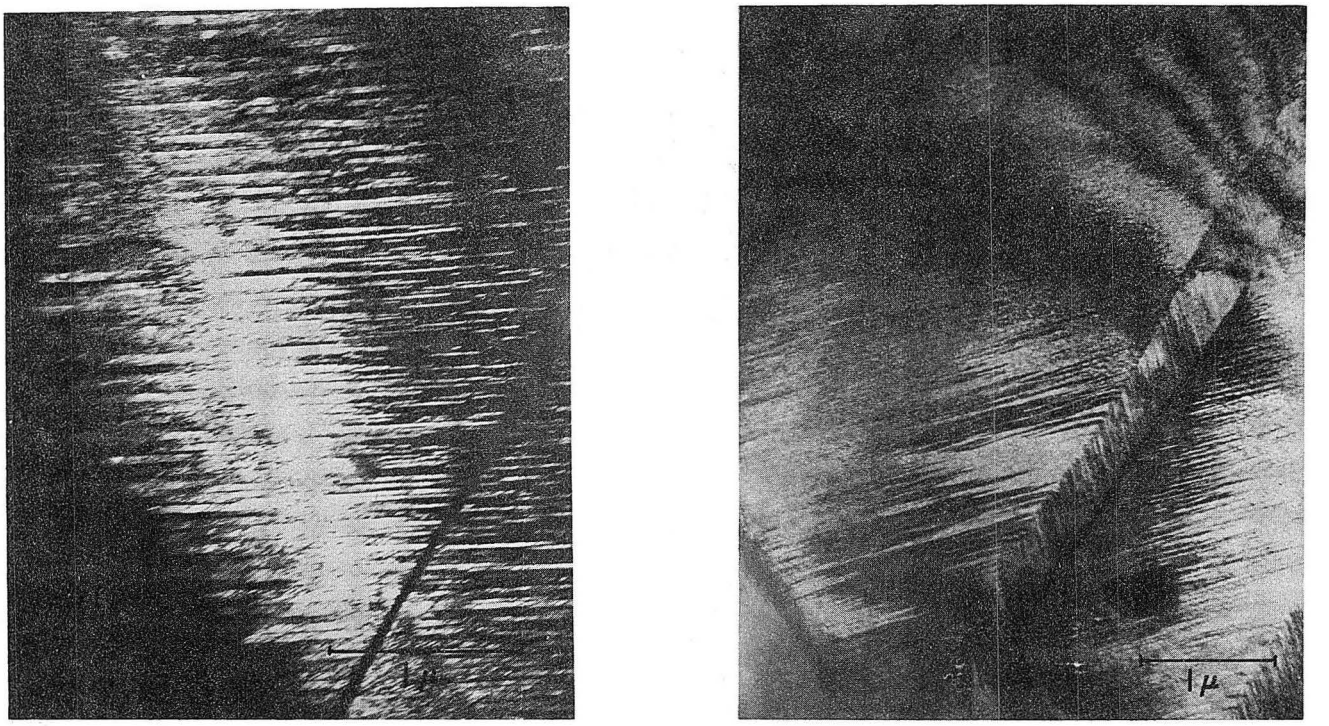

(a) (b)

ZN-4624

Fig. 14

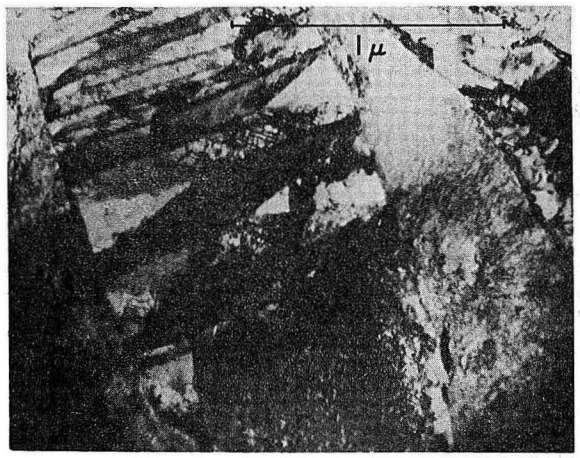

(a)

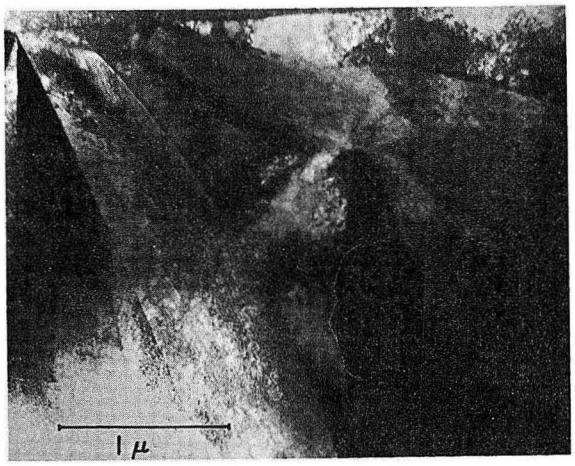

(b)

ZN-4625

Fig. 15

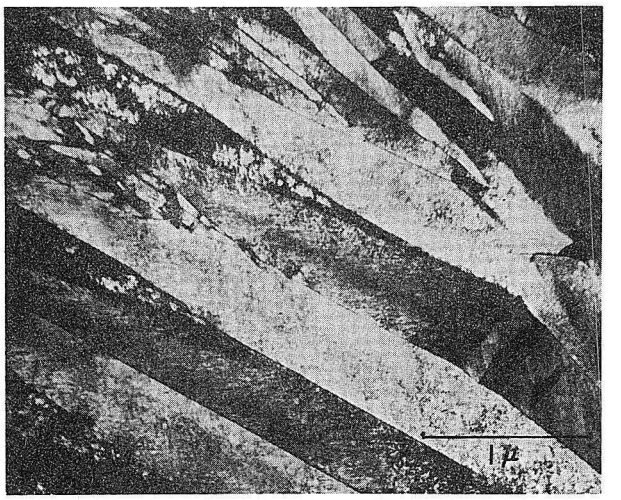

(a)

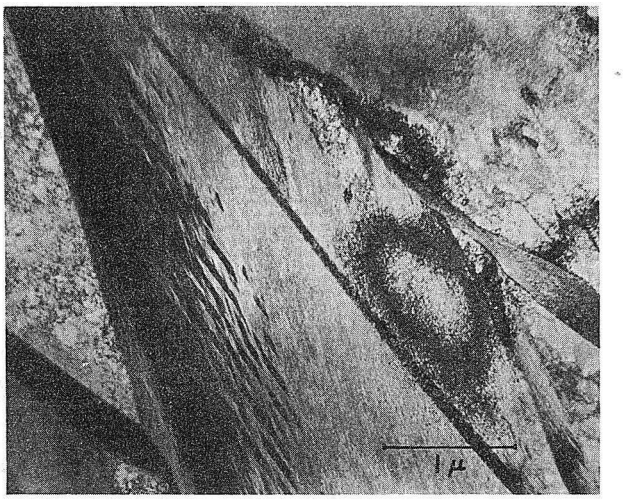

(b)

ZN-4626

Fig. 16

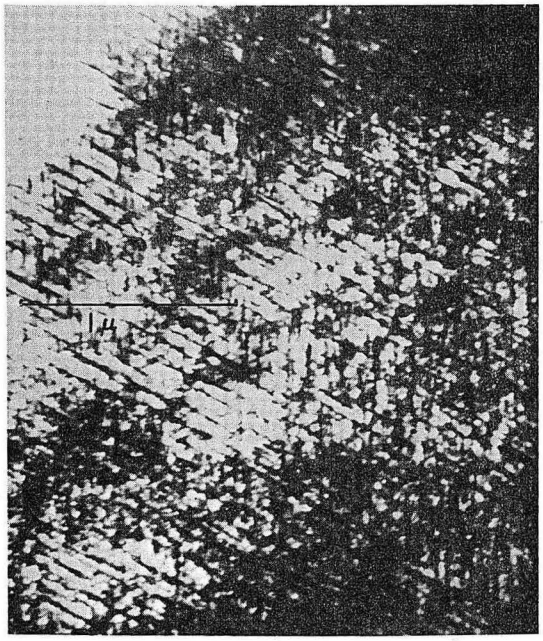

(a)

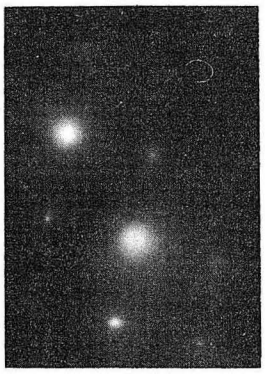

(b)

ZN-4627

Fig. 17

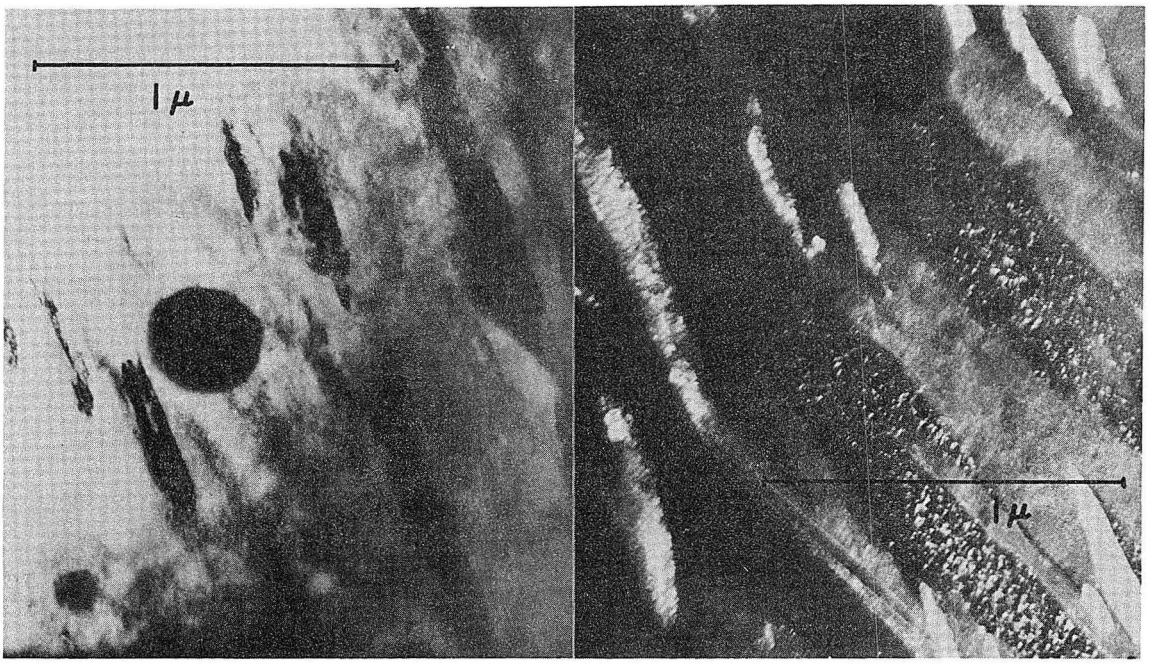

(a) (b)

ZN-4628

Fig. 18

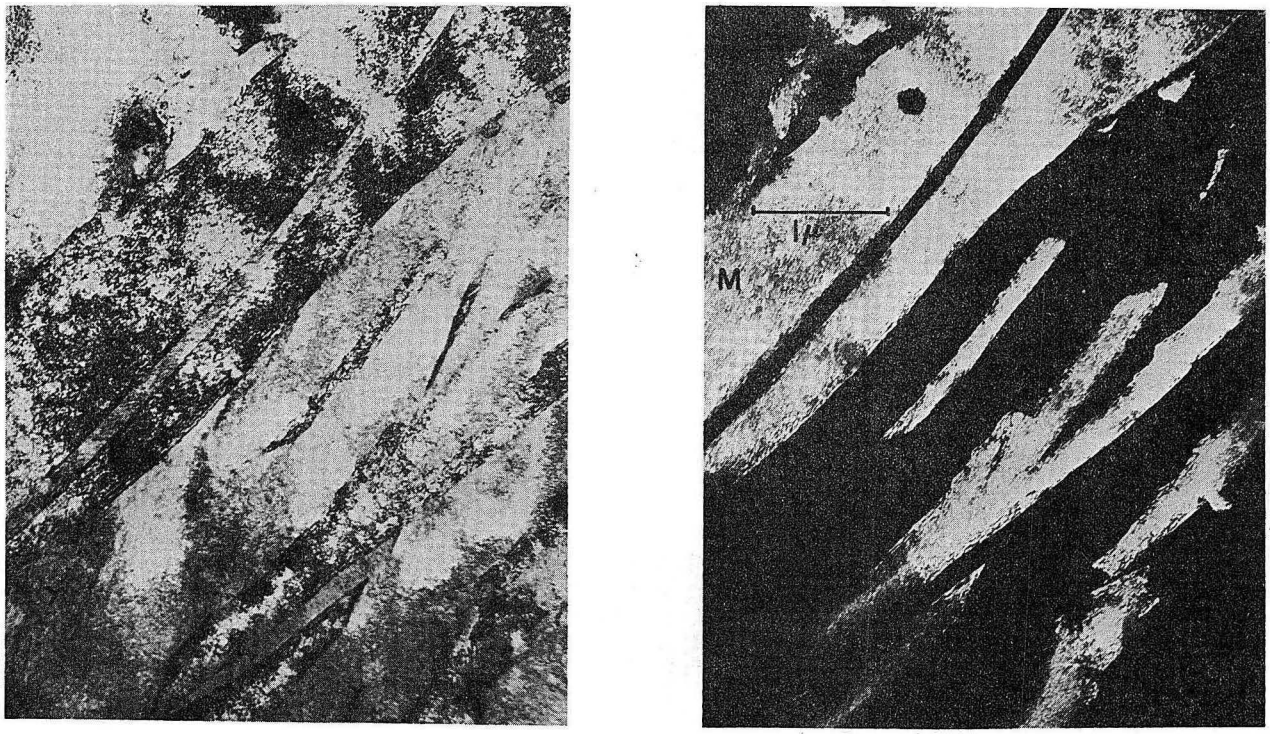

(a) (b)

ZN-4629

Fig. 19

ZN-4630

Fig. 20

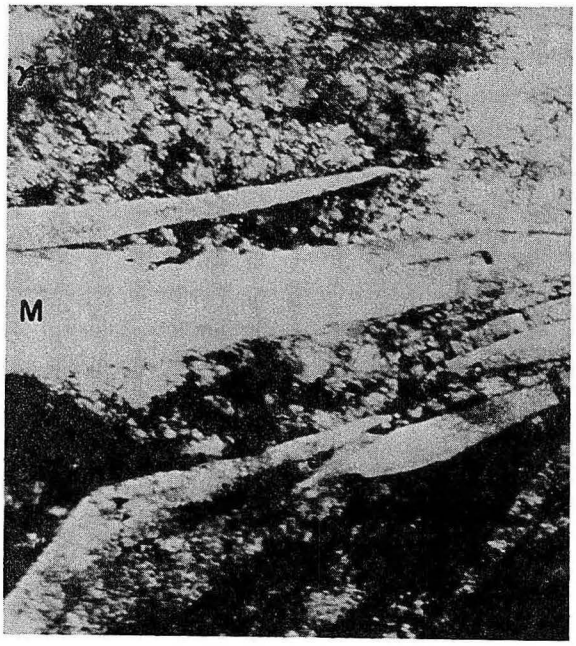

(a)

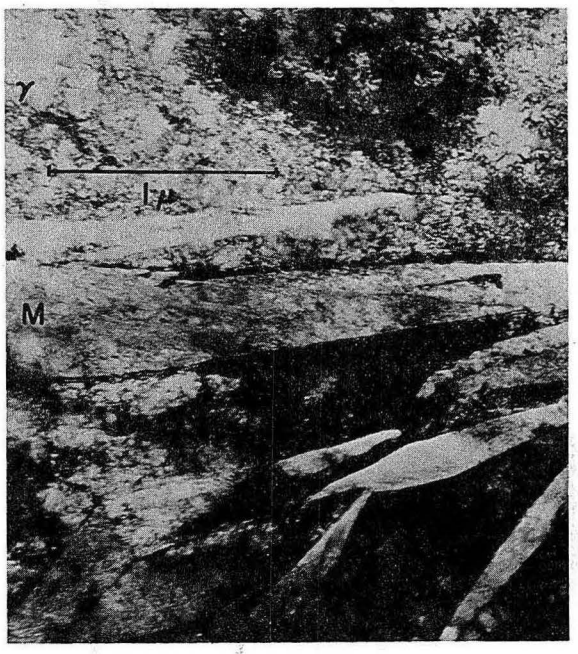

(b)

ZN-4631

Fig. 21

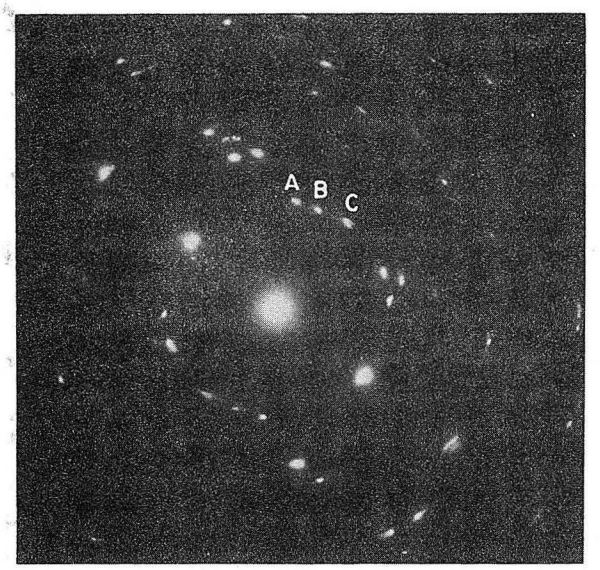

(a)

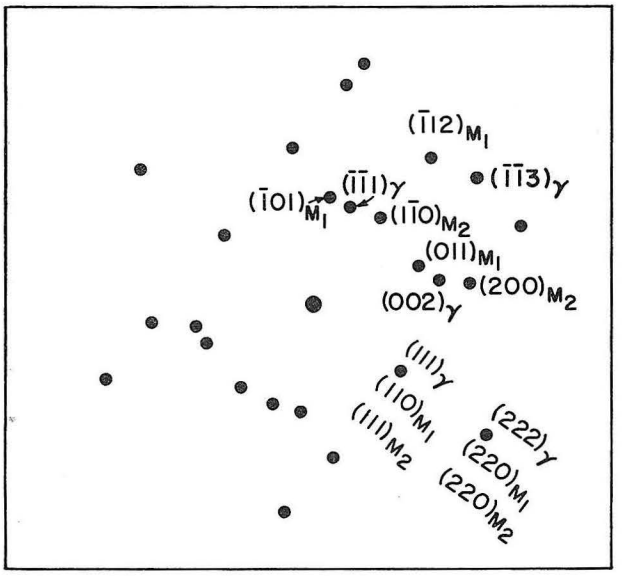

(b)

ZN-4632

Fig. 22

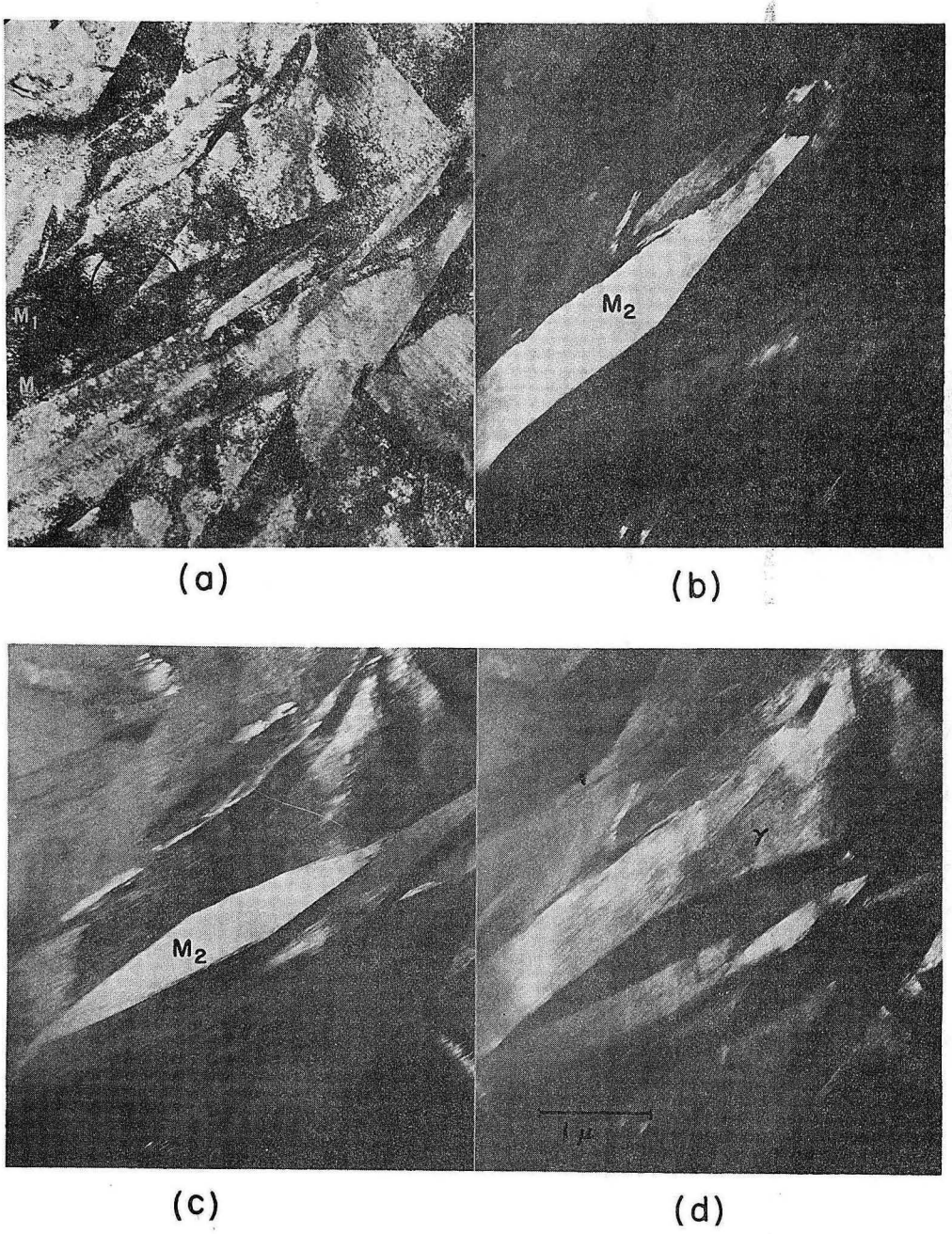

ZN-4633

Fig. 23

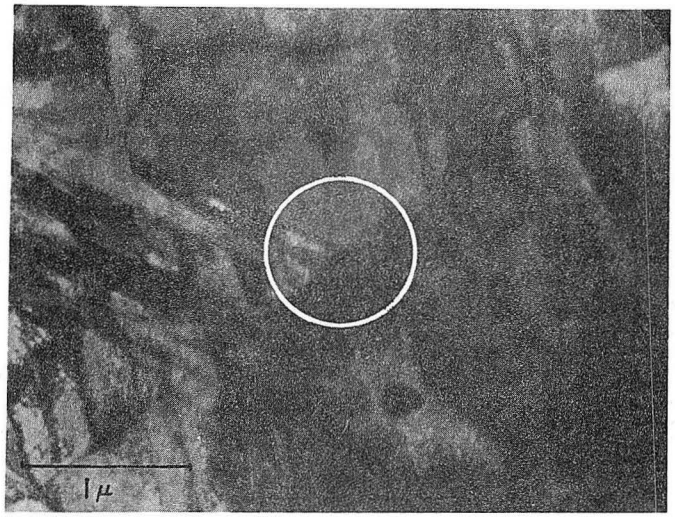

(a)

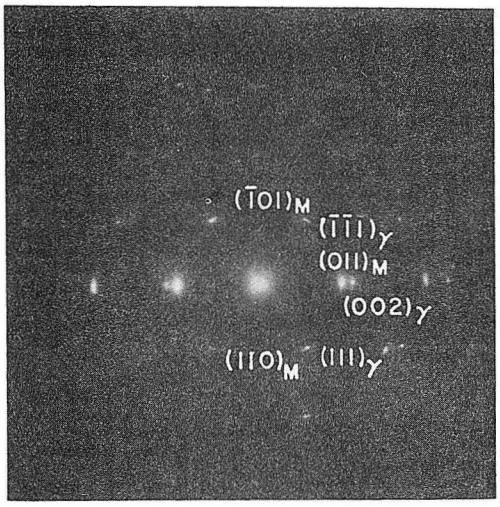

(b)

ZN-4634

Fig. 24

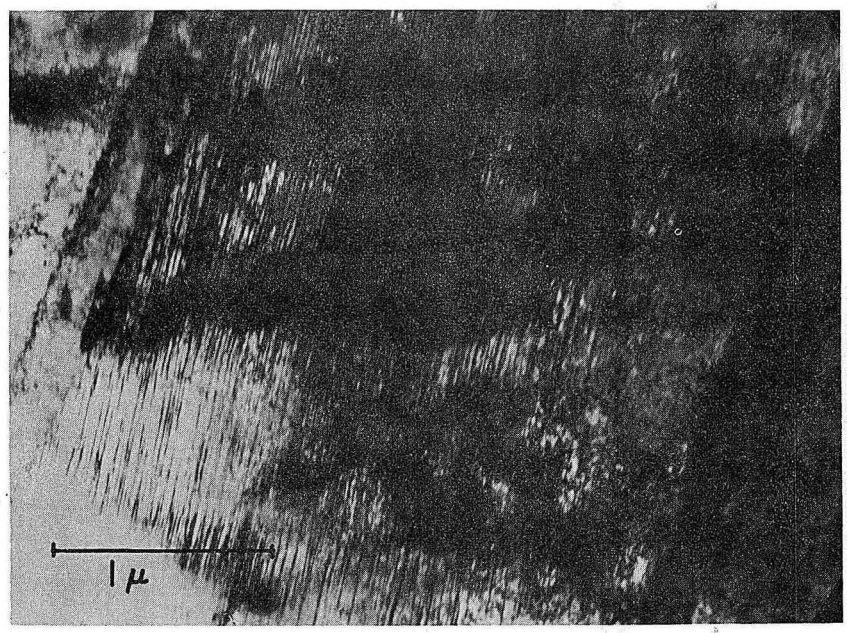

(a)

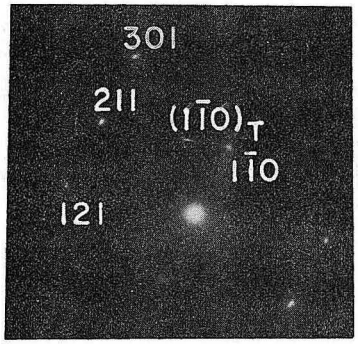

(b)

ZN-4635

Fig. 25

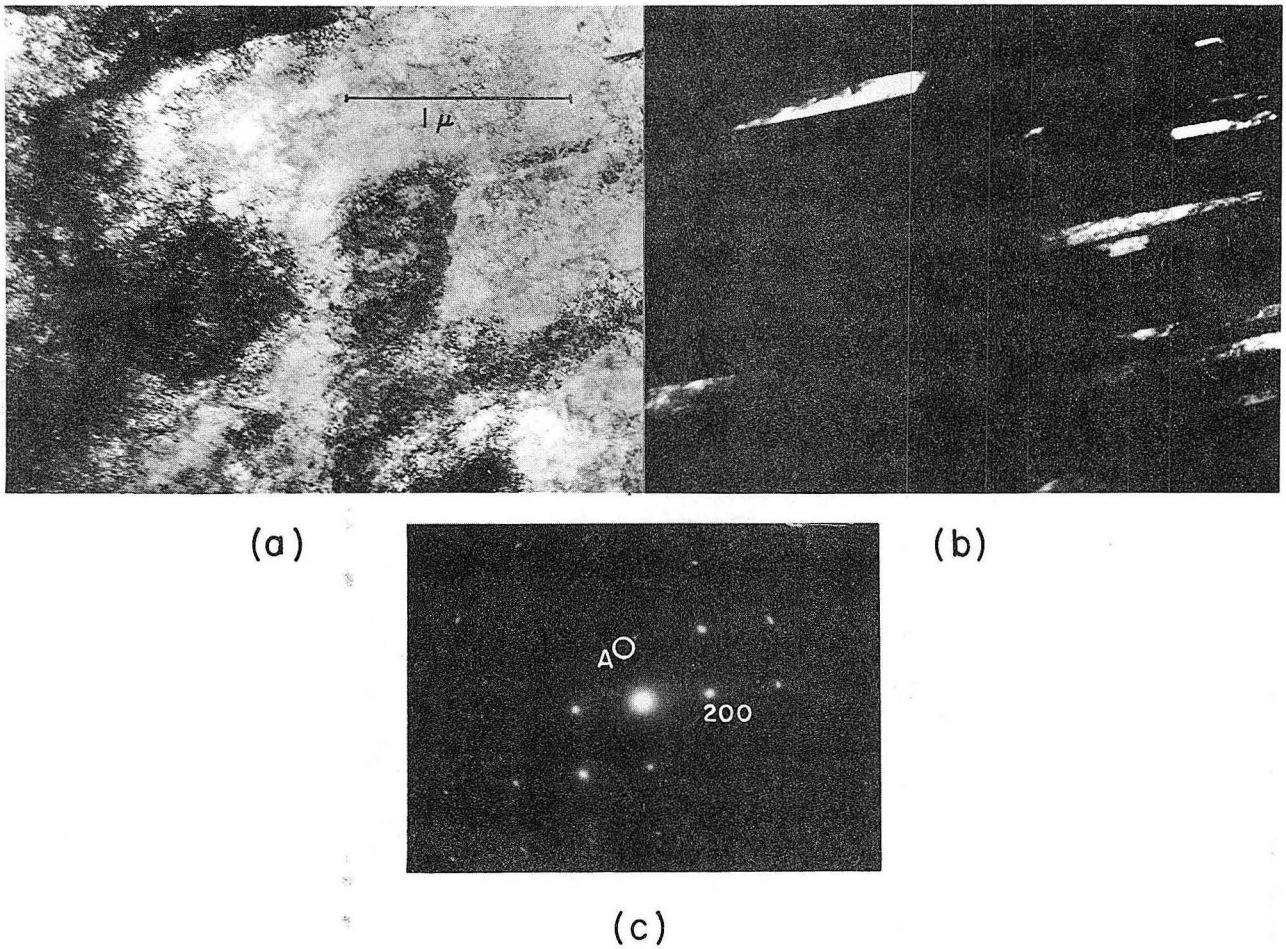

ZN-4636

Fig. 26

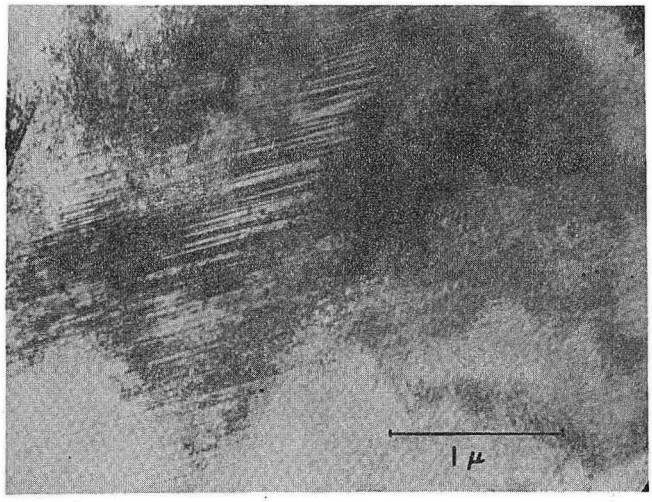

(a)

(b)

ZN-4637

Fig. 27

(a)

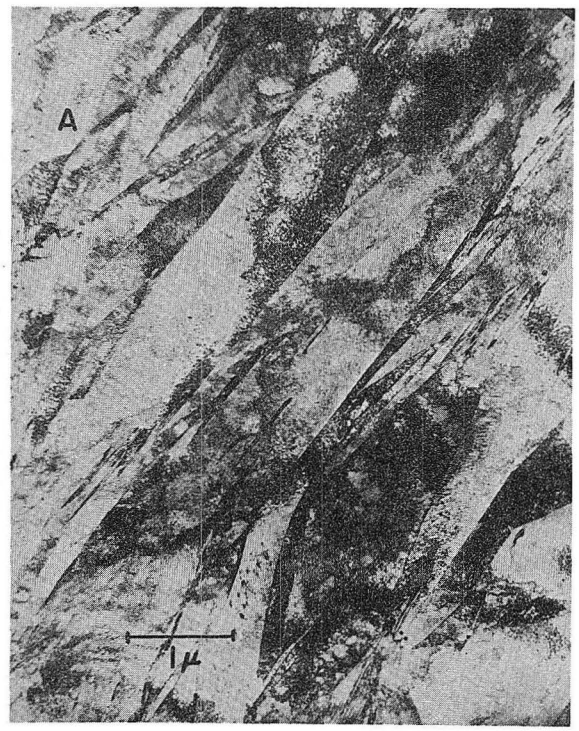

(b)

ZN-4638

Fig. 28

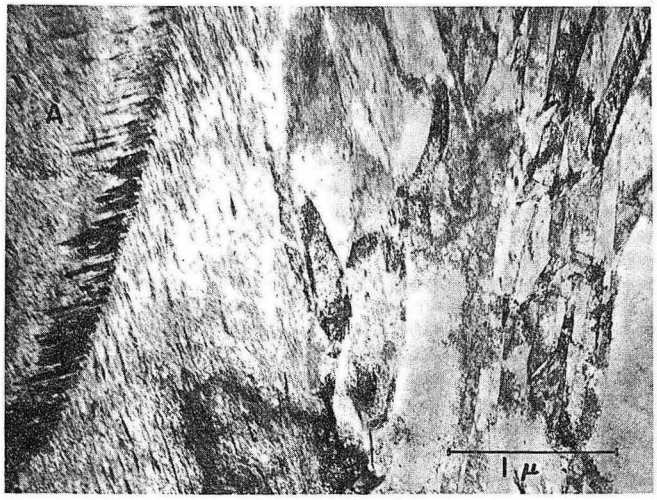

(a)

(b)

ZN-4639

Fig. 29

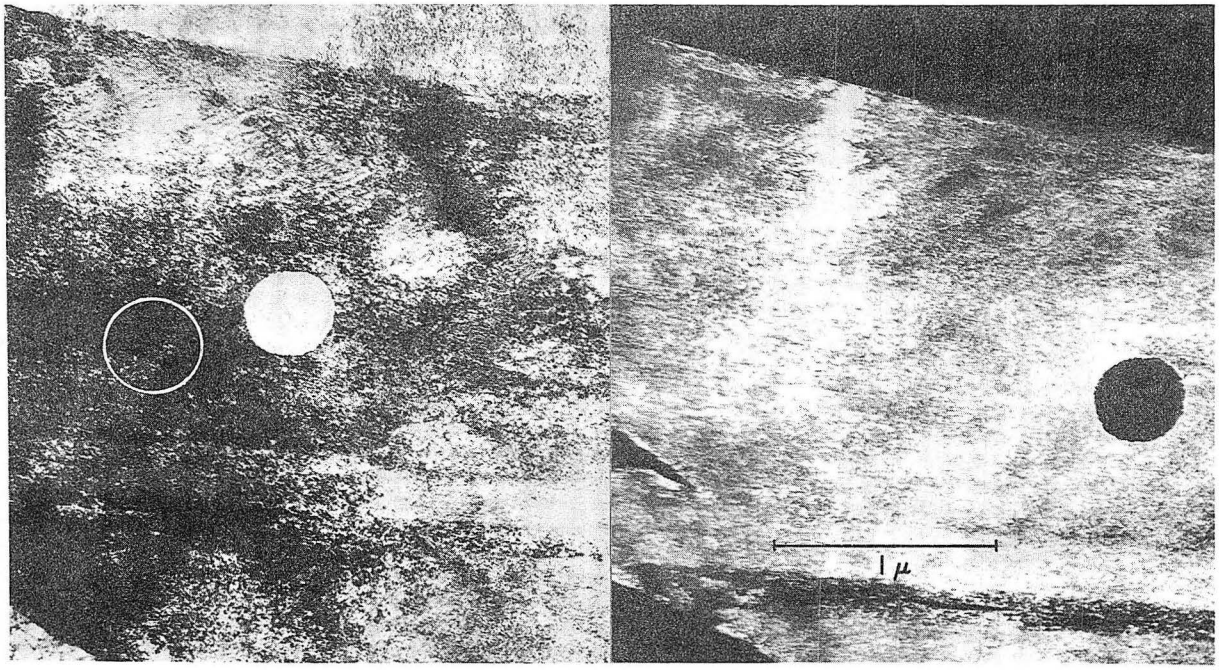

(a) (b)

ZN-4640

Fig. 30

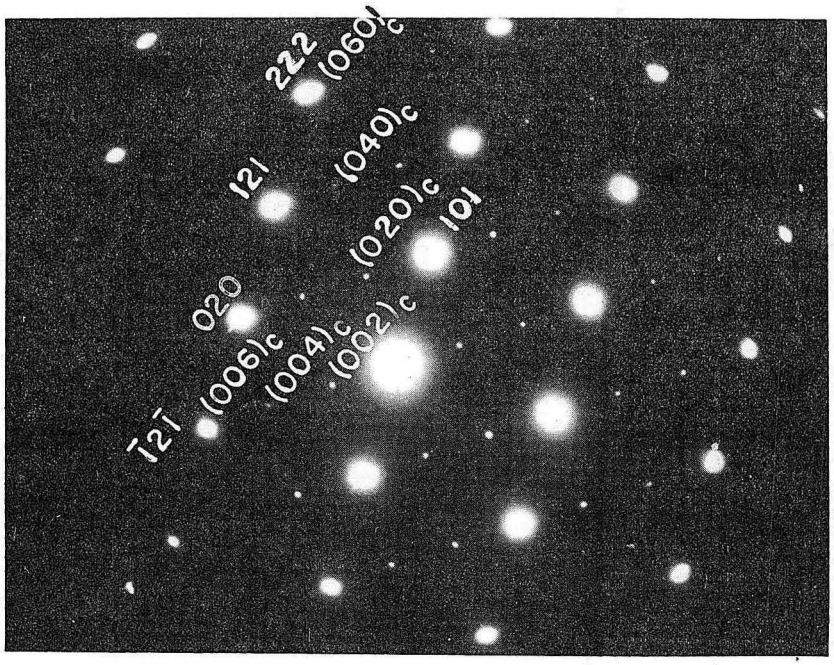

ZN-4641

Fig. 31

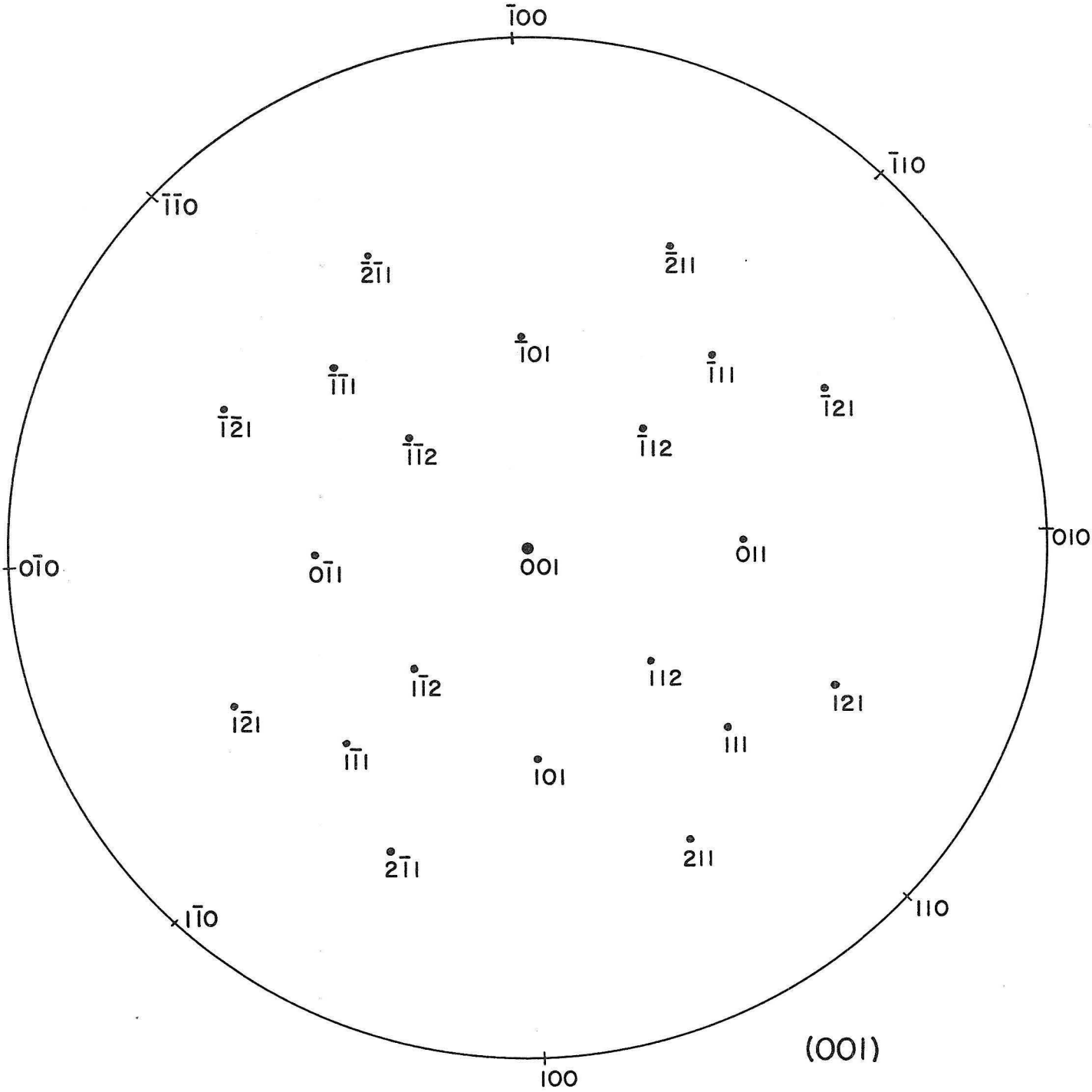

MUB-4979

Fig. 32

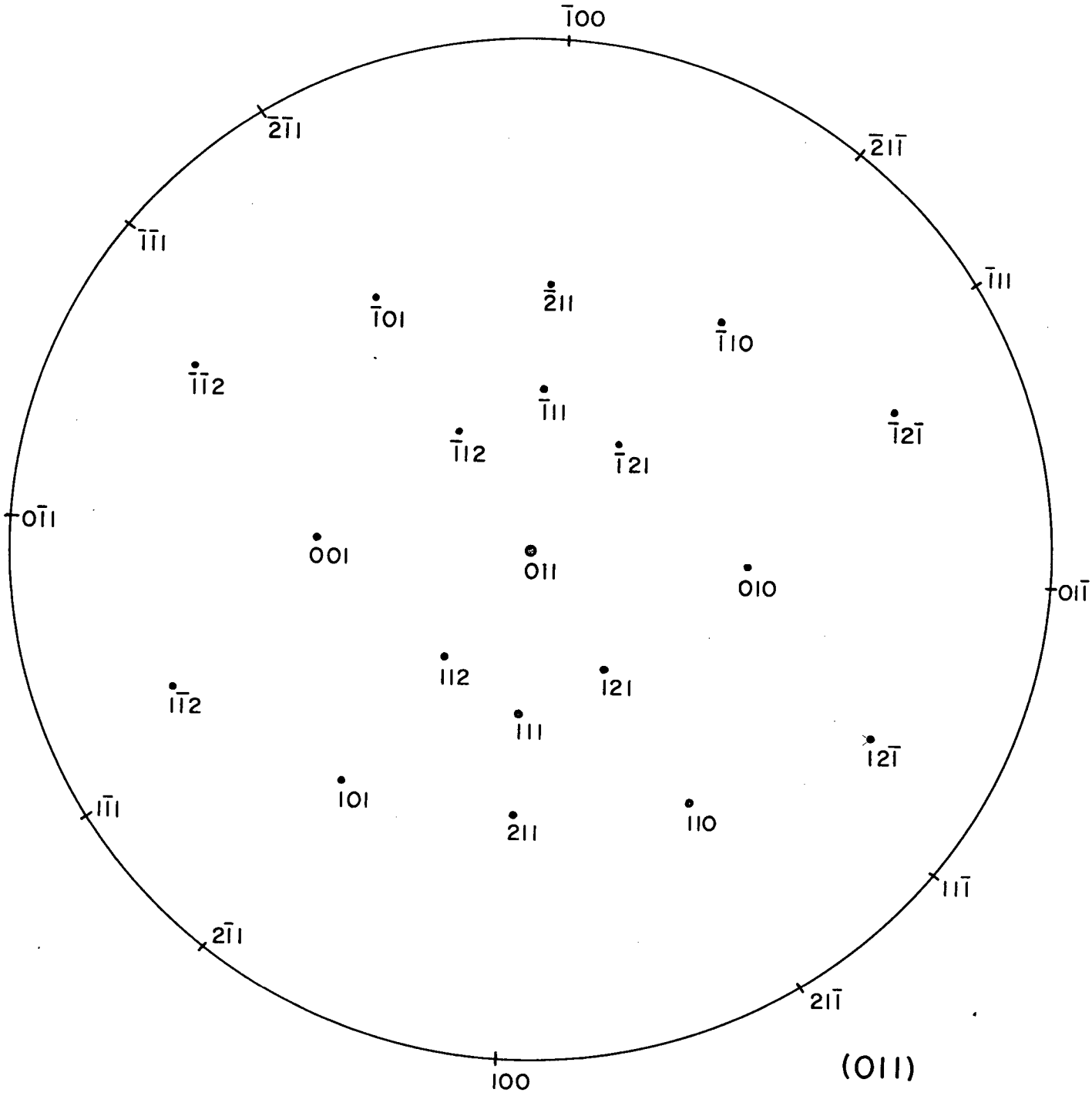

MUB-4980

Fig. 33

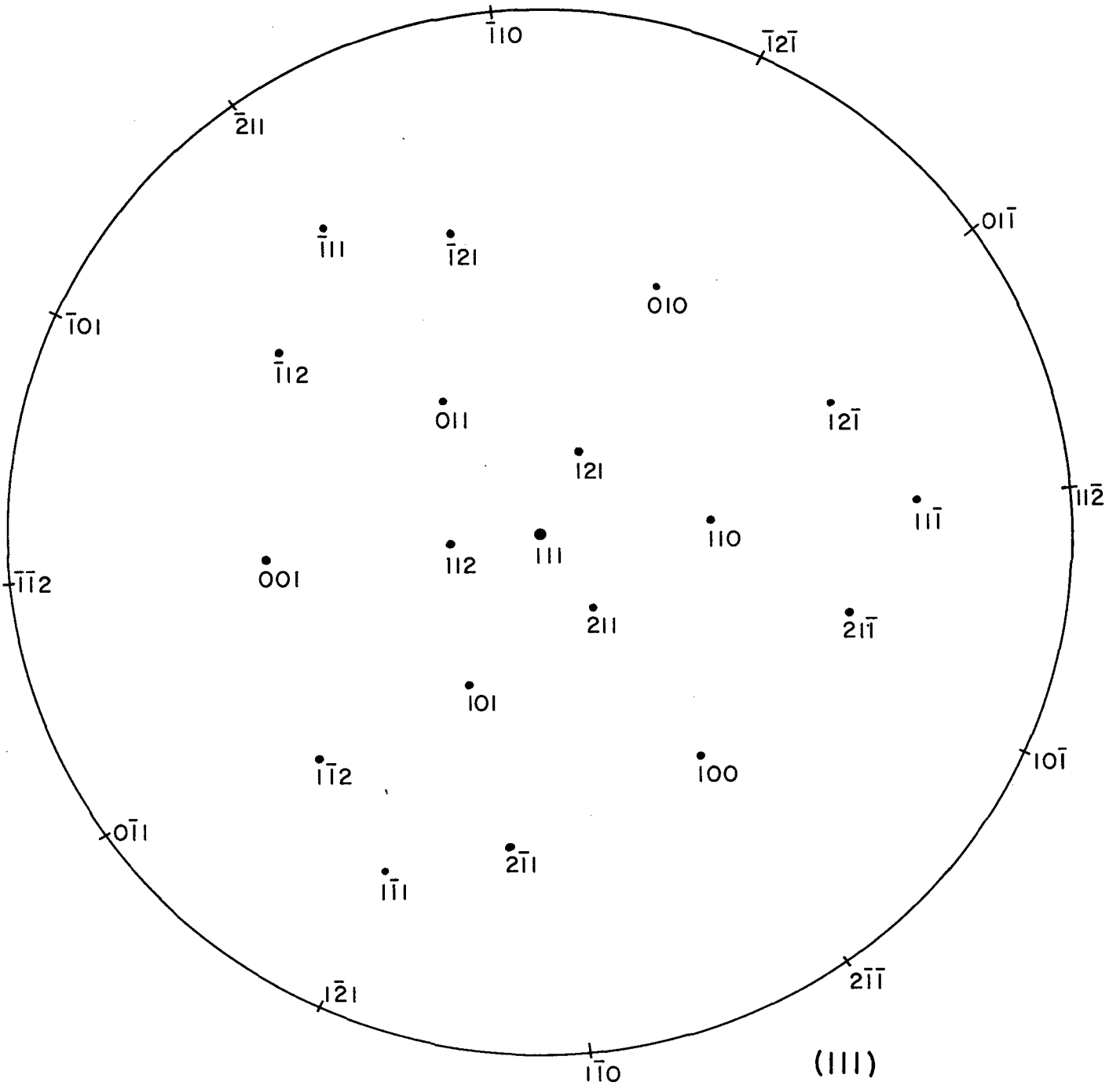

MUB-4981

Fig. 34

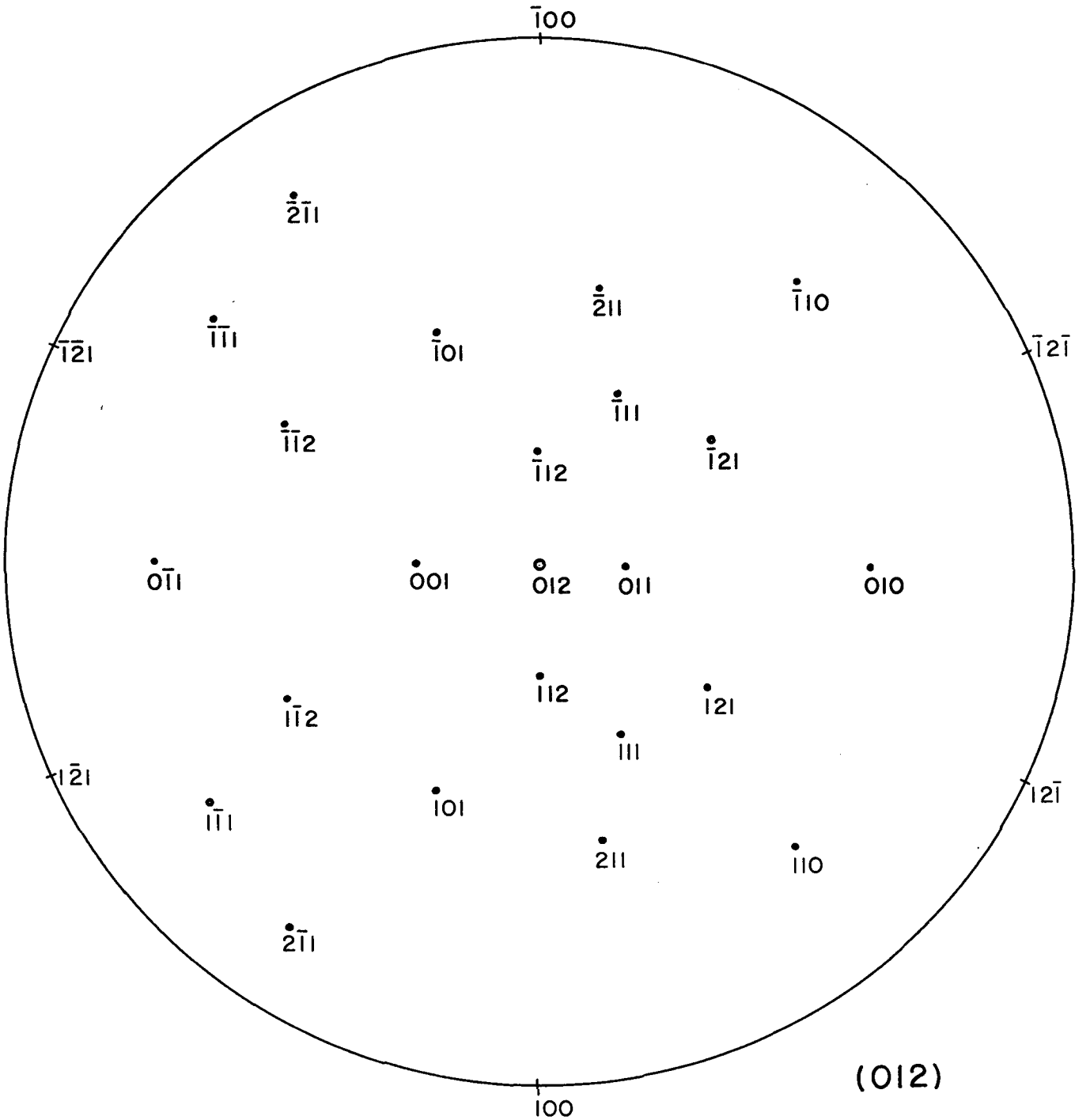

MUB-4982

Fig. 35

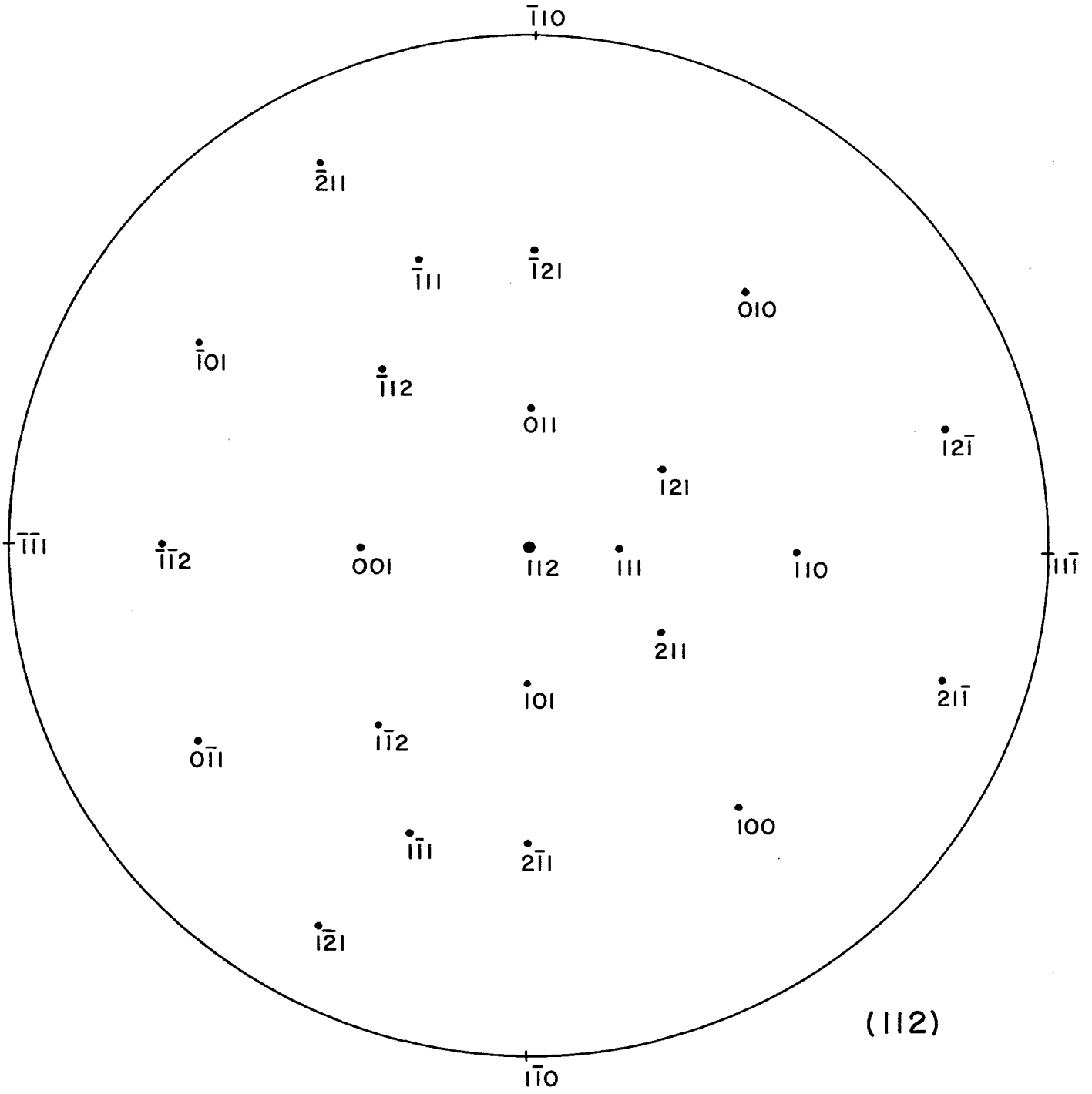

MUB-4983

Fig. 36

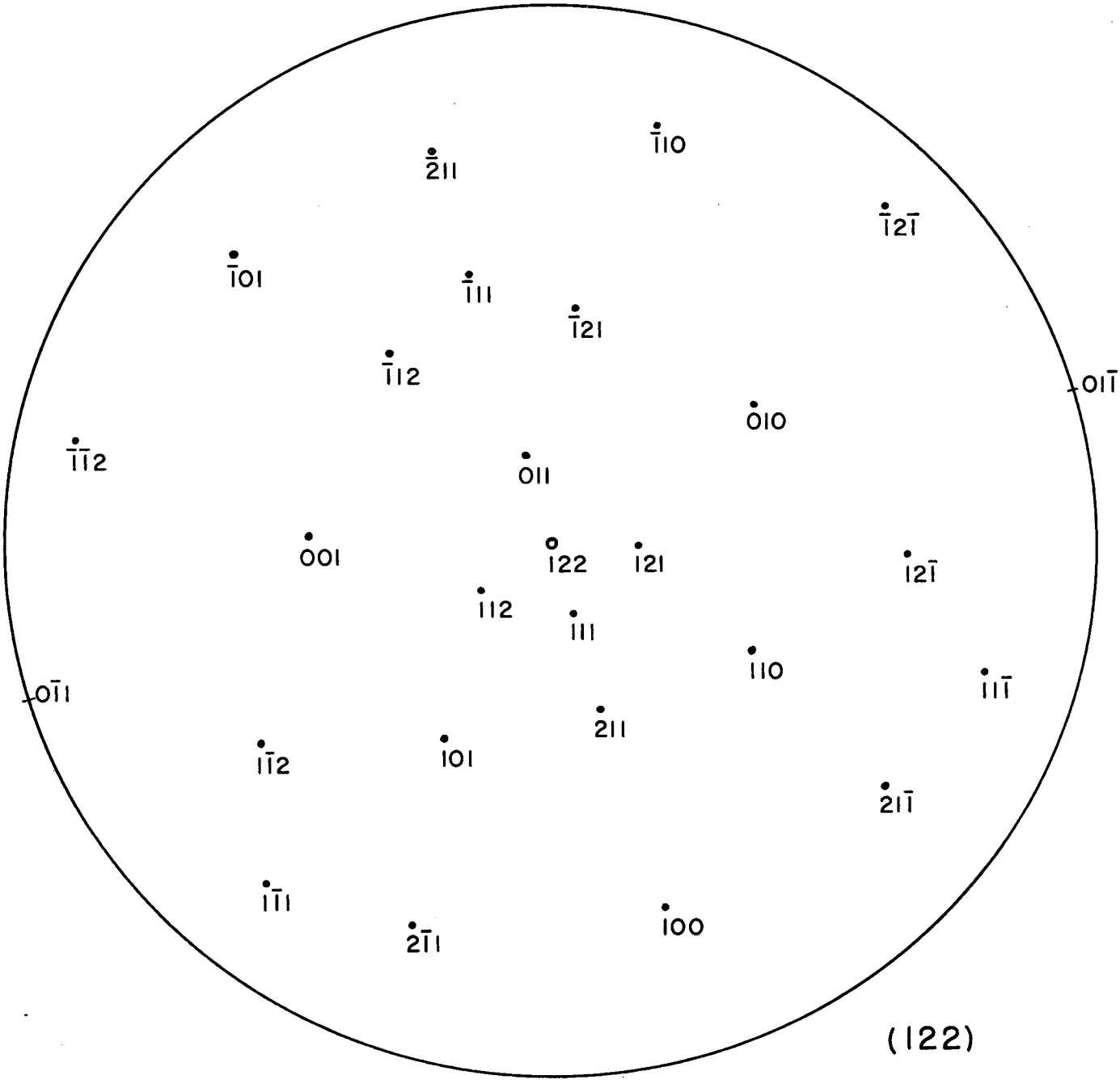

MUB-4984

Fig. 37

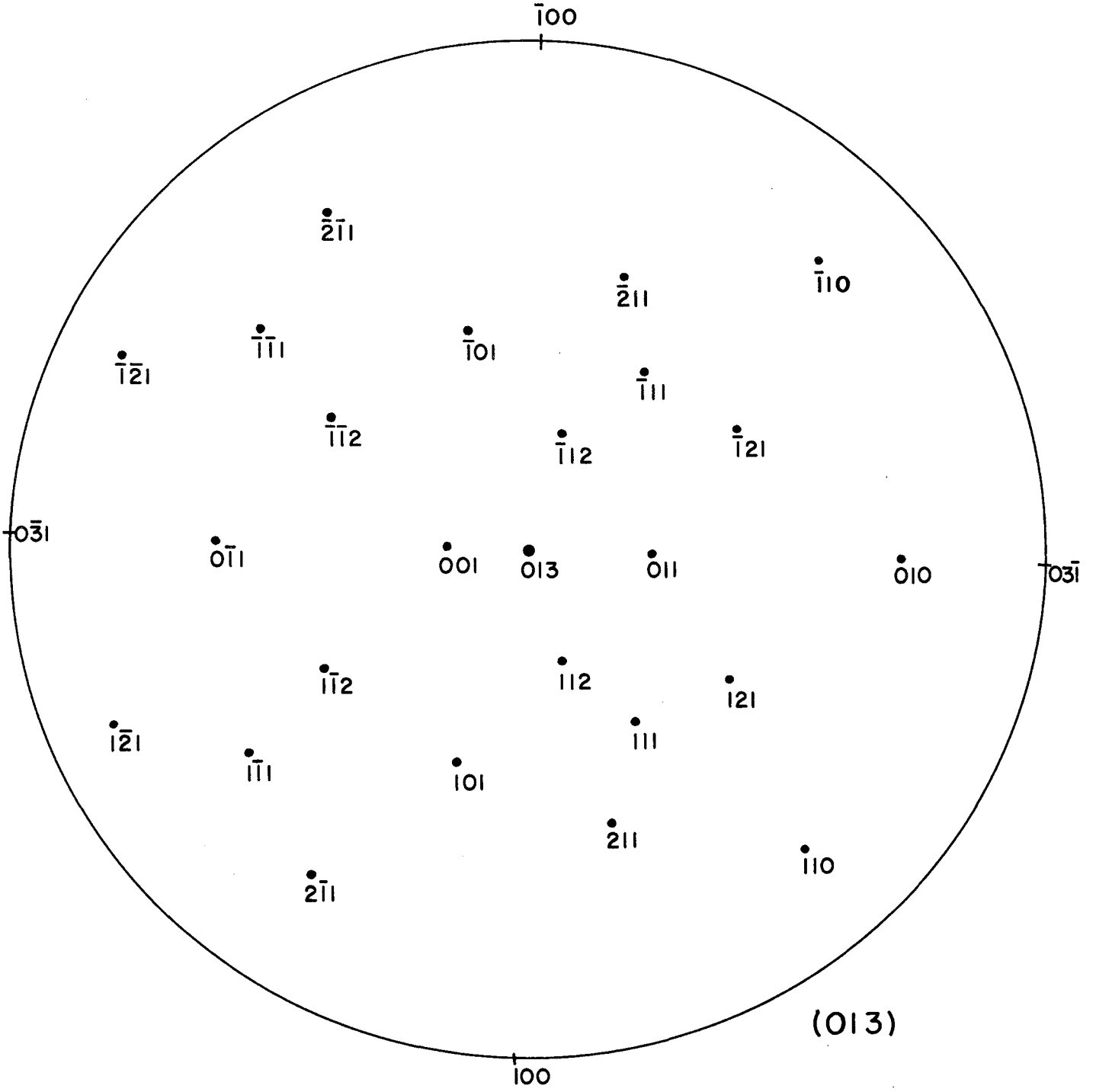

MUB-4985

Fig. 38

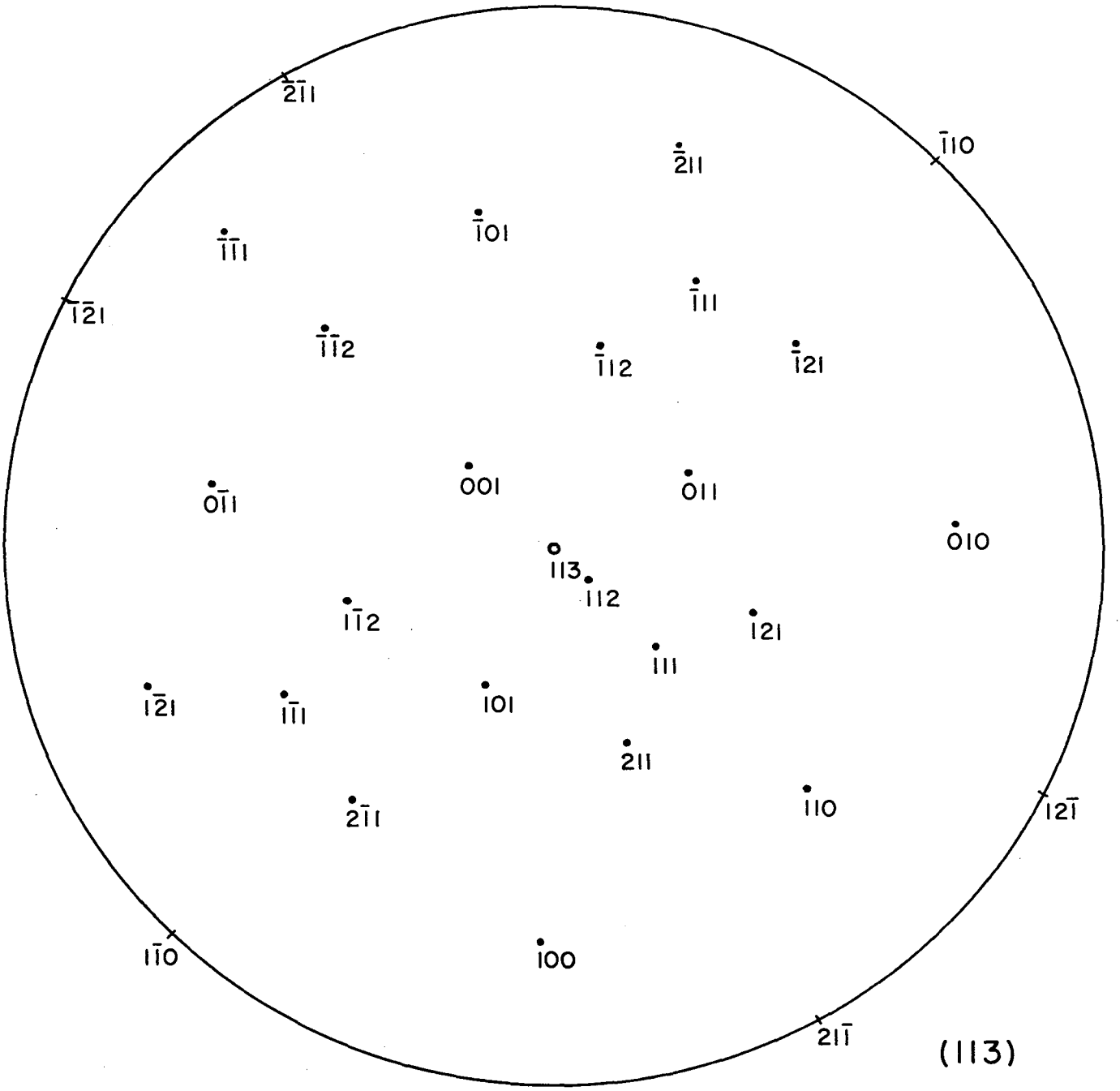

MUB-4986

Fig. 39

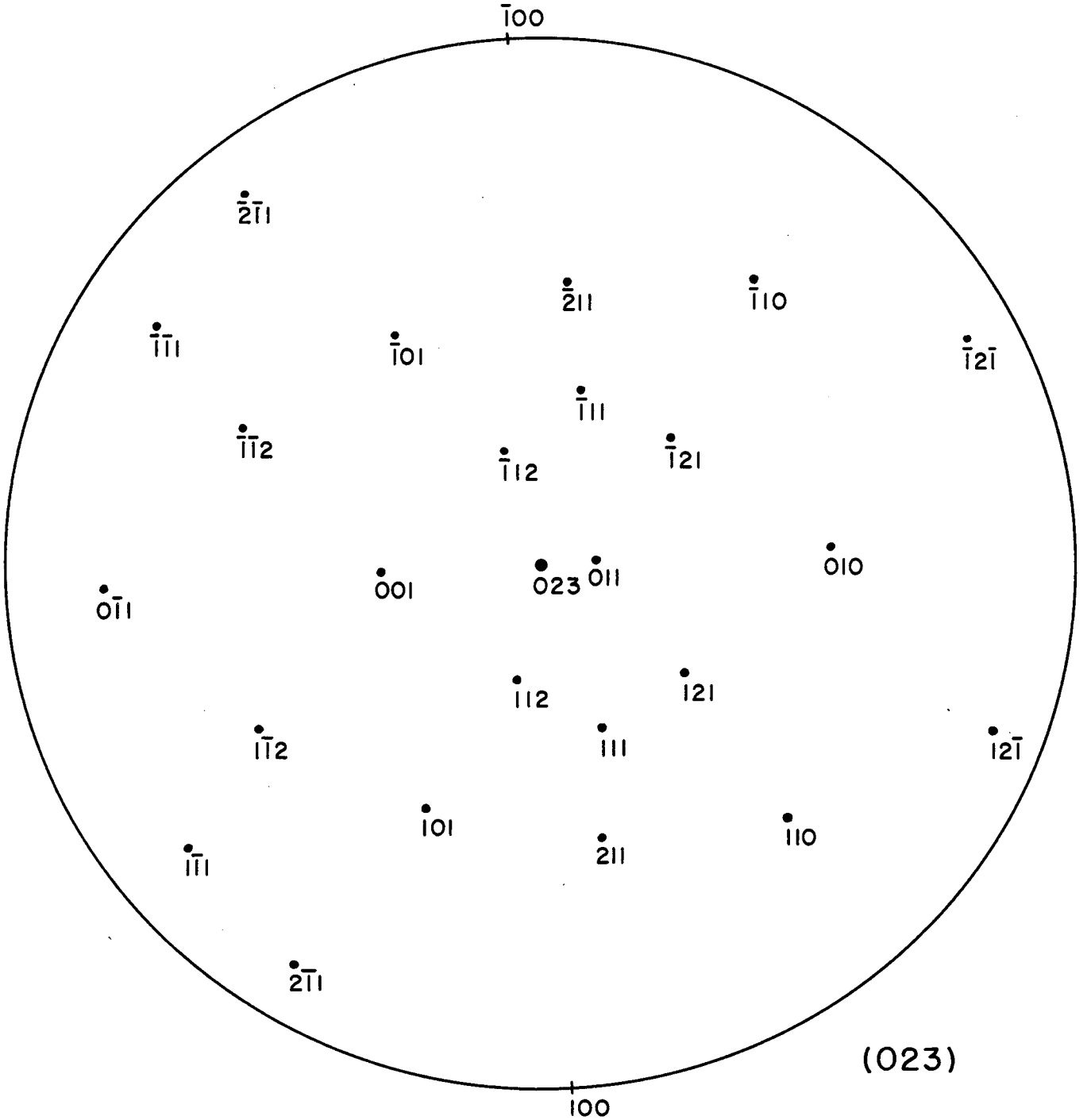

MUB-4987

Fig. 40

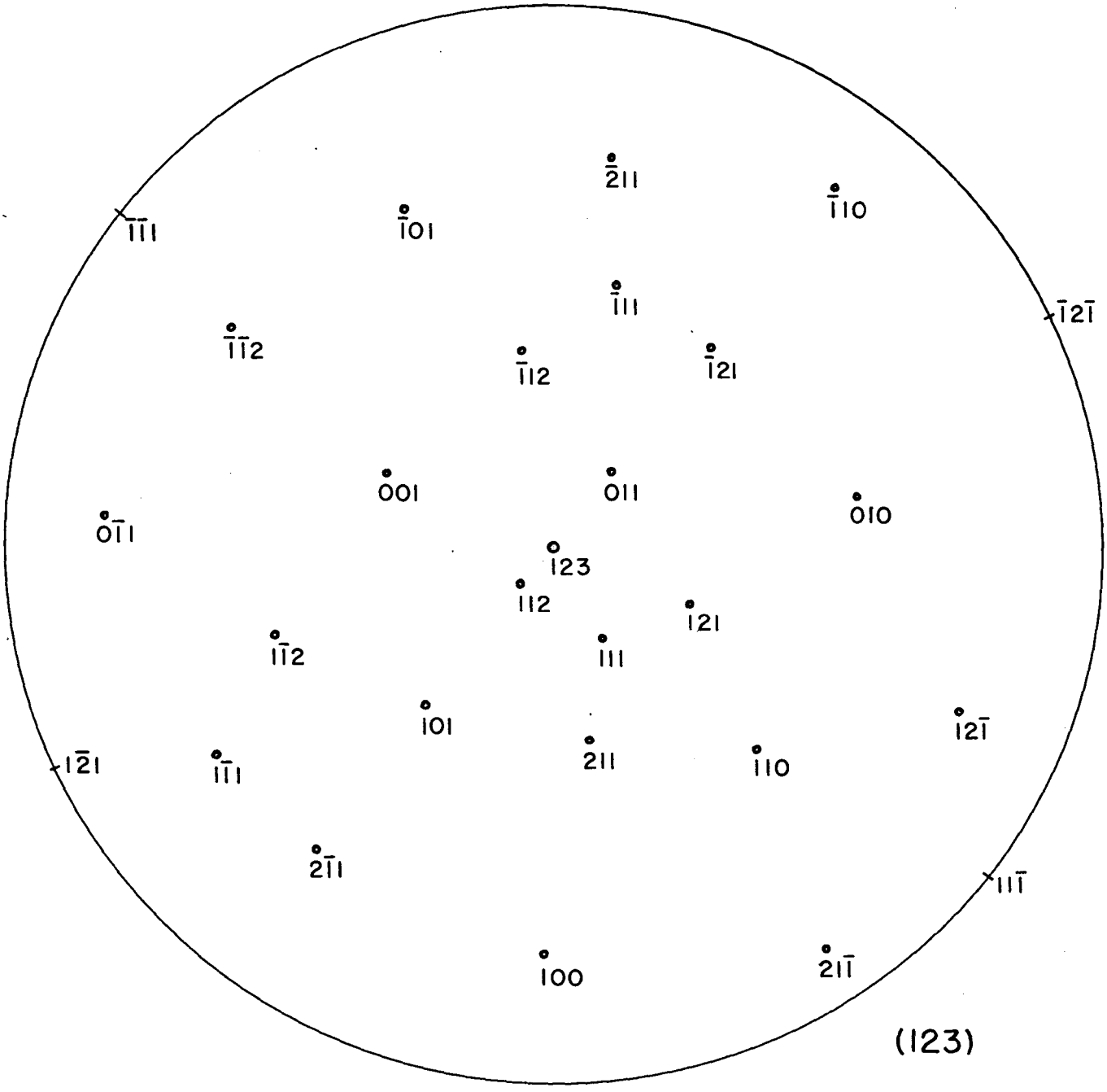

MUB-4988

Fig. 41

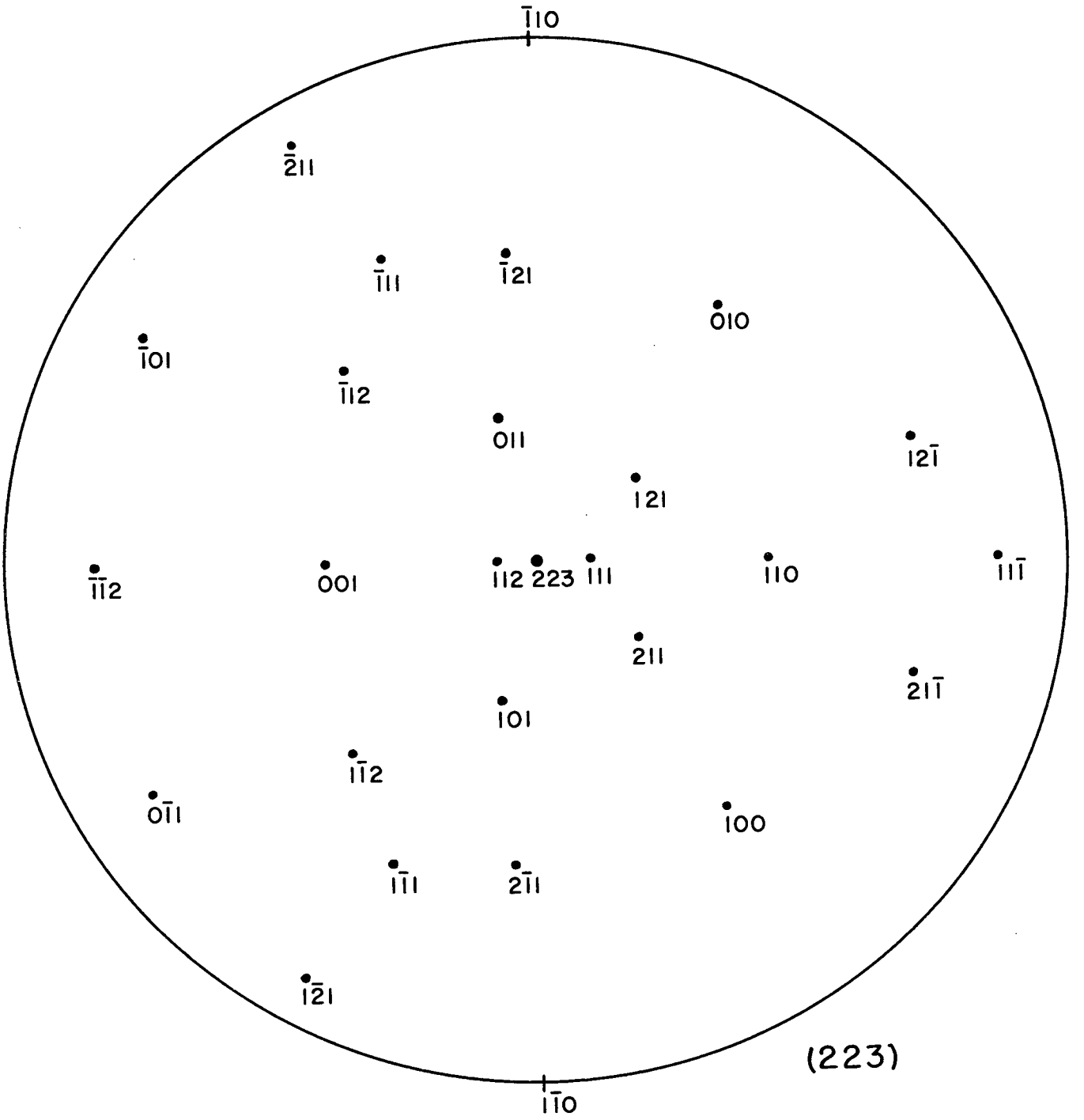

MUB-4989

Fig. 42

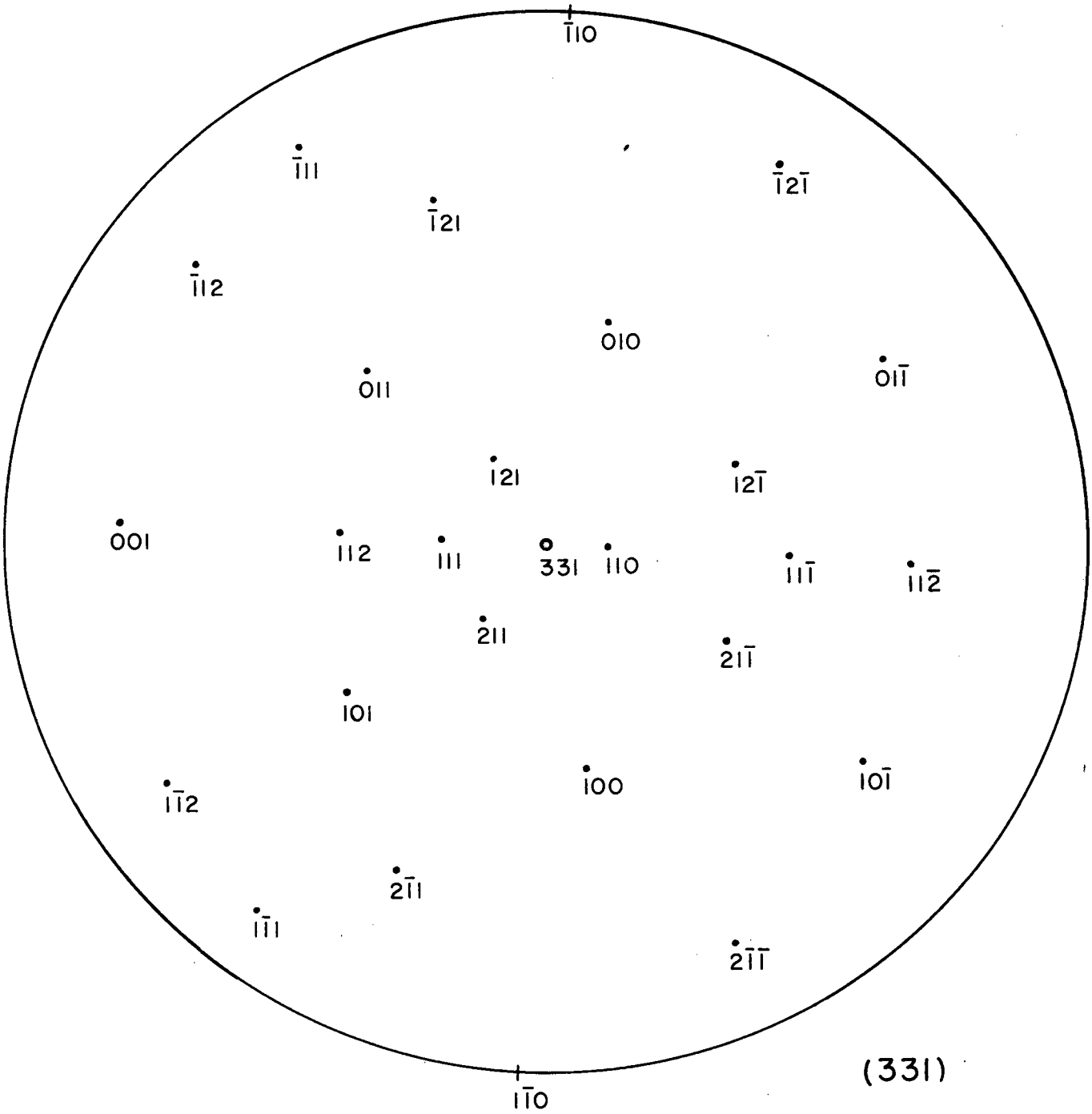

MUB-4990

Fig. 43

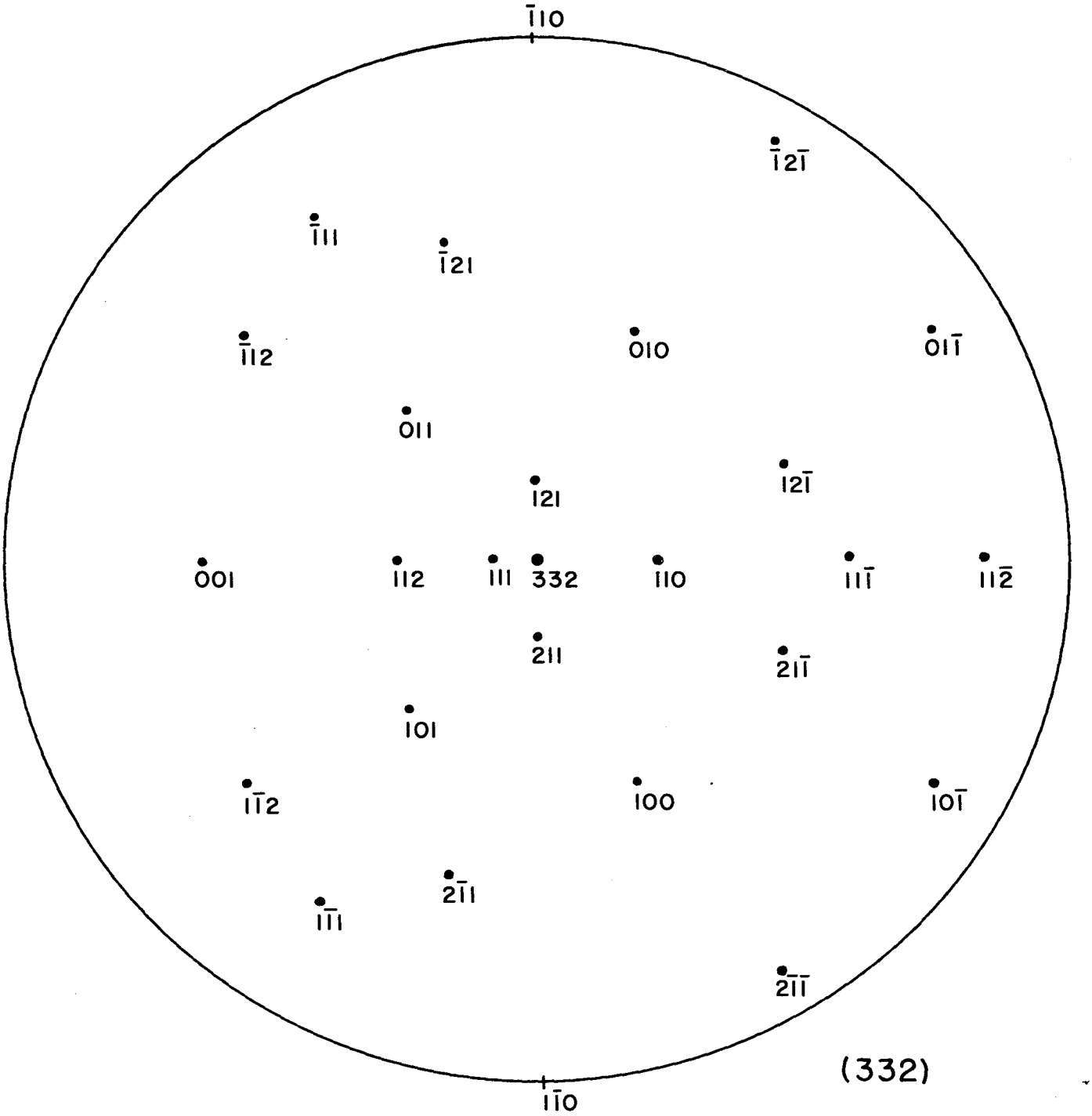

MUB-4991

Fig. 44

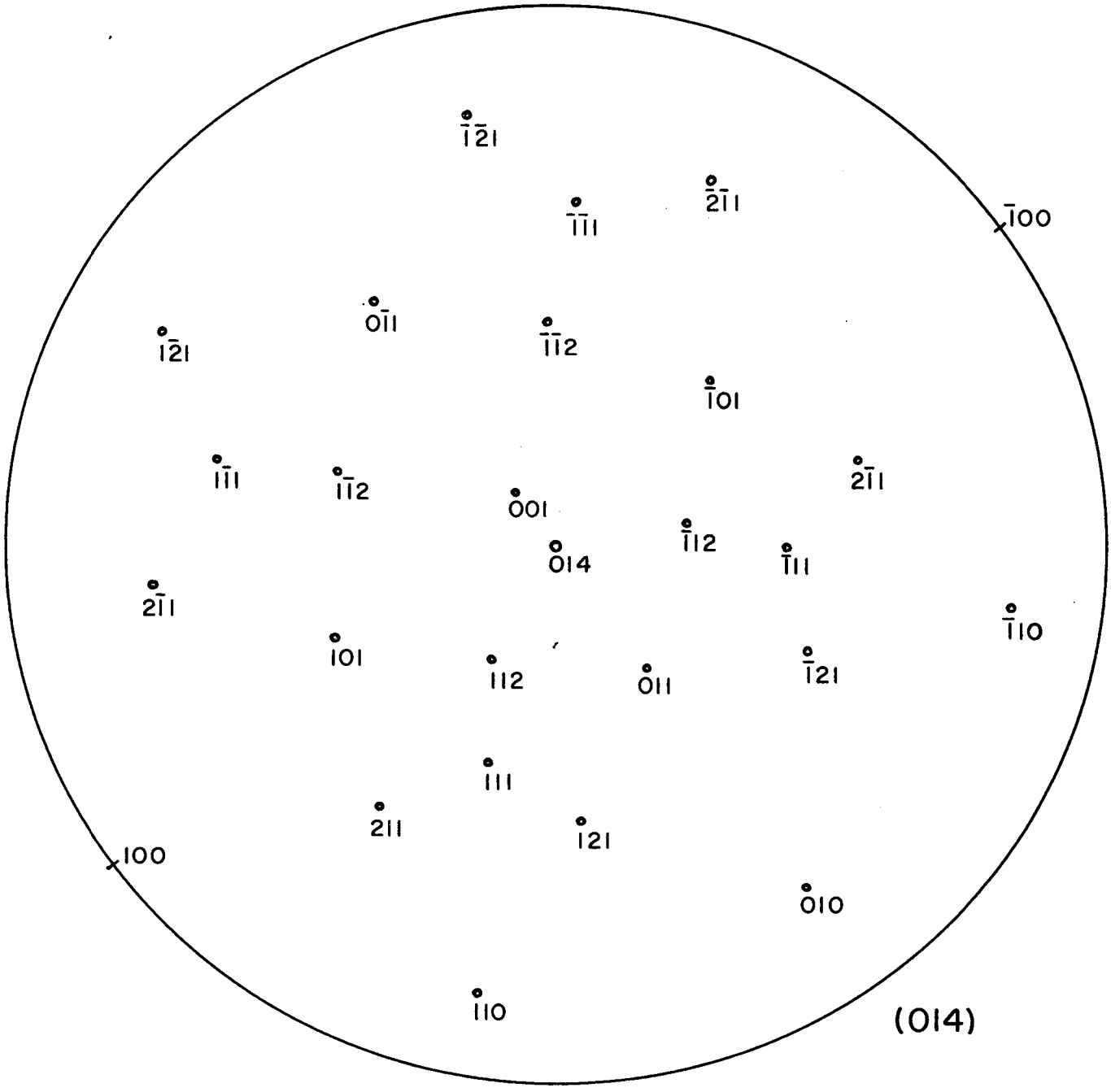

MUB-4992

Fig. 45

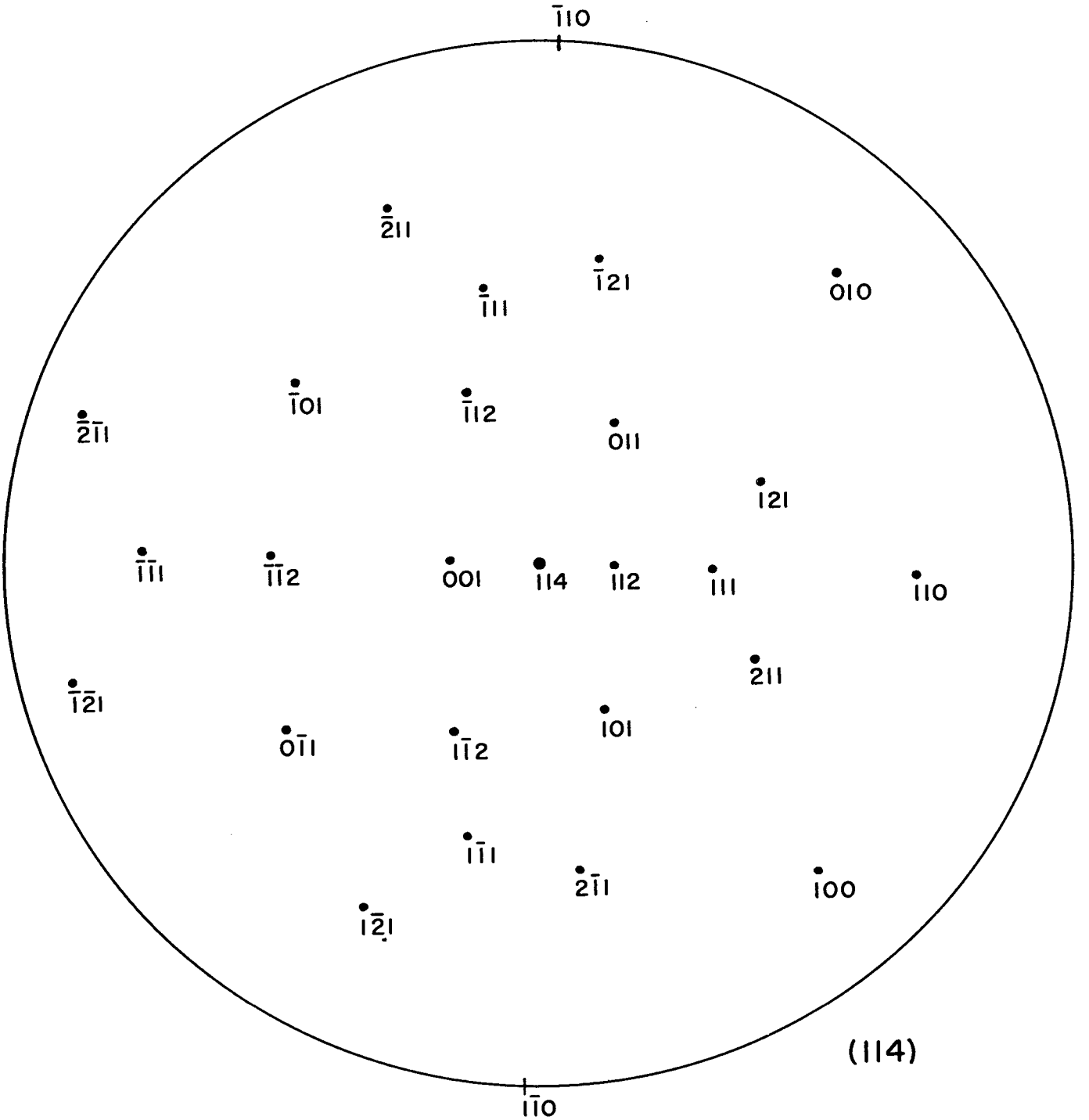

MUB-4993

Fig. 46

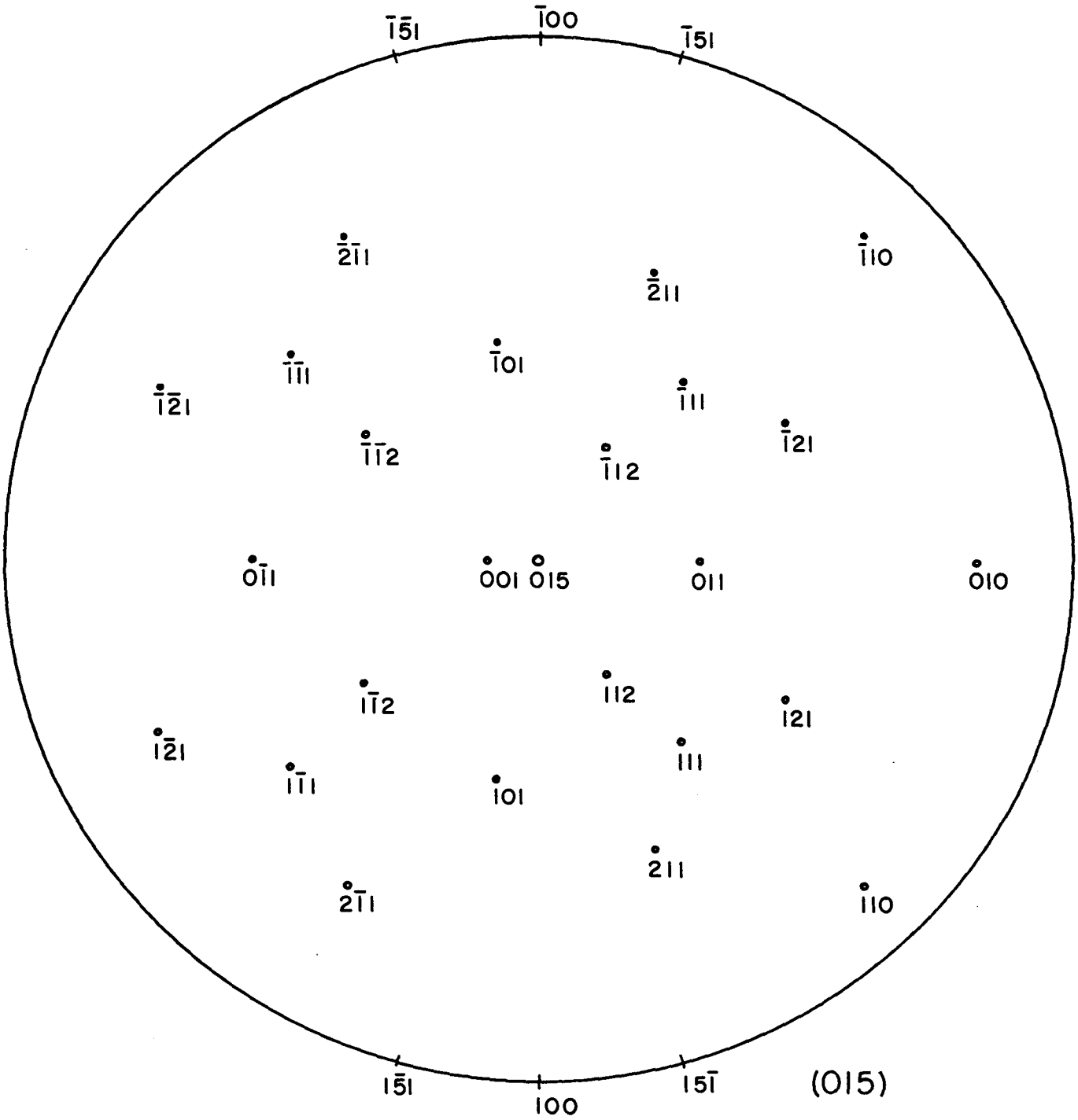

MUB-4994

Fig. 47

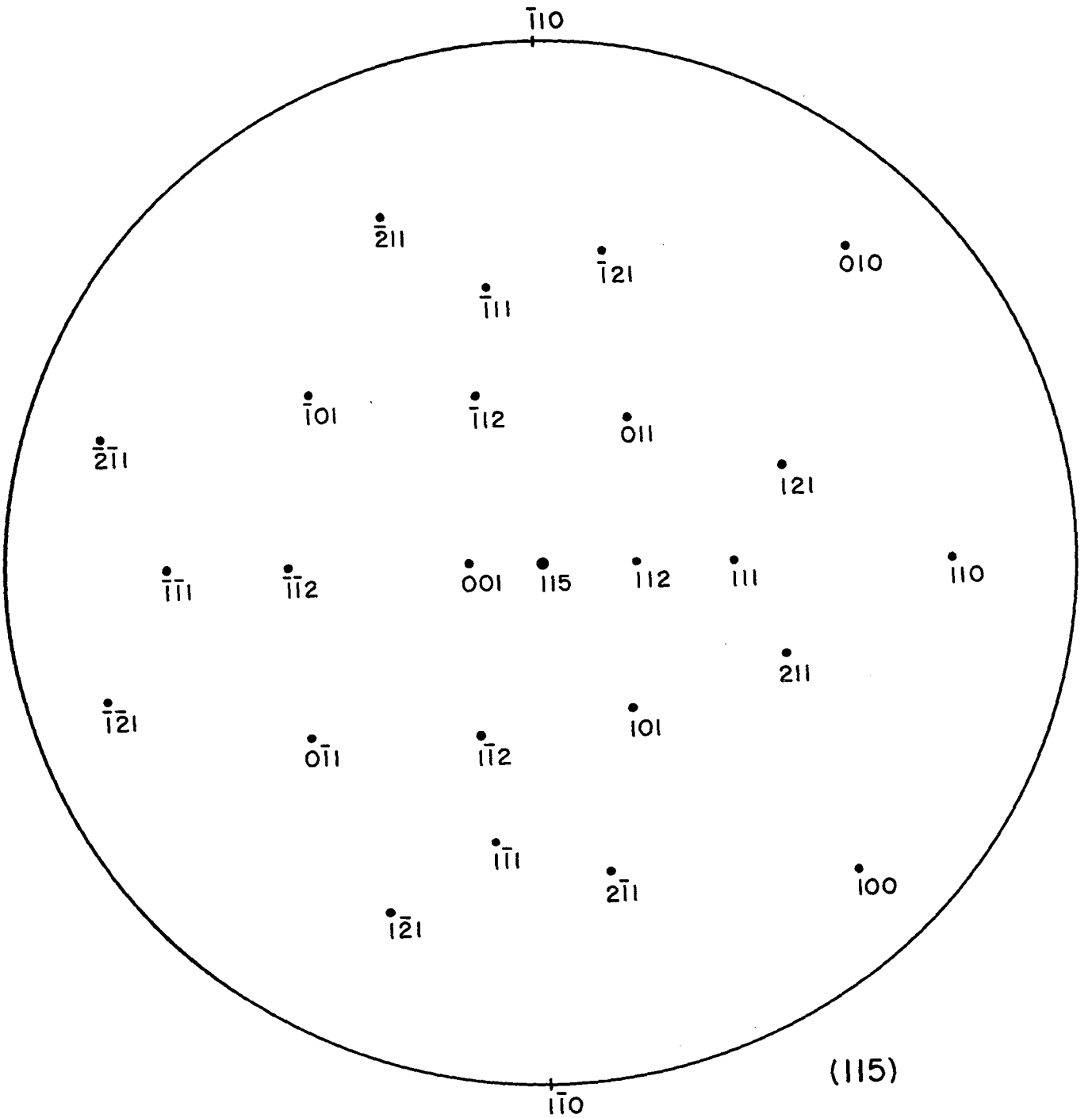

MUB-4995

Fig. 48

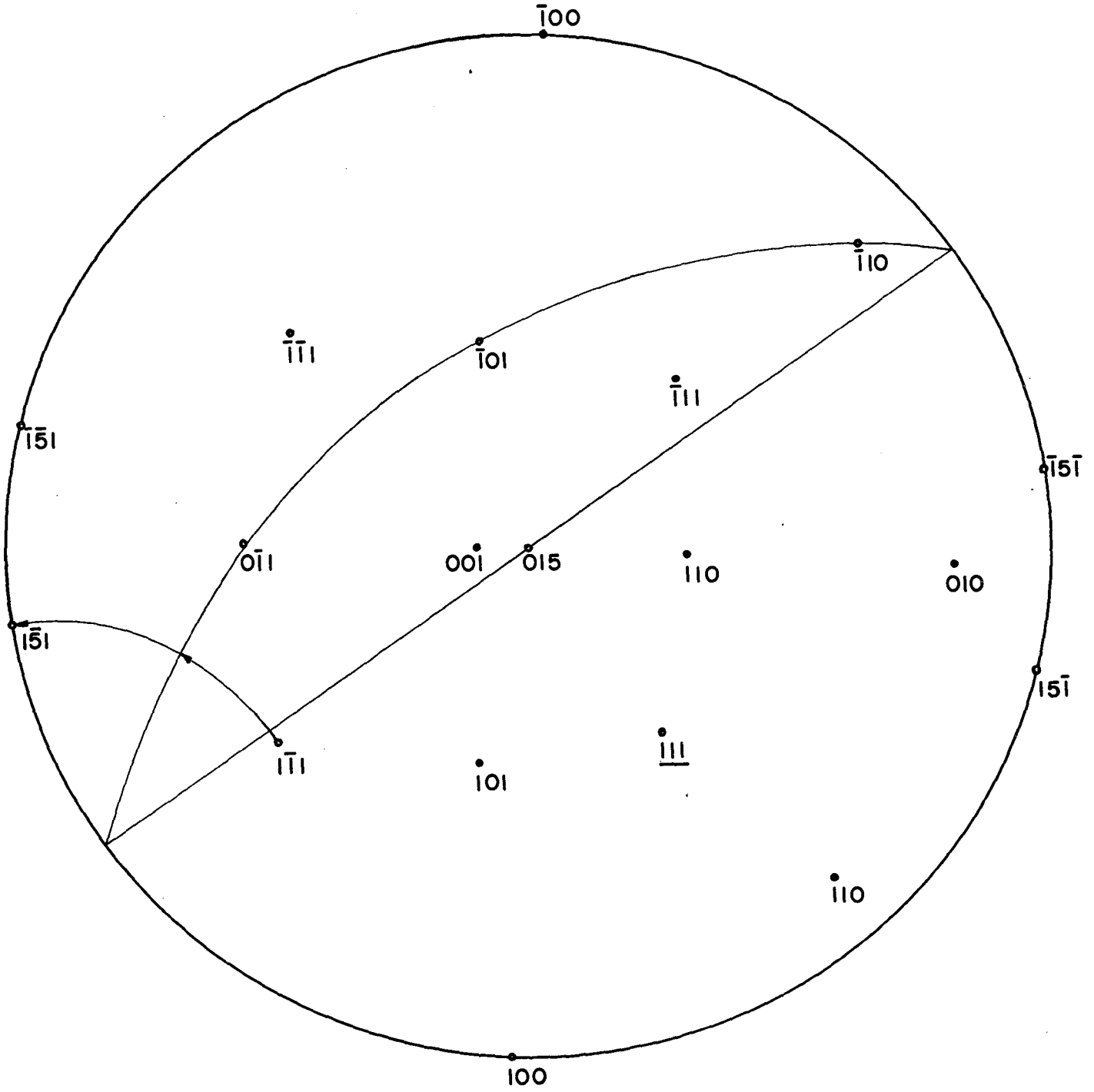

MUB-4996

Fig. 49

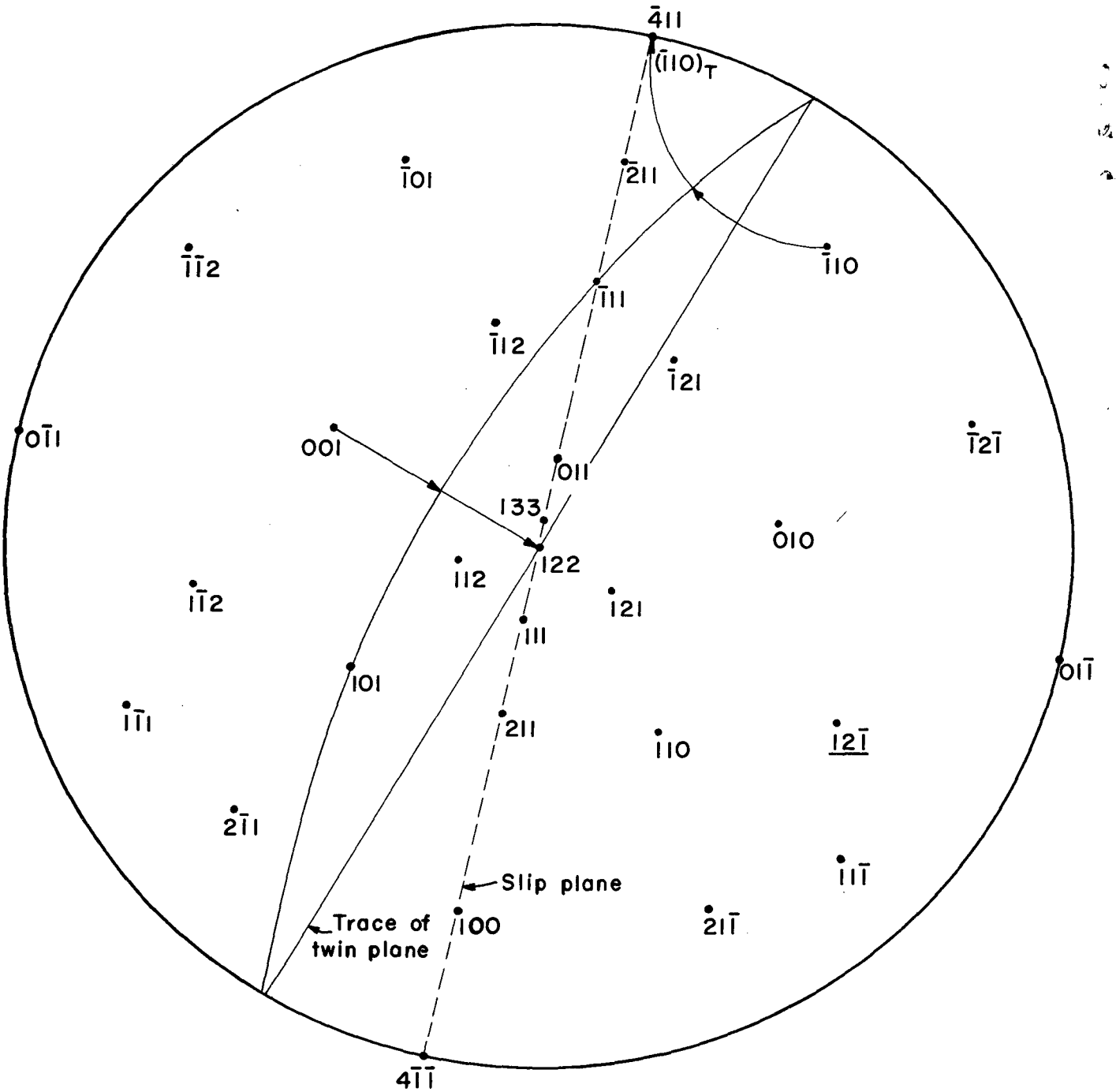

MUB-4997

Fig. 50

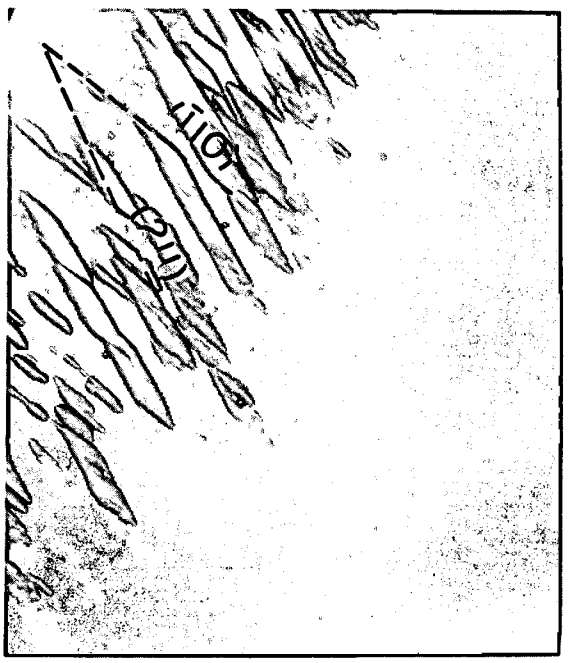

ZN-4642

Fig. 51

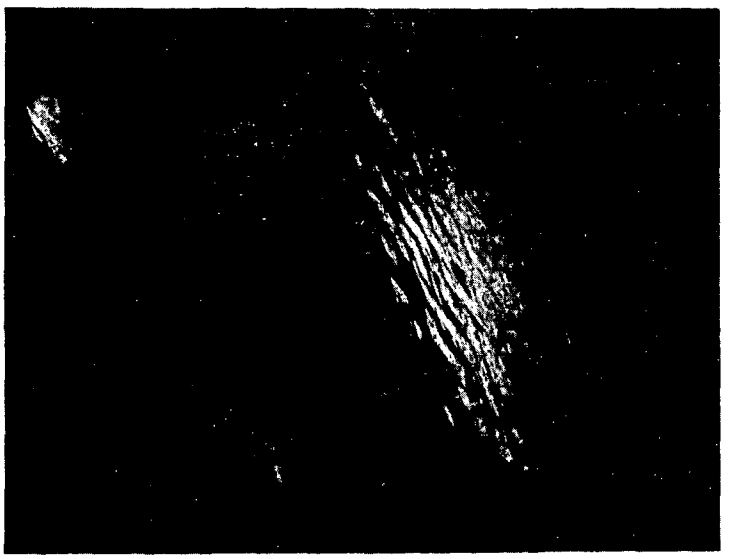

(a)

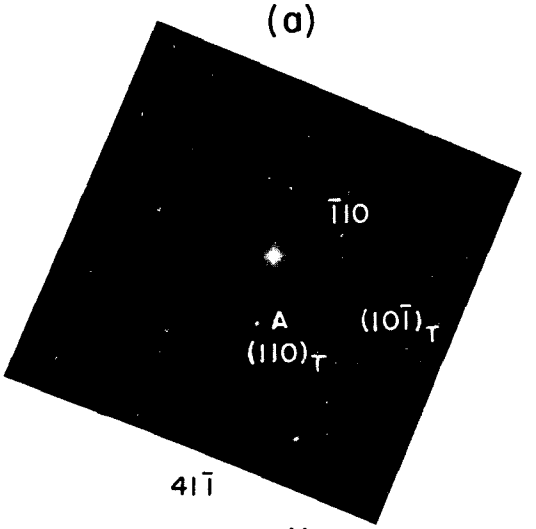

(b)

ZN-4643

Fig. 52

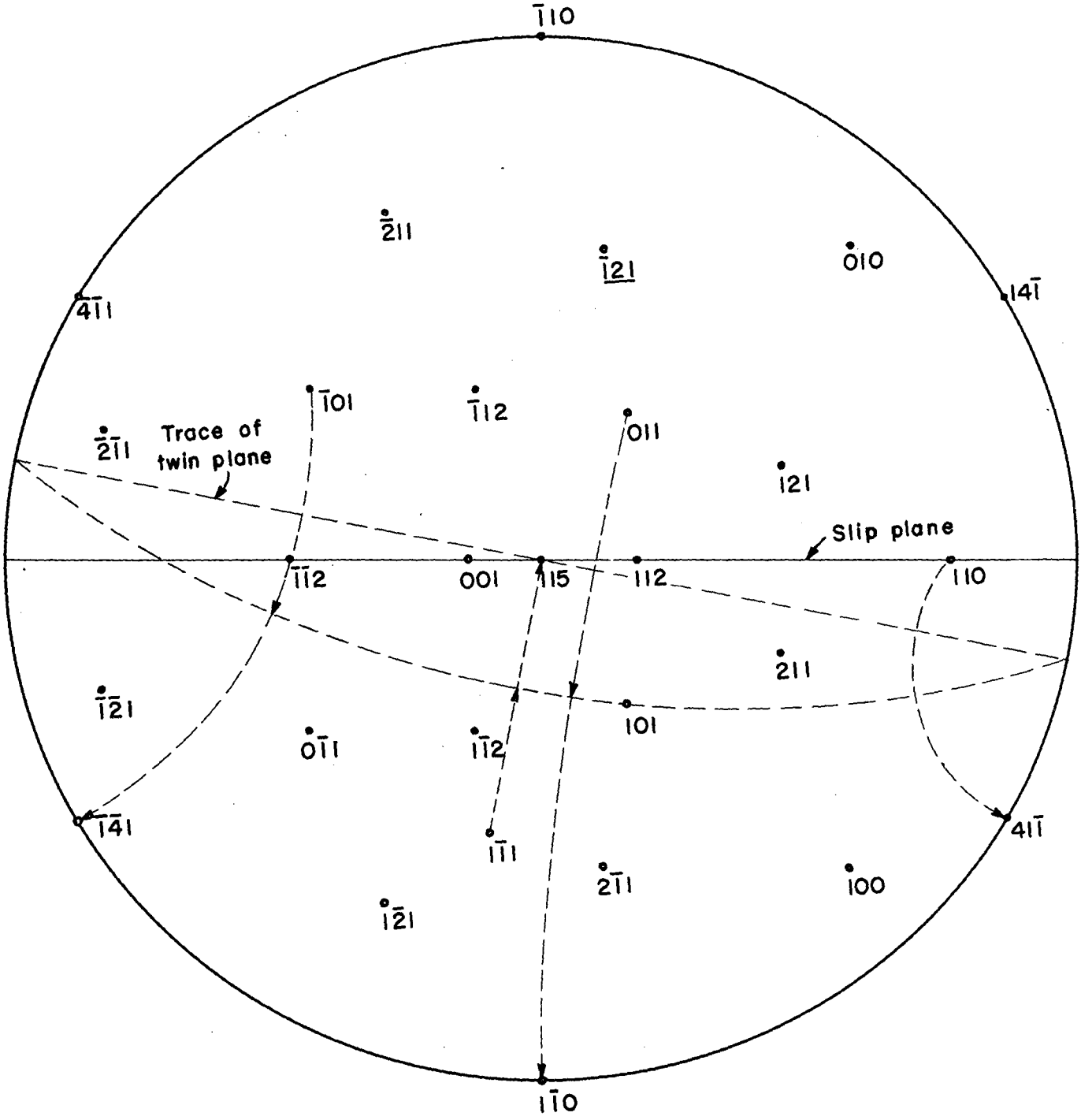

MUB-4998

Fig. 53

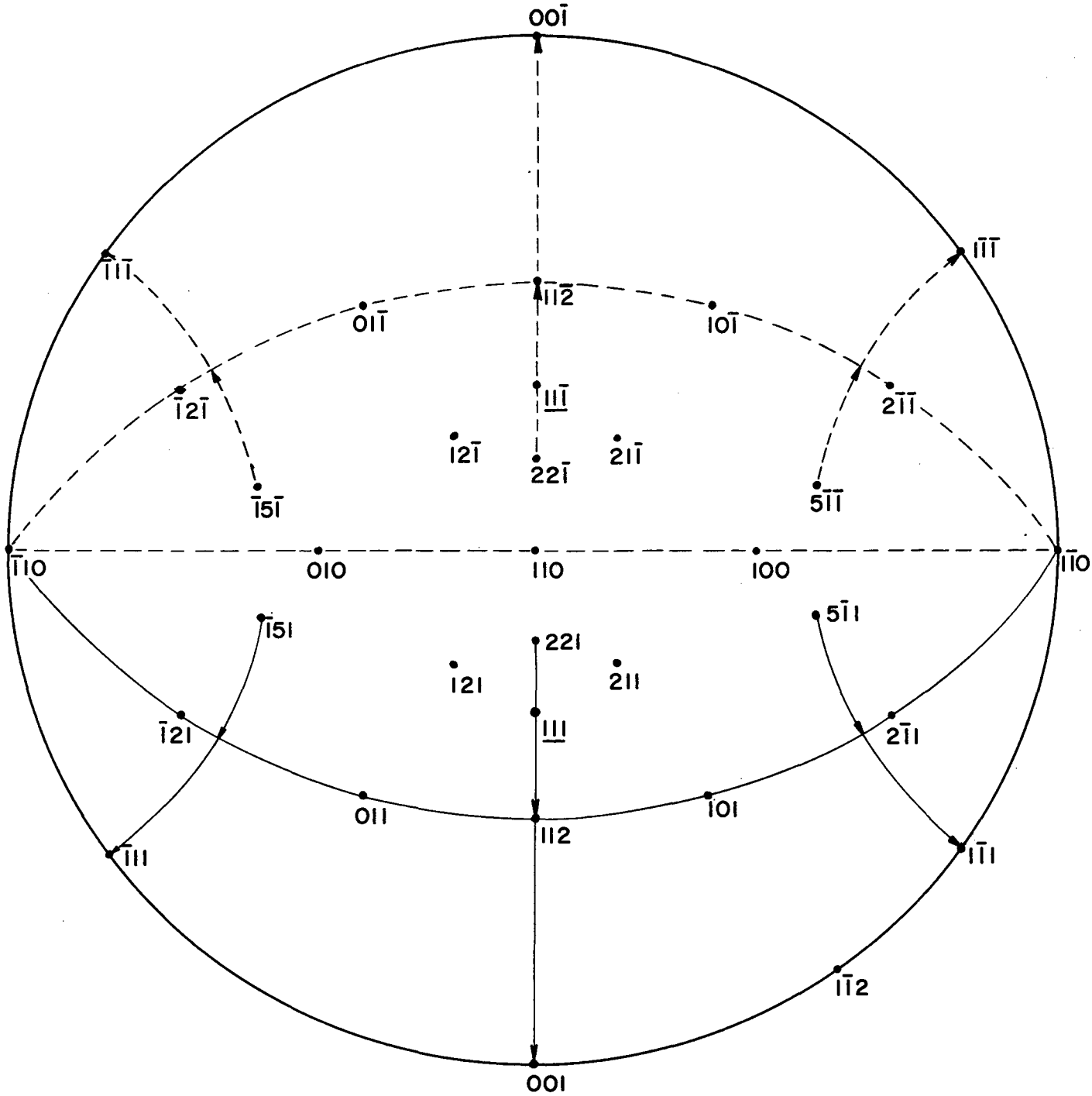

MUB-4999

Fig. 54

This report was prepared as an account of Government sponsored work. Neither the United States, nor the Commission, nor any person acting on behalf of the Commission:

A. Makes any warranty or representation, expressed or implied, with respect to the accuracy, completeness, or usefulness of the information contained in this report, or that the use of any information, apparatus, method, or process disclosed in this report may not infringe privately owned rights; or

B. Assumes any liabilities with respect to the use of, or for damages resulting from the use of any information, apparatus, method, or process disclosed in this report.

As used in the above, "person acting on behalf of the Commission" includes any employee or contractor of the Commission, or employee of such contractor, to the extent that such employee or contractor of the Commission, or employee of such contractor prepares, disseminates, or provides access to, any information pursuant to his employment or contract with the Commission, or his employment with such contractor.